Přírodovědecká fakulta
Faculty of Science

Jihočeská univerzita v Českých Budějovicích
University of South Bohemia in České Budějovice

High light, UV light, and green light: effects on the plant assimilation apparatus during acclimation

Habilitation Thesis

Michal Štroch

2023

Acknowledgements

I would like to thank all my colleagues from the Department of Physics at the University of Ostrava, with whom I have worked over the years, for their support, help, and fruitful cooperation. I am grateful to my former Ph.D. students Zuzana Kmecová-Materová and Jan Semer for their excellent work. My thanks also go to my coworkers from the Department of Biophysics at Palacký University in Olomouc and from the Laboratory of Ecological Plant Physiology at the Global Change Research Institute in Brno (Czechglobe) for the possibility of cooperation, which resulted in the joint publications that are an important part of the thesis. I would like to name especially Roman Kouřil and Petr Ilík from Palacký University and Otmar Urban and Karel Klem from Czechglobe. I also thank Dr. Claus Buschmann (Botanical Institute, Karlsruhe Institute of Technology, Germany) for the opportunity to work in his lab. Finally, I would like to thank my family for their support.

'The great tragedy of Science - the slaying of a beautiful hypothesis by an ugly fact'.

Thomas Henry Huxley (Liverpool, England, 1870)[*]

[*] 1870 September 15, Nature, Section: The British Association – Liverpool Meeting, 1870, Address of Thomas Henry Huxley, President, Start Page 400, Quote Page 402, Column 1, Macmillan and Company, London.

Contents

List of the attached publications

Publications related to the topic of the thesis are included in the appendix. Citations of these publications are marked with bold Roman numerals in the text (**Papers I-VIII**). Publications are not arranged chronologically, but in the order in which they appear in the thesis.

Paper I

Štroch M, Vrábl D, Podolinská J, Kalina J, Urban O, Špunda V (2010) Acclimation of Norway spruce photosynthetic apparatus to the combined effect of high irradiance and temperature. *Journal of Plant Physiology* 167: 597-605

Paper II

Štroch M, Karlický V, Ilík P, Ilíková I, Opatíková M, Nosek L, Pospíšil P, Svrčková M, Rác M, Roudnický P, Zdráhal Z, Špunda V, Kouřil R (2022) Spruce versus Arabidopsis: different strategies of photosynthetic acclimation to light intensity change. *Photosynthesis Research* 154: 21-40

Paper III

Štroch M, Lenk S, Navrátil M, Špunda V, Buschmann C (2008) Epidermal UV-shielding and photosystem II adjustment in wild type and *chlorina f2* mutant of barley during exposure to increased PAR and UV radiation. *Environmental and Experimental Botany* 64: 271-278

Paper IV

Klem K, Holub P, **Štroch M**, Nezval J, Špunda V, Tříska J, Jansen MAK, Robson TM, Urban O (2015) Ultraviolet and photosynthetically active radiation can both induce photoprotective capacity allowing barley to overcome high radiation stress. *Plant Physiology and Biochemistry* 93: 74-83

Paper V

Holub P, Nezval J, **Štroch M**, Špunda V, Urban O, Jansen MAK, Klem K (2019) Induction of phenolic compounds by UV and PAR is modulated by leaf ontogeny and barley genotype. *Plant Physiology and Biochemistry* 134: 81-93

Paper VI

Štroch M, Materová Z, Vrábl D, Karlický V, Šigut L, Nezval J, Špunda V (2015) Protective effect of UV-A radiation during acclimation of the photosynthetic apparatus to UV-B treatment. *Plant Physiology and Biochemistry* 96: 90-96

Paper VII

Materová Z, Sobotka R, Zdvihalová B, Oravec M, Nezval J, Karlický V, Vrábl D, **Štroch M**, Špunda V (2017) Monochromatic green light induces an aberrant accumulation of geranylgeranyled chlorophylls in plants. *Plant Physiology and Biochemistry* 116: 48-56

Paper VIII

Karlický V, Kmecová Materová Z, Kurasová I, Nezval J, **Štroch M**, Garab G, Špunda V (2021) Accumulation of geranylgeranylated chlorophylls in the pigment-protein complexes of *Arabidopsis thaliana* acclimated to green light: effects on the organization of light-harvesting complex II and photosystem II functions. *Photosynthesis Research* 149: 233-252

Abbreviations

A	antheraxanthin
A_{max}	the light-saturated CO_2 assimilation rate
A_N	the net CO_2 assimilation rate
ATP	adenosine triphosphate
Cars	carotenoids
Car *x+c*	total carotenoids content
Chl	chlorophyll
clo f2	chlorophyll *b*-less barley mutant *chlorina f2*
D	chlorophyll fluorescence parameter that expresses the efficiency of thermal energy dissipation
D1, D2	the photosystem II reaction center proteins
DEPS	de-epoxidation state of xanthophyll cycle pigments, calculated as (zeaxanthin + antheraxanthin)/(violaxanthin + antheraxanthin + zeaxanthin)
ELIPs	Early Light-Induced Proteins
F_V/F_M	the maximum quantum yield of photosystem II photochemistry
GGR	geranylgeranyl reductase
GL	green light
HL	high light
HPLC	high-performance liquid chromatography
HRS	high radiation stress - application of high intensities of PAR (1000 µmol m^{-2} s^{-1}), UV-A (10 W m^{-2}) and UV-B (2 W m^{-2}) for 4 hours
HT	high temperature
Lhca1-6	light-harvesting proteins of photosystem I
Lhcb1-6	light-harvesting proteins of photosystem II
LHCI, LHCII	light-harvesting complex of photosystem I and photosystem II
LL	low light
NL	normal light (100 µmol m^{-2} s^{-1})
NPQ	non-photochemical quenching (general meaning), non-photochemical quenching of maximal chlorophyll fluorescence (as chlorophyll fluorescence parameter)
P680	the primary electron donor in photosystem II
P700	the primary electron donor in photosystem I
PAR	photosynthetically active radiation
PSI, PSII	photosystem I, photosystem II
Rubisco	ribulose-1,5-bisphosphate carboxylase/oxygenase
SV_0	non-photochemical quenching of minimal chlorophyll fluorescence
UV	ultraviolet
V	violaxanthin
VAZ	the pool of xanthophyll cycle pigments, i.e. the sum of violaxanthin, antheraxanthin, and zeaxanthin
WL	white light
Z	zeaxanthin

Preface

Light is essential for plants, both as a primary source of energy for photosynthesis and as an informational signal that regulates plant metabolism and development. However, sunlight can be an environmental stress when its intensity is in excess of what can be used in photosynthetic reactions. Furthermore, ultraviolet-B radiation (UV-B) as an integral part of the solar spectrum is potentially damaging to plants. Excess light can cause photoinhibition and the accumulation of harmful reactive oxygen species, which damage DNA, proteins, and lipids. On the other hand, exposure to insufficient levels of light can also have detrimental effects because it limits photosynthetic activity, resulting in reduced plant growth and development. Due to a sessile lifestyle of plants, they cannot escape adverse light conditions as readily as single-cellular photosynthetic organisms through phototaxis, and therefore they have evolved a number of protective mechanisms to cope with such conditions. Plants exhibit a remarkable ability to adjust their physiology, biochemistry, morphology, and anatomy in response to long-term changes in the light environment (within days). This phenomenon is called acclimation, which allows plants to use light energy efficiently while avoiding photooxidative cellular damage to their leaves.

The topic of the presented habilitation thesis is acclimation of the assimilatory apparatus of plants to different light conditions. The thesis summarizes selected results of my research activity related to this topic that were published in the years 2008-2022. The relevant publications are included in the Appendix. Citations of these publications are marked with bold Roman numerals in the text (**Papers I-VIII**). Other cited papers, where I am the main author or co-author, are written in bold.

Acclimation of the plant photosynthetic apparatus to different levels of photosynthetically active radiation was the subject of my research already during my doctoral studies, which I finished in 2006. At that time, we observed a specific acclimation response to high light in Norway spruce, different from other higher plants. We presented a hypothesis about the different organization of light-harvesting complexes of photosystem II, which has been recently proved. That is why I returned to this issue after a decade, and thanks to new methodological approaches we could study the specific high-light acclimation response of the spruce photosynthetic apparatus in greater detail (**Paper II**). The findings of this study form the core of the first part of the thesis. As elevated irradiance in the natural environment is usually accompanied by elevated temperature, we have also studied the effect of high temperature during high-light acclimation of spruce. This is the subject of **Paper I**, which is included in the first part of the thesis.

In nature, plants are exposed to a light spectrum that, of course, includes UV light in addition to visible light. Thus, my other research interest is the UV acclimation response, which is covered in the second part of the thesis. This part is based on four papers dealing with the effects of UV radiation in acclimation of the assimilatory apparatus of barley plants (**Papers III-VI**). The emphasis is placed on the significance and interrelation of mechanisms that protect the photosynthetic apparatus under increased UV dose, such as an accumulation of xanthophyll cycle pigments and UV-absorbing phenolic compounds with their photoprotective screening and antioxidative function.

The next logical step in studying the effects of light environment on plants was to extend our research to the influence of spectral quality of visible light. The third part of the thesis deals with acclimation to green light. We have revealed an abnormal accumulation of unknown pigment in barley grown under monochromatic green light (500-590 nm). Therefore, we focused on identifying this pigment and found it to be a chlorophyll *a* derivative, an intermediate of the chlorophyll synthesis pathway with incomplete hydrogenation of its phytyl side chain (**Paper VII**). In a subsequent study with

Arabidopsis acclimated to green light, we did not detect just one chlorophyll *a* derivative as in barley, but various derivatives of both chlorophyll *a* and chlorophyll *b* with different degrees of phytyl chain saturation (**Paper VIII**). In this work, we studied the localization of chlorophyll derivatives in individual pigment-protein complexes and the adverse effects of their accumulation on the assembly and function of photosystem II complexes.

1. Acclimation to high light: specific strategy of the spruce photosynthetic apparatus

1.1. Short-term regulatory mechanisms

Photosynthetically active radiation is essential for plants as a basic driving force for photosynthesis. However, it is also a stress factor when its intensity is in excess of what can be used in photochemical reactions in chloroplast thylakoid membranes. Excess light energy has the potential to cause photooxidative damage to thylakoid membranes, resulting in a sustained decrease in photosynthetic efficiency, a phenomenon termed photoinhibition (Powles 1984). Therefore, the need for photoprotection increases in order to reduce excess energy accumulation under high-light conditions. The most sensitive part of the photosynthetic machinery to photoinhibition is photosystem II (PSII), which possesses one of the strongest oxidizers in nature, the primary electron donor P680. P680 is composed of chlorophyll (Chl) *a* dimer, undergoes oxidation upon photon excitation, and is required to oxidize water. When electrons are not available from water to re-reduce $P680^+$, the long-lived powerful oxidant $P680^+$ can oxidize the nearest pigments and amino acids, eventually leading to degradation of the PSII reaction center protein D1. Another scenario of D1 degradation occurs when electron donation from P680 to oxidized plastoquinone is inhibited by the build-up of reduced plastoquinone. Then, charge recombination leads to the formation of a triplet excited state of P680. In this state, P680 can interact with atmospheric triplet oxygen, forming highly reactive harmful singlet oxygen (Barber 1995).

In order to cope with changes in light intensity, plants have developed a number of regulatory mechanisms that enable them to adjust the composition and function of their photosynthetic apparatus to a particular light environment. There are several short-term mechanisms that occur within minutes. For example, the so-called state transitions balance the distribution of excitation energy between PSI and PSII by relocating a mobile pool of the PSII light-harvesting complex (LHCII), especially under low-light conditions (Fig. 1; for a review, see Allen 2017). Light-induced chloroplast movement is another short-term mechanism. Under low-intensity blue light, the chloroplasts accumulate at the most illuminated cell walls to increase light capture. On the other hand, under high-intensity blue light, chloroplasts can relocate to the cell walls parallel to the light direction to minimize light absorption and protect themselves against potential photodamage (Fig. 2; for a review, see Wada 2016). To avoid absorption of excessive light energy, some plants can also decrease light absorption through movement of leaves that can be regulated by PSII photoinhibition (Huang et al. 2014).

Another important photoprotective process known as non-photochemical quenching (NPQ) is rapidly induced (within seconds to minutes). More precisely, it is the main component of NPQ called energy-dependent quenching (qE), as it is dependent on the “energization” of the thylakoid. By this process, excess light energy is safely dissipated as heat in the LHCII antenna, which can be monitored as a light-induced quenching of Chl fluorescence (Baker 2008, Murchie and Lawson 2013). Thus, NPQ prevents overexcitation of PSII reaction centers and reduces the risk of photodamage to the thylakoid membranes under high-light conditions (for recent reviews, see Bassi and Dall’Osto 2021, Ruban and Wilson 2021). Rapidly induced and reversible NPQ is activated by the pH gradient across the thylakoid membrane, which is generated as a result of electron transport. The signal transduction into a quenching state is obtained by two complementary processes. The first one is the activation of a luminal enzyme violaxanthin de-epoxidase, catalyzing the de-epoxidation of violaxanthin to zeaxanthin via the intermediate antheraxanthin in the so-called xanthophyll cycle (Jahns and Holzwarth 2012). The second process involves the protonation of two glutamate residues on the luminal loops of the

PSII protein PsbS. Low luminal pH-induced PsbS protonation and the binding of zeaxanthin to PSII produce conformational changes in antenna complexes that allow the formation of a quenching state (Fig. 3). Several physical mechanisms underlying the quenching processes have been proposed: energy transfer from Chl *a* to a low-lying excited state of lutein, charge-transfer quenching that involves a charge separation within a Chl-zeaxanthin heterodimer producing a transient zeaxanthin radical cation, Chl-Chl interaction quenching, and quenching due to excitonic interactions between Chls and carotenoids (Bassi and Dall'Osto 2021).

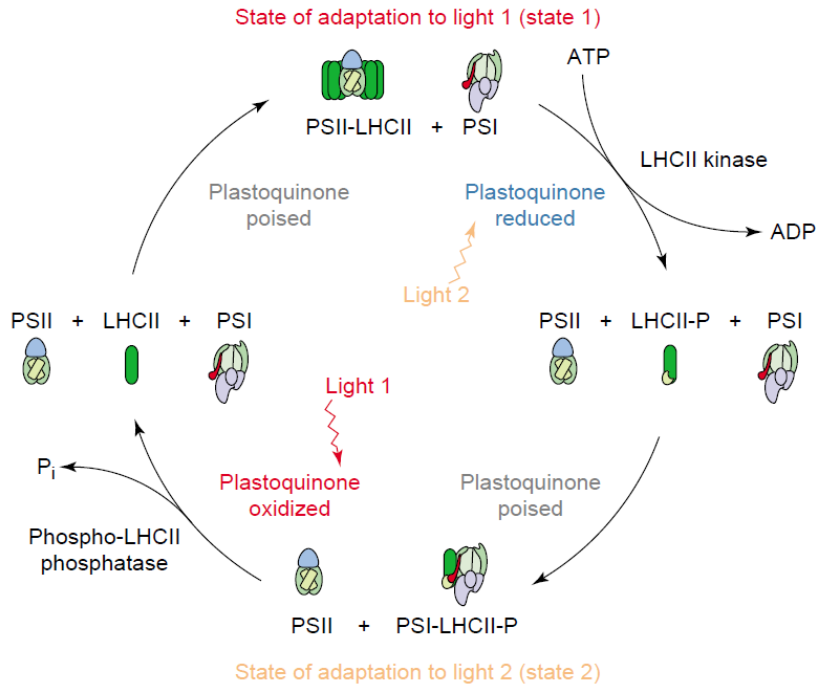

Fig. 1 Overview of state transitions, i.e. transitions between state 1 and state 2. In state 1, the mobile pool of LHCII is bound to PSII. When PSII is favoured for light energy absorption, the plastoquinone pool is over-reduced, LHCII kinase becomes activated and catalyzes phosphorylation of LHCII. The phosphorylated LHCII detaches from PSII, migrates towards PSI and incorporates into its antenna system. This results in state 2, when phosphorylated LHCII transfers excitation energy to PSI. The process is reversed via dephosphorylation of LHCII by a phosphatase and re-binding of LHCII to PSII (Allen and Forsberg 2001).

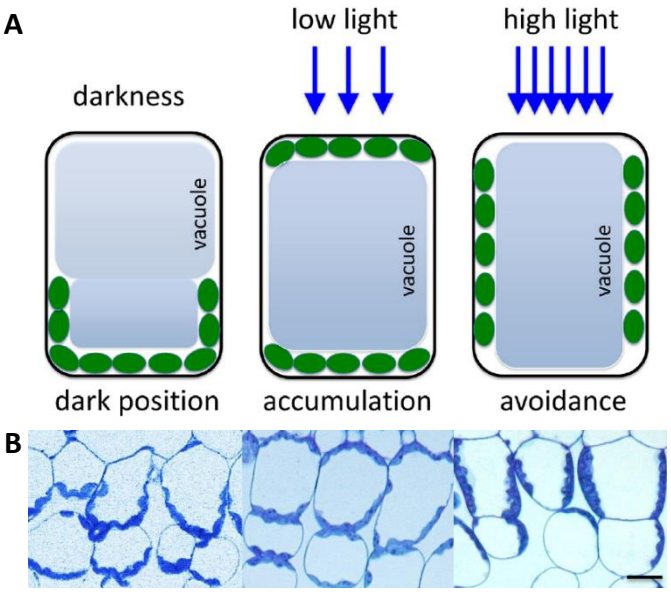

Fig. 2 (A) Schematic drawings of chloroplast positions in darkness, and during the accumulation response under low light and avoidance response under high light in plant palisade cells. In darkness, chloroplasts are present at the bottom of the cell. Under low light, they re-distribute to the upper and lower sides of the cell. Under high light, the chloroplasts migrate to the side walls of the cell. **(B)** The corresponding chloroplast positions captured in photographs of the *Arabidopsis thaliana* leaf sections; bar: 20 µm (for further details of the methodology, see Wada 2013).

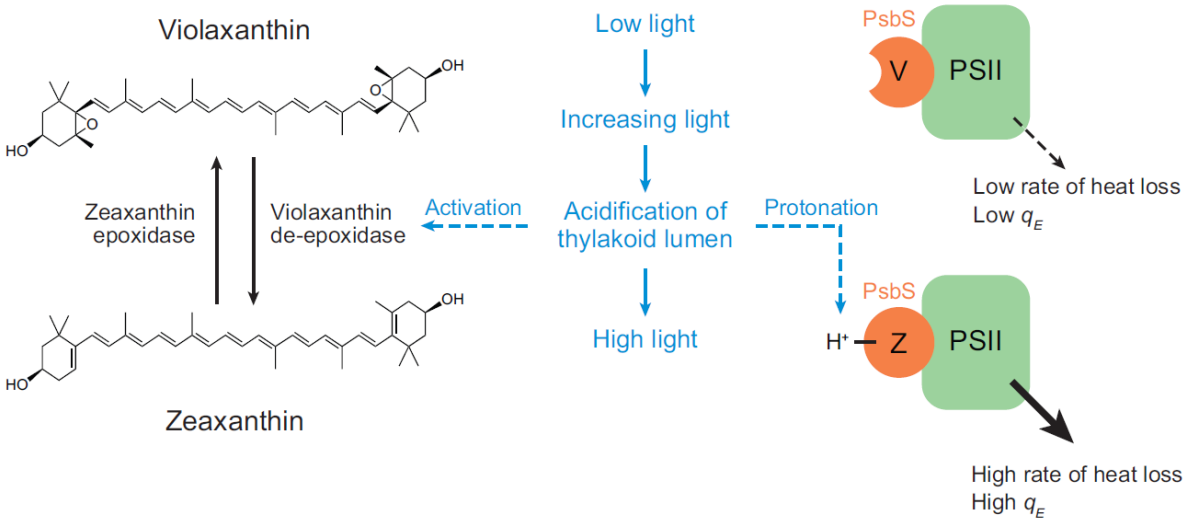

Fig. 3 Mechanism of energy-dependent quenching (qE). At low light, which is limiting for photosynthesis, violaxanthin (V) is associated with the PSII antenna and PSII has a low rate of heat dissipation (low qE). At higher light intensities, acidification of the thylakoid lumen causes protonation of the PSII protein PsbS and conversion of V to zeaxanthin (Z), which binds to the PSII antenna, resulting in a high rate of heat dissipation (high qE). When light intensity decreases, deprotonation of PsbS occurs and Z is converted back to V, which decreases qE (Baker 2008).

As mentioned above, thermal energy dissipation in LHCII can be monitored as a light-induced non-photochemical quenching of Chl fluorescence. If Chl fluorescence is measured under strong light involving a blue spectral component, a chloroplast avoidance reaction occurs. Therefore, the absorption cross-section of chloroplasts decreases during illumination. This effect significantly affects the partitioning of excitation energy within PSII and cannot be neglected, for example, during measurements of action spectra (i.e., spectral dependences) (**Semer et al. 2018**). The fate of absorbed light energy in PSII can be assessed by a widely used measurement of pulse-amplitude modulated (PAM) Chl fluorescence, the intensity of which is lowered by the chloroplast avoidance reaction (Pfündel et al. 2018). This fact motivated us to evaluate which of the commonly used fluorescence parameters are affected by changes in PSII absorption during illumination. We have performed such a theoretical analysis and for parameters that are distorted by changing PSII absorption, we have derived new alternative parameters, independent of the change in PSII absorption during measurement (**Semer et al. 2019**). We experimentally verified the independence of our derived parameters on the change in PSII absorption due to chloroplast relocalization using the *Arabidopsis thaliana* phototropin double mutant *phot1 phot2*, which is defective in chloroplast movement. Commonly used formulae to express the quantum yield of NPQ (Hendrickson et al. 2004, Kramer et al. 2004) neglect the effect of lowering fluorescence intensity caused by the chloroplast avoidance reaction, which can result in overestimation of NPQ. The formula for determining the quantum yield of NPQ, introduced by us, removes the effect of changes in PSII absorption during illumination (without the need for additional measurements) and gives the correct estimate of light-induced thermal energy dissipation in PSII.

1.2. Long-term acclimation response

The responses of plants to longer-term changes in light intensity (within days) involve various morphological, biochemical, and physiological changes at the level of leaf and chloroplast and are collectively called light acclimation (Walters 2005, Eberhard et al. 2008, Schöttler and Tóth 2014). In response to different light intensities, many plant species are able to acclimate through the development of sun or shade leaves. At light levels that are limiting to photosynthesis, light energy must be captured and utilized with the highest possible efficiency. Plants under low light (LL) develop larger and thinner leaves with lower stomatal density and CO_2 assimilation rates. In contrast, plants acclimated to high light (HL) are limited in photosynthetic electron transport rather than light capture and have smaller and thicker leaves with higher photosynthetic rates, both on a leaf area and Chl basis (e.g., Kurasová et al. 2002, Bailey et al. 2004, Lichtenthaler et al. 2007). Shade leaves have large chloroplasts with a greater proportion of granal stacked membranes, while sun leaves have small chloroplasts with thin grana stacks (Lichtenthaler 2015; Fig. 4). To support elevated photosynthetic capacity, chloroplasts of sun leaves contain greater amounts of components of the electron transport chain, ATP synthase, and enzymes of the Calvin cycle, particularly the CO_2-fixing enzyme Rubisco (for a review, see Schöttler and Tóth 2014).

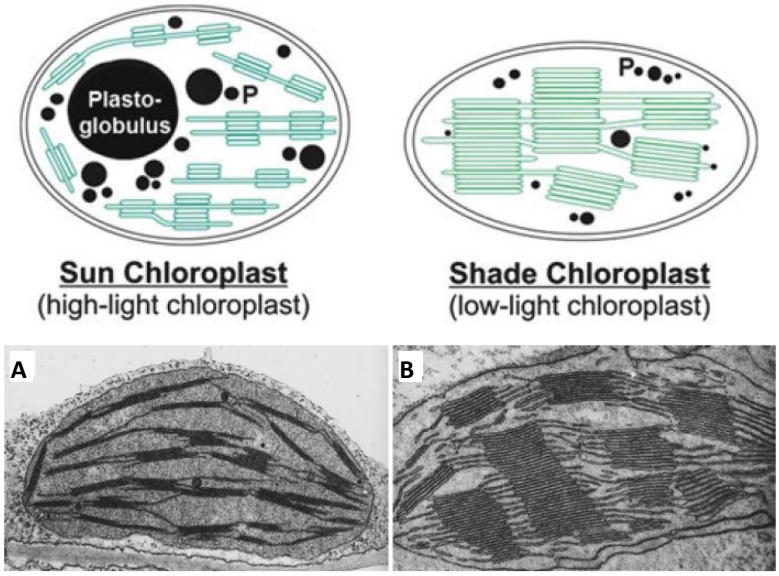

Fig. 4 Scheme showing the differences in the ultrastructure of chloroplasts of sun and shade leaves. Sun-type chloroplasts exhibit a lower degree of stacking of thylakoids (lower amounts of appressed membranes), lower and narrower grana stacks, and rather large plastoglobuli (P) that function primarily as a reservoir for excess lipids, such as α-tocopherol and plastoquinone-9 (Lichtenthaler 2015). Examples showing small grana stacks in chloroplast of a sun leaf of tobacco **(A)** and substantial thylakoid stacking in chloroplast of a shade leaf of snapdragon **(B)** (taken from Schulze et al. 2019, references therein).

Specific modifications of the photosynthetic apparatus at the protein level lead to structural and functional changes of PSI and PSII (Anderson 1986). The PSII-LHCII supercomplex of higher plants is composed of a dimeric core complex and a variable number of light-harvesting proteins (Lhcb1-6). A major part of LHCII is formed by LHCII trimers, which consist of Lhcb1-3 proteins and are specifically associated with the core complex via monomeric antenna proteins Lhcb4-6 (Su et al. 2017). Unlike PSII, the plant PSI complex is monomeric and consists of the core complex, which binds four monomeric

Lhca1-4 proteins forming LHCI (Bai et al. 2021). Plants respond to LL exposure by two main adjustments of their photosynthetic apparatus. The first is an enlargement of LHCII via up-regulation of Lhcb1 and Lhcb2 proteins and the second is a decrease in the abundance of PSII, which is reflected in the increase in the PSI/PSII ratio (Bailey et al. 2001, Ballottari et al. 2007, Albanese et al. 2016). These modifications lead to an enlarged absorption cross-section of PSII complexes, thereby compensating for the potentially detrimental effects of LL conditions on the photosynthetic performance of plants.

Under HL conditions, on the other hand, plants have to cope with a surplus of absorbed light energy, and therefore its amount is down-regulated by a reduction of the LHCII antenna size. This is achieved by selective and coordinated down-regulation of the monomeric Lhcb6 protein and the Lhcb1-3 proteins that form LHCII trimers (Ballottari et al. 2007, Kouřil et al. 2013, Albanese et al. 2016). At the same time, Lhcb4.3 (one of the Lhcb4 isoforms, also referred to as Lhcb8) is strongly up-regulated by HL (Floris et al. 2013, Albanese et al. 2016, 2018). This isoform was found to weaken the binding of the M trimer (moderately bound LHCII trimer) to the PSII core (Albanese et al. 2019). In contrast to LHCII, LHCI does not change significantly in HL. PSI modulates light absorption by changing the PSI/PSII ratio and the amount of LHCII proteins associated with PSI (Ballottari et al. 2007, Wientjes et al. 2013).

1.3. Basic characteristics of the spruce acclimation strategy - earlier studies

Our earlier studies were aimed at characterization of the acclimation response of the photosynthetic apparatus to HL under controlled environment conditions (i.e., using growth chambers) in Norway spruce (*Picea abies* [L.] Karst.) and barley (*Hordeum vulgare* L.), as representatives of evergreen conifers and rapidly growing annuals, respectively (**Kurasová et al.** 2002, **2003a**, **2003b**, **Štroch 2006**, **Štroch et al. 2008**). Very high intensities of light were used in these acclimation studies, namely 1000 and 1200 µmol m^{-2} s^{-1}. For measurements we used the primary barley leaves that were grown from seeds under HL for 8-9 days and one year-old needles of 5 year-old spruce saplings that were acclimated to HL for 25 or 10 days.

We have revealed a different strategy of acclimation to HL in these two plant species. Barley responded to HL particularly by reducing LHCII size and increasing the photosynthetic CO_2 assimilation rate. The reduction of the LHCII antenna was estimated from the increase in the Chl *a*/*b* ratio (Fig. 5A), since trimeric LHCII complexes undergoing acclimative degradation are the most enriched in Chl *b* (e.g., Bailey et al. 2004, Ballottari et al. 2007, Kouřil et al. 2013, Albanese et al. 2016). Photosynthetic activity determined at the corresponding acclimation irradiance showed a three-fold increase compared to barley grown under LL (100 µmol m^{-2} s^{-1}) (Fig. 5B). Photosynthetic capacity (CO_2 assimilation rate at saturating irradiance and CO_2 concentration) also increased significantly in barley upon acclimation to HL (Fig. 5C; **Kurasová et al. 2003b**). One of the typical acclimation responses to HL is increased capacity for NPQ (Demmig-Adams 1998, Bailey et al. 2004), which seems to be of minor importance in photoprotection during acclimation of barley to HL.

Unlike barley, the typical manifestation of acclimation to HL, i.e., diminution of LHCII complexes and increased photosynthetic capacity, was not observed in spruce (Fig. 5A, C). The key protective process in acclimation of the spruce photosynthetic apparatus to HL is the enhanced efficiency of de-epoxidation of xanthophyll cycle pigments, which is associated with a pronounced NPQ. The level of de-epoxidation state (DEPS) can be calculated as (Z+A)/(V+A+Z), where V, A, and Z are violaxanthin and the de-epoxidized xanthophylls antheraxanthin and zeaxanthin, respectively. DEPS was found to be

always higher for spruce needles compared to barley leaves of both LL- and HL-acclimated plants. DEPS under acclimation irradiance and also maximal capability to de-epoxidize V to A+Z were significantly higher in spruce (Fig. 5D, E). In addition, both LL and HL spruce showed a pronounced retention of Z+A in darkness, while in LL barley almost all A and Z were epoxidized back to V after one hour in darkness (Fig. 5F; **Kurasová et al. 2003b**). Extremely slowed-down epoxidation in HL spruce was confirmed by **Štroch et al. (2008)**, when we observed DEPS above 55 % after 7 h in darkness.

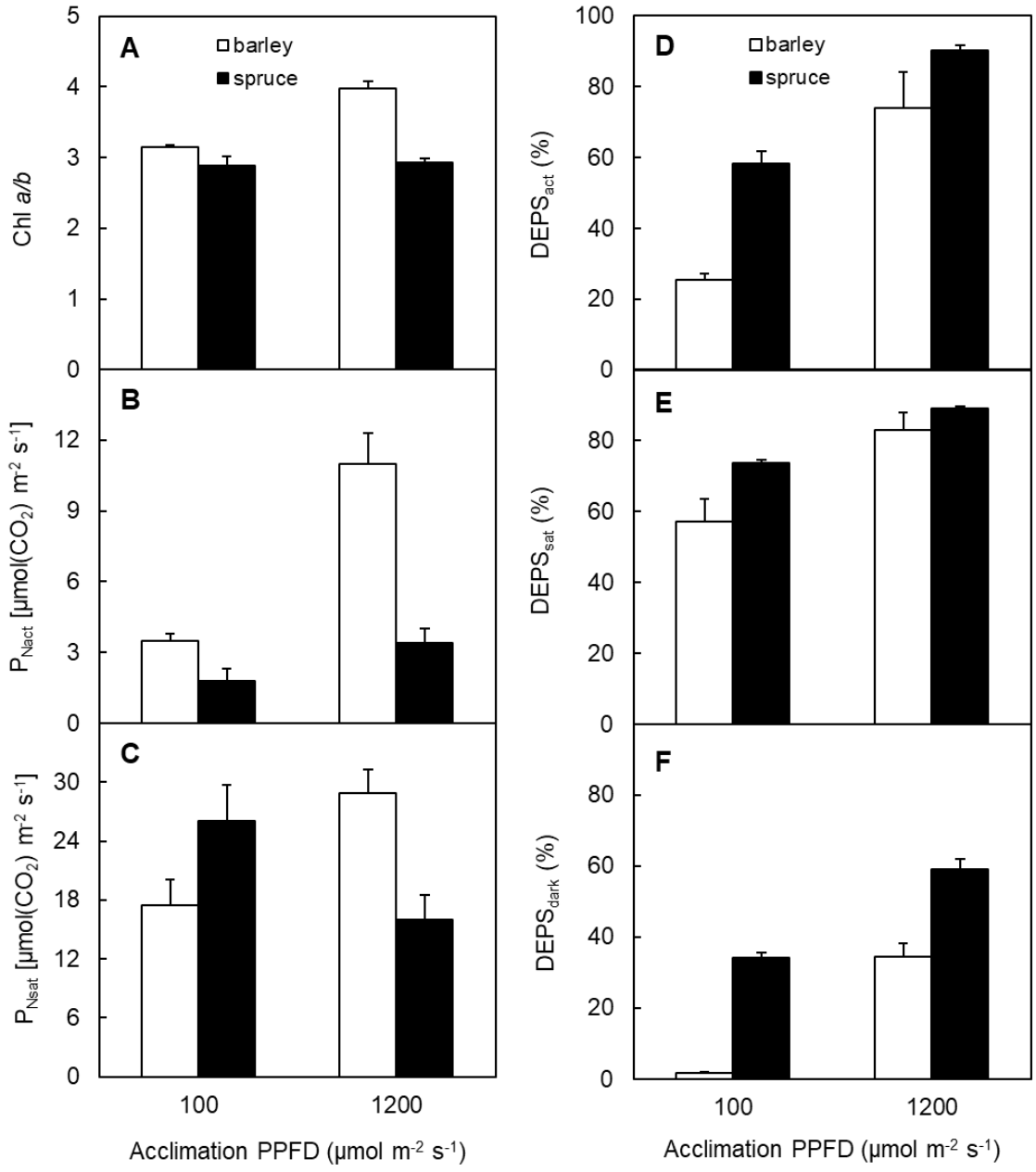

Fig. 5 The Chl *a/b* ratio **(A)**, the steady-state rate of CO_2 assimilation at corresponding acclimation conditions (P_{Nact}) **(B)**, the light- and CO_2-saturated CO_2 assimilation rate (P_{Nsat}) **(C)**, the de-epoxidation state of xanthophyll cycle pigments after 10 min-exposure to light intensity corresponding to the acclimation conditions ($DEPS_{act}$) **(D)**, or to high light intensity (approximately 2000 µmol m^{-2} s^{-1}; $DEPS_{sat}$) **(E)**, and after one hour in darkness ($DEPS_{dark}$) **(F)** for barley and spruce acclimated to low and high PPFD (photosynthetic photon flux density) (100 and 1200 µmol m^{-2} s^{-1}). DEPS was calculated as (Z+A)/(V+A+Z), where V, A, and Z are violaxanthin, antheraxanthin, and zeaxanthin, respectively. *n* = 6-10 ± S.D. Based on data from **Kurasová et al. 2003b**.

We revealed a strong negative linear correlation between the amount of sustained de-epoxidized xanthophylls and the maximum quantum yield of PSII photochemistry (F_V/F_M) in spruce (**Štroch et al. 2008**). HL spruce was characterized by a pronounced sustained decrease in F_V/F_M to values in the range of 0.55 – 0.65 (**Kurasová et al. 2003b**, **Štroch et al. 2008**). The great ability to induce NPQ in both LL and HL spruce has been documented by a pronounced non-photochemical quenching of minimal Chl fluorescence (SV_0; Gilmore and Yamamoto 1991) and also by its extremely rapid induction (Fig. 6; **Kurasová et al. 2003b**, **Štroch et al. 2008**). During HL acclimation, the spruce photosynthetic apparatus was capable to considerably speed up NPQ induction. After 10 days under HL 72 % of maximum SV_0 was induced during the first 20 s of illumination (**Štroch et al. 2008**). This rapid induction of NPQ seems to be enabled due to a pronouncedly slowed-down epoxidation reaction resulting in the high amount of Z persistent in darkness, which can lead to its rapid engagement in NPQ after onset of illumination.

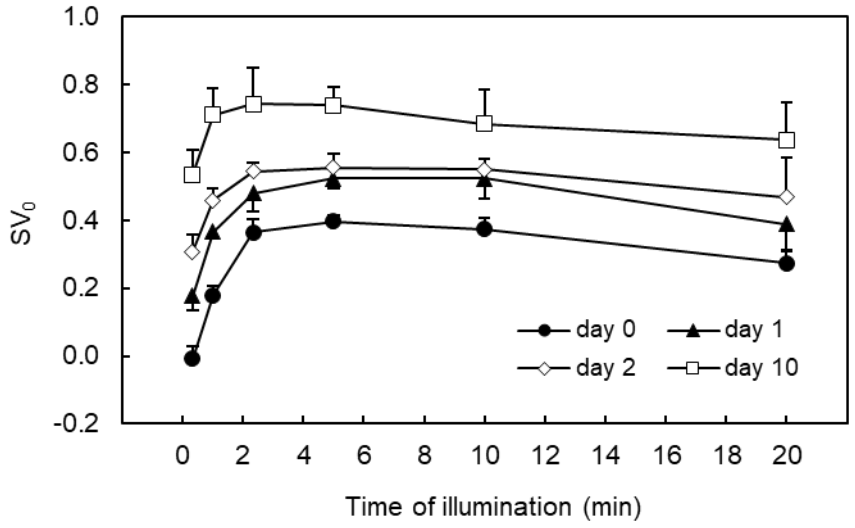

Fig. 6 Induction of non-photochemical quenching of minimal fluorescence (SV_0) upon exposure of dark-adapted spruce needles to light intensity of 1000 µmol m^{-2} s^{-1}. Measurements were made on spruce plants acclimated to low light (100 µmol m^{-2} s^{-1}; day 0) and during acclimation to high light (1000 µmol m^{-2} s^{-1}; after 1, 2, and 10 days of acclimation). *n* = 5-6 ± S.D. (**Štroch et al. 2008**)

It is known that, in contrast to rapidly growing annuals, slowly growing long-lived evergreens possess low intrinsic capacities for photosynthesis and a high need for protection of the photosynthetic apparatus against photodamage. The importance of NPQ in photoprotection of evergreens has been demonstrated in many studies (Demmig-Adams and Adams 2006), which agrees with the acclimation strategy of spruce described above. However, the surprising finding is the absence of LHCII antenna size reduction in spruce during HL acclimation, indicated by the stable Chl *a/b* ratio (Fig. 5A, **Kurasová et al. 2003b**, **Štroch et al. 2008**). The ratio of total chlorophylls to total carotenoids content (Chl *a+b*/Car *x+c*) decreased less pronouncedly after HL acclimation in spruce than in barley. HL-induced increase in VAZ pool was also much lower in spruce. We observed a 1.6-fold and three-fold increase in VAZ expressed on Chl *a+b* basis in HL spruce and HL barley, respectively, as compared to LL counterparts (**Kurasová et al. 2003b**). These results indicate less flexibility in photosynthetic pigment composition at HL acclimation of spruce. As the LHCII size does not change in spruce during HL acclimation, the possible explanation for the increase in VAZ/Chl lies in the *de novo* synthesis of VAZ.

We suppose that the major fraction of newly synthesized xanthophyll cycle pigments is localized in the lipid bilayer rather than bound to pigment-protein complexes.

The acclimative LHCII degradation accompanied by an increase in Chl *a/b* occurs within 3 days after transfer of LL-acclimated plants to elevated irradiance (Andersson and Aro 1997, Yang et al. 1998). Therefore, we can rule out that 10 or 25 days under HL in our experiments could be an insufficient time for the induction of LHCII proteolysis. However, it should be noted that the absence of LHCII size modulation applies to spruce that is suddenly exposed to excess light for several days. Under field conditions, there are differences in Chl *a/b* within the vertical profile of the spruce trees. Sun-exposed needles exhibit significantly higher Chl *a/b* than shaded needles (e.g., Špunda et al. 1998, Urban et al. 2012). This implies that spruce has the potential to adjust LHCII size during long-term growth, but another acclimation strategy occurs upon acute HL stress in fully developed needles.

1.4. Acclimation of the spruce photosynthetic apparatus to an elevated, but non-excessive light level

In subsequent laboratory experiments, we wanted to get closer to the natural conditions. Therefore, instead of a constant (thus unnatural) light level, we used diurnal courses of both light intensity and air temperature (**Paper I**). The four-year-old spruce seedlings were gradually acclimated to three consecutive regimes with different light intensity and temperature. First, plants were acclimated to LL conditions with moderate temperature, simulating cloudy days (LL; maximum light intensity was 300 µmol m^{-2} s^{-1} at "midday", temperature in the range of 15-25 °C). Then the light intensity was increased, while the temperature remained the same, to simulate sunny days with moderate temperature (HL; maximum light intensity was 1000 µmol m^{-2} s^{-1} at "midday"). Finally, the temperature was increased with the unchanged HL level to simulate hot sunny days (HL-HT; temperature was in the range of 20-35 °C throughout the day). Each acclimation regime lasted 13 days. In addition to HL-induced acclimation response, this experimental design allowed us to examine also the effect of elevated temperature itself under HL conditions.

We observed a strong inhibition of the net CO_2 assimilation rate (A_N) during most of the day after HL acclimation, which was even more pronounced under elevated temperature in HL-HT treatment (Fig. 7A). This is in agreement with the inability of spruce to adjust its photosynthetic capacity to elevated growth temperature (Way and Sage 2008). The depression of photosynthesis is also related to a reduced strength of the sink for assimilates, as our experiments were performed during late autumn (**Paper I**). We identified insufficient stomatal opening as the main reason for reduced A_N, based on a good correlation between stomatal conductance (G_S) and A_N (Fig. 7B). Thus, both HL and mainly HL-HT treatments should lead to considerably enhanced demands for photoprotection.

Despite the pronounced inhibition of A_N after acclimation to both HL and HL-HT conditions, the maximum quantum yield of PSII photochemistry (F_V/F_M) remained at optimal level, pointing to the absence of PSII photoinhibition (Fig. 8A). Elevated temperature did not represent an additional stress factor to HL, with respect to the functional state of PSII. From this point of view, the light intensity in the HL and HL-HT regimes can be considered non-excessive. F_V/F_M only slightly decreased after the first day under HL, but at the end of HL acclimation (after 13 days) it fully recovered.

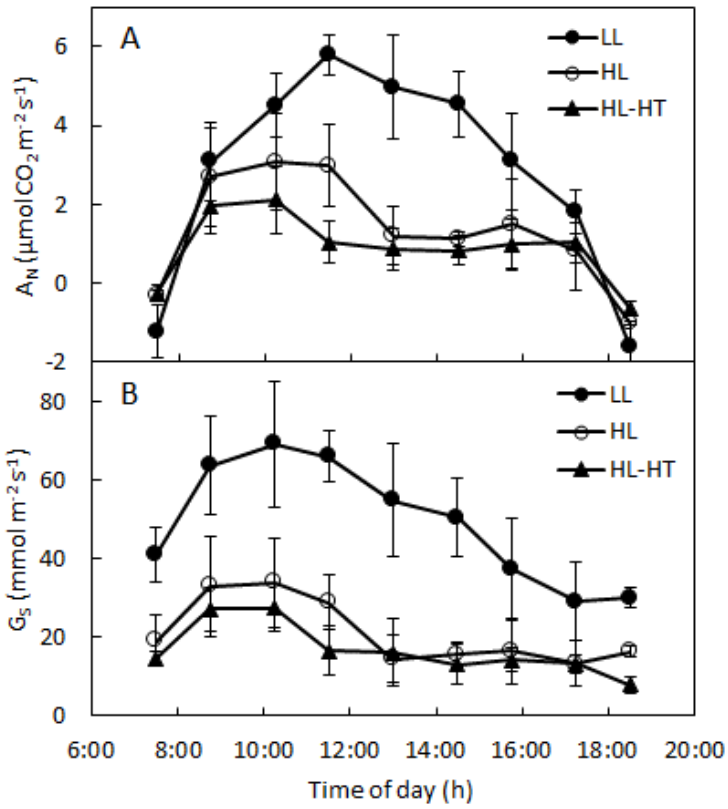

Fig. 7 Diurnal courses of **(A)** the net CO_2 assimilation rate (A_N) and **(B)** stomatal conductance (G_S) in spruce acclimated to low light (LL; maximum of 300 µmol m^{-2} s^{-1} and 25 °C at "midday"), high light (HL; maximum of 1000 µmol m^{-2} s^{-1} and 25 °C at "midday") and high light with elevated temperatures (HL-HT; maximum of 1000 µmol m^{-2} s^{-1} and 35 °C at "midday"). "Midday" corresponds to 13:00. *n* = 6 ± S.D. (**Paper I**)

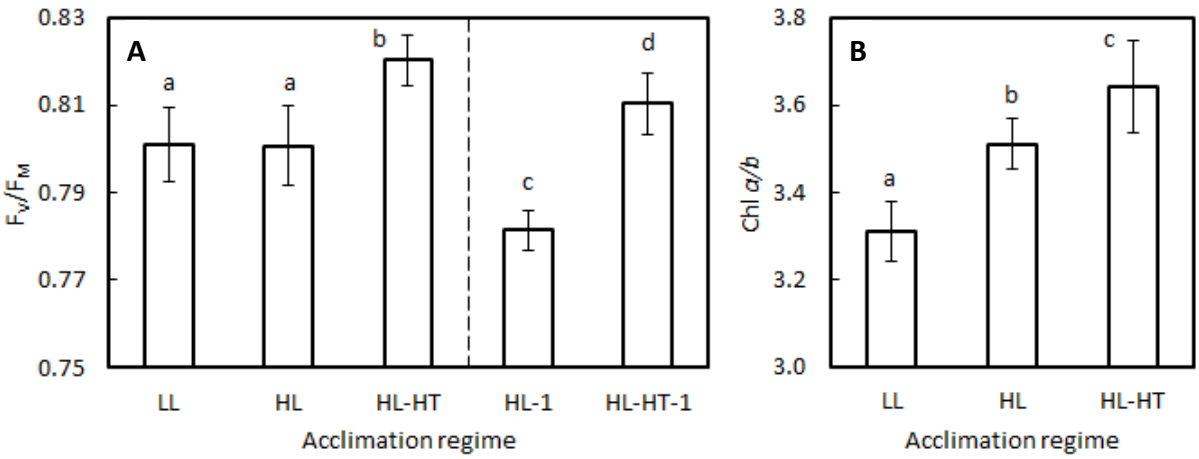

Fig. 8 (A) The maximum quantum yield of PSII photochemistry (F_V/F_M) and **(B)** the Chl *a*/*b* ratio in spruce acclimated to low light (LL; maximum of 300 µmol m^{-2} s^{-1} and 25 °C at "midday"), high light (HL; maximum of 1000 µmol m^{-2} s^{-1} and 25 °C at "midday") and high light with elevated temperatures (HL-HT; maximum of 1000 µmol m^{-2} s^{-1} and 35 °C at "midday"). F_V/F_M was determined after 12 h of dark-adaptation at the end of LL, HL, and HL-HT treatments (i.e., after 13 days) and after the first day under HL (HL-1) and HL-HT conditions (HL-HT-1). Data followed by the same letter indicate non-significant differences ($p > 0.05$; Student's *t*-test). *n* = 6-10 ± S.D. (**Paper I**)

In contrast to our earlier studies of spruce acclimation to HL (Chapter 1.3.), we observed a HL-induced increase in Chl *a/b*, indicating a typical acclimative reduction of the LHCII antenna size (Fig. 8B). In this study, the light dose per day was only 34 % of that used in earlier experiments, when the spruce seedlings were exposed to a constant light intensity of 1200 µmol m^{-2} s^{-1} for 16 h per day (**Kurasová et al. 2003b**). Apparently, the light dose or distribution of the light intensity during a day affects the resulting response of spruce during HL acclimation. The degree of light stress in spruce could be a determining factor for the triggering of LHCII proteolysis, in that sense that under an acute excessive light level above some threshold, a strategy of photoprotection other than LHCII reduction is activated. The reduction of F_V/F_M can be considered as a marker of excessive light level. On the one hand, LHCII reduction (increase in Chl *a/b*) and no PSII photoinhibition (unchanged F_V/F_M) were found in spruce acclimated to elevated irradiance with simulated diurnal course in growth chambers (**Paper I**) as well as in sun-exposed needles compared to shaded needles of Norway spruce trees (Kalina et al. 2001, Grebe et al. 2020). On the other hand, the absence of LHCII reduction (stable Chl *a/b*) together with a pronounced PSII photoinhibition (F_V/F_M depression) was found in spruce acclimated to excess irradiance (**Kurasová et al. 2003b**, **Štroch et al. 2008**).

Because permanent PSII photoinhibition was not observed in HL- and HL-HT-acclimated spruce, efficient regulation of the utilization of HL in photochemical and/or non-photochemical de-excitation processes had to be ensured. The efficiency of thermal energy dissipation, evaluated by the fluorescence parameter D (Demmig-Adams et al. 1996), showed an asymmetric daily course for LL-acclimated spruce with significantly higher values during the afternoon compared to the corresponding morning values (Fig. 9A). As expected, the D values increased after HL acclimation. Taking into account the greatest suppression of A_N after acclimation to HL-HT (Fig. 7A), we also expected a high level of photoprotective thermal dissipation in this treatment. However, HL-HT acclimation surprisingly resulted in a decrease of D throughout the day. For HL-HT-acclimated plants, we observed a symmetric daily course of D, with afternoon values close to those of LL-acclimated plants, although the light intensity was more than three times higher under HL-HT conditions.

The diurnal courses of the de-epoxidation state of xanthophyll cycle pigments (DEPS) matched the response of D (Fig. 9B). Thus, xanthophyll cycle-dependent thermal energy dissipation was a dominant component of the D parameter. DEPS of HL-acclimated spruce reached a high maximum value of 86 %, which confirms very efficient violaxanthin de-epoxidation in the spruce photosynthetic apparatus compared to other plant species (**Kurasová et al. 2003b**). DEPS determined in darkness after HL-HT acclimation showed the lowest value. This may be the reason for the highest F_V/F_M value (Fig. 8A), as the retention of de-epoxidized xanthophylls in darkness is usually associated with F_V/F_M reduction (**Štroch et al. 2008**).

The decreased requirement for thermal energy dissipation under HL-HT conditions indicates a positive effect of elevated acclimation temperature on the capacity of PSII photochemical de-excitation. Indeed, after HL-HT acclimation the PSII electron transport rate (ETR; Genty et al. 1989) increased in comparison with the preceding LL and HL acclimation regimes (Fig. 9C). This implies an enhanced contribution of non-assimilatory electron transport pathways to the total electron flux, which seems to be the dominating protective process leading to the optimal function of PSII under HL-HT conditions. It is probable that photorespiration fulfils this role in PSII photoprotection at elevated temperatures of HL-HT treatment (Franco et al. 2007).

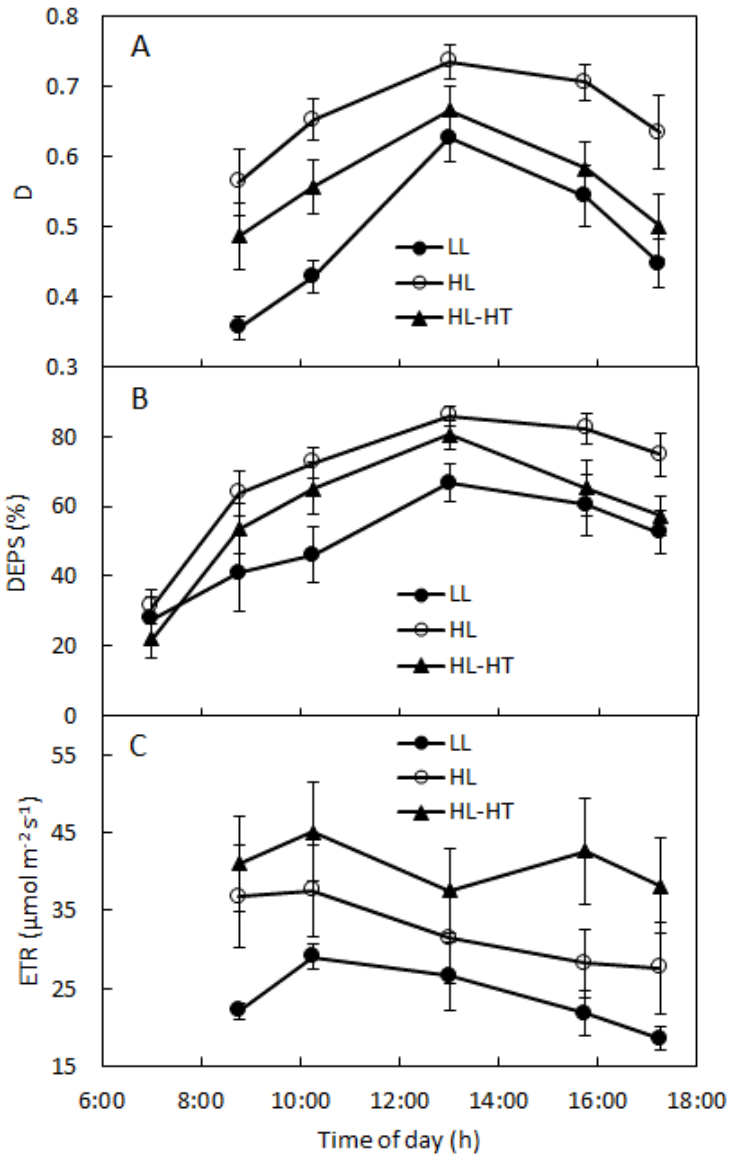

Fig. 9 Diurnal courses of **(A)** the efficiency of thermal energy dissipation (D), **(B)** the de-epoxidation state of xanthophyll cycle pigments (DEPS), and **(C)** PSII electron transport rate (ETR) in spruce acclimated to low light (LL; maximum of 300 µmol m^{-2} s^{-1} and 25 °C at "midday"), high light (HL; maximum of 1000 µmol m^{-2} s^{-1} and 25 °C at "midday"), and high light with elevated temperatures (HL-HT; maximum of 1000 µmol m^{-2} s^{-1} and 35 °C at "midday"). "Midday" corresponds to 13:00. DEPS was calculated as (Z+A)/(V+A+Z), where V, A, and Z are violaxanthin, antheraxanthin, and zeaxanthin, respectively. DEPS values at 7:00 correspond to the samples collected after 12 h of the dark period. *n* = 6-10 ± S.D. (**Paper I**)

1.5. Different composition of PSII and PSI light-harvesting proteins in Norway spruce

One of the typical acclimation responses to HL is the enhanced capacity of violaxanthin (V) de-epoxidation (Ballottari et al. 2007), which has usually been attributed to an increased accessibility of V to V de-epoxidase caused by a reduction of the LHCII antenna size (Brugnoli et al. 1998). However, we observed a very high V convertibility in HL-acclimated Norway spruce (around 90 %) despite the unchanged LHCII size (Fig. 5A, E; **Kurasová et al. 2003b**, **Štroch et al. 2008**). At the time of these earlier findings we hypothesized that the spruce photosynthetic apparatus possesses a specific spatial organization of LHCII pigment-protein complexes that allows easy release of bounded V into the lipid

phase and better accessibility of V to V de-epoxidase. Thus, we assumed that the high extent of xanthophyll cycle-dependent NPQ in HL spruce could be related to the proposed different PSII organization (**Kurasová et al. 2003b**).

Our hypothesis of the different organization of LHCII complexes in the spruce photosynthetic apparatus has been proved in the breakthrough work of Kouřil et al. (2016), who revealed that the structure and composition of PSII supercomplexes are not conserved among higher plants. They have found that the Lhcb3 and Lhcb6 proteins are missing in the gymnosperm genera *Picea* and *Pinus* (family Pinaceae) and *Gnetum* (order Gnetales). As a consequence, the M trimers (LHCII trimers moderately bound to the PSII core) associate with the PSII core complex in a different orientation in Norway spruce, which results in a specific form of PSII supercomplex that is unique among land plants (Fig. 10). This could be linked to the observed reduced PSII macro-organization in the thylakoid membrane and more significant 77 K Chl fluorescence emission of PSII supercomplexes at 695 nm than at 685 nm, conversely than in model plants such as *Arabidopsis thaliana* (Karlický et al. 2016). Recently, Kouřil et al. (2020) have reported very large unique PSII supercomplexes containing up to eight LHCII trimers in spruce, which exceeds the LHCII antenna size of PSII supercomplex in the green alga *Chlamydomonas reinhardtii*, currently considered to be the largest known PSII supercomplex (Shen et al. 2019, Sheng et al. 2019).

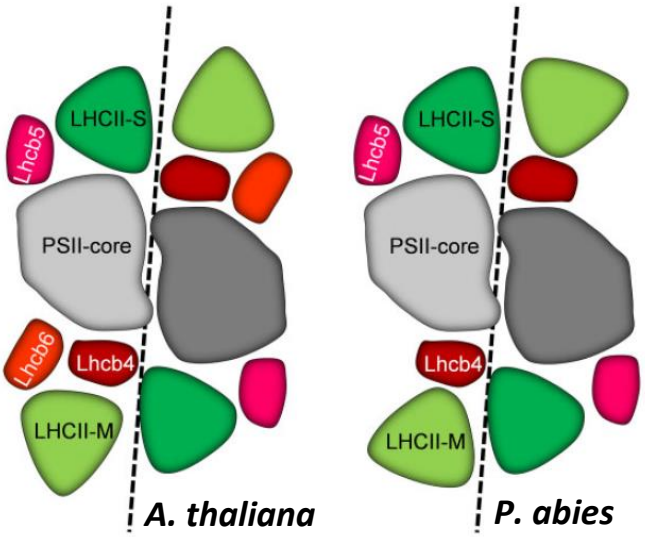

Fig. 10 Scheme of the organization of PSII supercomplexes in *Arabidopsis thaliana* and Norway spruce (*Picea abies*) based on current structural data available. *P. abies* lacks the LHCII minor antenna protein Lhcb6, and the binding of LHCII-M trimer to PSII core is in a different orientation than in *A. thaliana* (Arshad et al. 2022).

In addition to the absence of the Lhcb3 and Lhcb6 proteins, the PSII and PSI complexes of Norway spruce (and other Pinaceae members) have other unique characteristics. Grebe et al. (2019) revealed that genes coding for the Lhcb4.1 and Lhcb4.2 proteins have been lost from the genome, while the gene for the Lhcb4.3 protein has been retained. Regarding PSI subunits, Norway spruce lacks the Lhca6 protein (like other gymnosperms) but additionally the Lhca5 protein (Grebe et al. 2019). Thus, the composition of light-harvesting proteins of both PSII and PSI in the Pinaceae family (and order Gnetales) is distinct from not only angiosperms but also other gymnosperms. The absence of Lhca5 and Lhca6 proteins is consistent with the loss of the NDH-1 genes and the absence of the PSI-NDH supercomplexes (Nystedt et al. 2013, Grebe et al. 2019), since Lhca5 and Lhca6 are needed for the

formation of the PSI-NDH supercomplex (Peng et al. 2009, Kouřil et al. 2014). Consequently, NDH-dependent cyclic electron flow around PSI is lacking in Norway spruce.

Interestingly, the modified protein composition of the Norway spruce PSII complex has a striking similarity to alterations in the amount of LHCII proteins occuring during HL acclimation of higher plants, i.e., reduction of the Lhcb3 and Lhcb6 proteins and increase of the Lhcb4.3 isoform (Kouřil et al. 2013, Albanese et al. 2016). According to Kouřil et al. (2016), the loss of the Lhcb3 and Lhcb6 proteins may be a result of the evolutionary pressure imposed on spruce by exposure to HL conditions. The gymnosperm families evolved after the greatest extinction event in Earth history, which probably opened the canopy for a very long time period, exposing the surviving plants to HL (see Kouřil et al. 2016 and references therein). It is possible that this evolutionary modification of the composition of LHCII proteins in Pinaceae and Gnetales could be one of the factors that contribute to the reduced plasticity of LHCII (stable Chl *a/b* ratio) in spruce grown under excess light observed in our previous studies (**Kurasová et al. 2003**, **Štroch et al. 2008**).

1.6. Low plasticity of electron transport protein complexes in light acclimation of spruce and its functional consequences

In light of the new findings on PSII and PSI structure in spruce, we decided to study its specific HL acclimation response in greater detail. We performed the acclimation study that included other modern experimental methods to obtain more detailed information compared to our earlier studies, such as circular dichroism spectroscopy to analyze the PSII-LHCII macro-organization or monitoring the redox state of the PSI primary electron donor (P700) to assess the functional state of PSI (**Paper II**). We used mass spectrometry for analysis of the composition of the protein subunits of PSII and PSI to test our hypothesis of a fixed LHCII antenna size during acclimation of spruce to excess light. This hypothesis was based on a stable Chl *a/b* ratio, which, however, can also be affected by changes in the PSII/PSI stoichiometry in addition to changes in the LHCII size. As Chl *a/b* is higher in PSI than in PSII (Caffarri et al. 2014), an increase in the PSII/PSI ratio typically observed at HL acclimation tends to decrease Chl *a/b*, contrary to the reduction of LHCII that results in a higher Chl *a/b* value. The increased PSII/PSI ratio could mask the LHCII reduction in the evaluation of the Chl *a/b* ratio.

Thus, we focused on light acclimation-related changes in the stoichiometry of protein complexes involved in primary photosynthetic reactions and on the consequences of these changes for the regulation of electron transport in thylakoid membranes. The acclimation response of spruce (slowly growing long-lived evergreen species) was compared with a model for rapidly growing short-lived annuals, *Arabidopsis thaliana*. This approach allowed us to identify different strategies in the acclimation response in these two species. As our intention was to use plants cultivated under well-defined environmental conditions, spruce and Arabidopsis seedlings were grown from seeds in growth chambers. First, the plants were pre-grown at a light intensity of 100 µmol m^{-2} s^{-1} (Arabidopsis for 32 days and spruce for 11 weeks). The seedlings were then exposed to three light intensities for 10-14 days: low light (LL; 20 µmol m^{-2} s^{-1}), control normal light (NL; 100 µmol m^{-2} s^{-1}) and high light (HL; 800 µmol m^{-2} s^{-1}). After the light acclimation phase, fully developed Arabidopsis leaves and primary needles of spruce were used for all measurements (**Paper II**). The intensity of HL was lower than in our previous studies using 1000 and 1200 µmol m^{-2} s^{-1} (see Chapter 1.3.), but strong enough to induce a stress response in spruce, as will be documented below by a significant drop in the maximum quantum yield

of PSII photochemistry (F_V/F_M), very high PSII excitation pressure or up-regulation of light stress-related proteins.

1.6.1. Structural adjustments of photosystem complexes

Our results confirmed that Arabidopsis, a representative of angiosperms, follows the well-known acclimation strategy of higher plants to cope with changes in light intensity at the level of the thylakoid membrane (e.g., Anderson 1986, Ballottari et al. 2007, Kouřil et al. 2013). With increasing acclimation light intensity, there was an increase in the PSII/PSI ratio, the relative abundance of cytochrome *f*, as well as an increase in the Chl *a/b* ratio corresponding to the reduction of the PSII peripheral light-harvesting system (higher PSII/LHCII ratio) (Fig. 11). In contrast, spruce seedlings showed a very low plasticity of the electron transport protein complexes. We found virtually no effect of light acclimation on the Chl *a/b*, PSII/PSI, and cytochrome *f*/PSI ratios. However, after HL acclimation we observed a 30% decrease in the PSII/LHCII ratio, an opposite trend to what was found in Arabidopsis (Fig. 11B). Because of the unchanged Chl *a/b* (2.8), this decrease in PSII/LHCII cannot be explained by the synthesis of trimeric LHCII. LHCII trimers that have a value of Chl *a/b* around 1.3 (Caffarri et al. 2014) would lower Chl *a/b*. Thus, the observed phenomenon can only be explained by a proportional degradation of both PSII and PSI-LHCI, accompanied by the storage of released Chls. This explanation would justify the lower PSII/LHCII ratio and at the same time the unchanged PSII/PSI and Chl *a/b* ratios in HL spruce. Interestingly, the LHCII antenna size in spruce was found to be large and comparable to that of LL Arabidopsis (Fig. 11B), suggesting that under all acclimation light intensities, the LHCII antenna of spruce remained adjusted to light-limiting conditions. However, the PSII/PSI ratio in spruce was high and similar to that of HL Arabidopsis (Fig. 11C). This implies a considerable imbalance between PSII and PSI functions in spruce.

To test the possibility of the retention of released Chls, we analyzed the level of stress proteins called ELIPs (Early Light-Induced Proteins), which are known to be associated with PSII core degradation and repair and have been proposed to play an important photoprotective role. They are able to bind free Chl *a* molecules and protect them against oxidation within the thylakoid membrane (Hutin et al. 2003). Indeed, in HL-acclimated spruce, we observed a dramatic increase in ELIPs, whereas in all Arabidopsis samples as well as in LL- and NL-acclimated spruce, the ELIPs were very close to (or even below) the mass spectrometry detection limit (**Paper II**).

Analysis of 77 K Chl fluorescence emission spectra has revealed three characteristics of spruce that are different from Arabidopsis. First, the emission from PSII in spruce was dominated by the band at a wavelength of 695 nm, whereas in Arabidopsis by the band at 685 nm (Fig. 12A). The origin and physiological significance of this phenomenon have not yet been elucidated. Second, the HL-NL difference spectrum in spruce clearly showed an increase in emission peaking at 680 nm after HL acclimation, much more pronounced than in Arabidopsis (Fig. 12B). The emission at this wavelength reflects the presence of LHCII antennae, which are weakly bound to the PSII core antenna (Belgio et al. 2012). Third, the enhanced emission around 700 nm in HL spruce indicates that a part of LHCIIs form aggregates (Chmeliov et al. 2016).

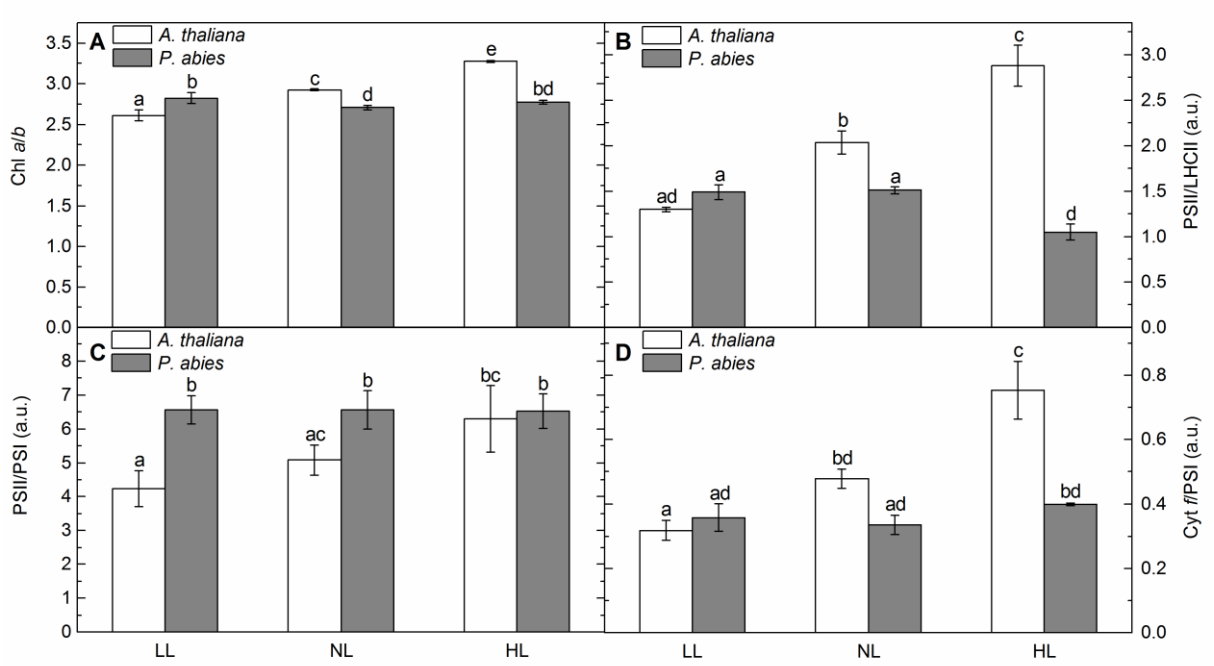

Fig. 11 (A) Chl *a/b*, **(B)** PSII/LHCII, **(C)** PSII/PSI, and **(D)** cytochrome *f*/PSI ratios for Arabidopsis (*A. thaliana*) and spruce (*P. abies*) acclimated to low light (LL; 20 µmol m^{-2} s^{-1}), normal light (NL; 100 µmol m^{-2} s^{-1}) and high light (HL; 800 µmol m^{-2} s^{-1}). The relative content of proteins was determined by mass spectrometry; PSII represents the sum of relative PG intensities of D1, D2, CP43 and CP47 proteins, LHCII – Lhcb1-3 proteins, and PSI - PsaA and PsaB proteins. Different letters represent statistically significant differences ($p < 0.05$, two-way ANOVA followed by Tukey's post hoc test). n = 4-5 ± S.D. (**Paper II**)

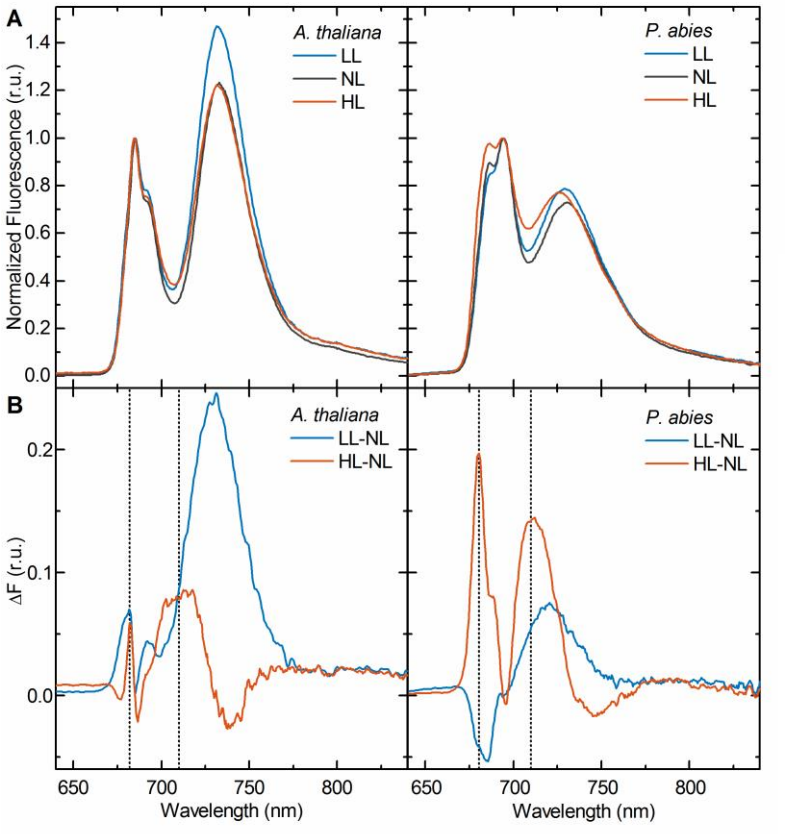

Fig. 12 (A) Normalized 77 K Chl fluorescence emission spectra measured at excitation wavelength of 475 nm in thylakoid membranes isolated from Arabidopsis (*A. thaliana*) and spruce (*P. abies*) acclimated to low light (LL; 20 µmol m^{-2} s^{-1}), normal light (NL; 100 µmol m^{-2} s^{-1}) and high light (HL; 800 µmol m^{-2} s^{-1}). Average spectra from three to five replicates are presented. **(B)** HL-NL and LL-NL difference spectra calculated from the corresponding emission spectra. The dotted lines highlight the wavelengths of 680 nm and 707 nm (**Paper II**).

A large LHCII antenna in spruce ensures efficient light harvesting under light-limiting conditions and makes spruce LL-tolerant species. However, it represents a burden for spruce grown in NL or even HL conditions. Without the ability to regulate the size of its LHCII antenna, spruce has to utilize different mechanisms to cope with the potentially dangerous surplus of excitation energy. One of these mechanisms may be regulated LHCII reorganization, which is detectable as a change in the long-range macro-organization of PSII-LHCII supercomplexes in the thylakoid membrane, measured by circular dichroism spectroscopy (Kovács et al. 2006, Tóth et al. 2016). In spruce, the extent of PSII-LHCII macro-organization was much smaller than in Arabidopsis, as shown by approximately ten times lower amplitudes of the Ψ-type bands (+)685 nm, (-)673 nm and (+)505 nm (compare Figs. 13A and 13B). In HL spruce, the macrodomain organization of PSII-LHCII was almost completely lost, which is probably associated with the weakening of PSII-LHCII interaction. A low degree of organization is usually associated with a high variability in the PSII-LHCII interaction, which corresponds to the finding that the random distribution of PSII complexes dominates in the grana membranes of spruce. PSII complexes in spruce are not arranged into the 2D crystalline arrays (Kouřil et al. 2020), which are often present in other higher plant species (Kouřil et al. 2012, Kirchhoff 2013) and which are one of the probable sources of the Ψ-type signal bands in circular dichroism spectra (Tóth et al. 2016).

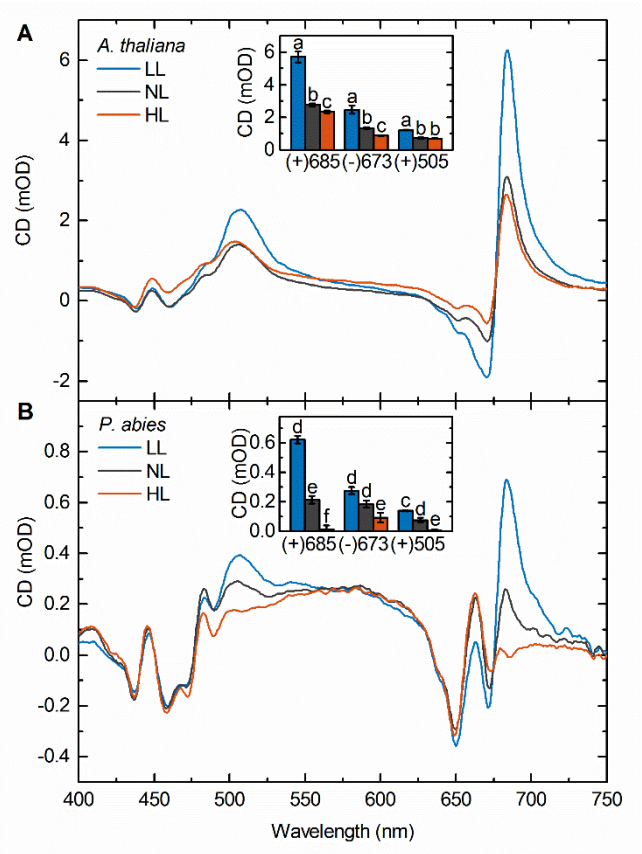

Fig. 13 Room-temperature circular dichroism (CD) spectra measured in thylakoid membranes isolated from **(A)** Arabidopsis (*A. thaliana*) and **(B)** spruce (*P. abies*) acclimated to low light (LL; 20 µmol m^{-2} s^{-1}), normal light (NL; 100 µmol m^{-2} s^{-1}) and high light (HL; 800 µmol m^{-2} s^{-1}). The insets show amplitudes of Ψ-type CD bands around (+)685 nm, (−)673 nm and (+)505 nm with reference wavelengths at 730 or 550 nm. Different letters in the insets represent statistically significant differences within the individual CD bands ($p < 0.05$, two-way ANOVA followed by Tukey's post hoc test). Averaged spectra normalized to the Q_y absorbance maximum are presented. n = 3-5 ± S.D. (**Paper II**)

1.6.2. Response of PSII and PSI function

The acclimation strategy of Arabidopsis ensured a successful adjustment of the PSII function to HL conditions, as documented by an optimal value of F_V/F_M after HL acclimation (Fig. 14A). However, in spruce, HL acclimation resulted in a significant decrease in F_V/F_M (mainly due to F_M quenching), which was associated with the retention of de-epoxidized xanthophylls (zeaxanthin and antheraxanthin) in darkness (Fig. 14B). This agrees with our previous studies with one-year-old needles of 5-year-old spruce saplings (**Kurasová et al. 2003b**, **Štroch et al. 2008**; Chapter 1.3.). Such response in HL spruce indicates the induction of "locked-in" NPQ (Demmig-Adams et al. 2012, 2014). This permanent quenching requires a large amount of loosely bound LHCIIs and is most likely based on the zeaxanthin-dependent formation of aggregates from LHCIIs (Fig. 12B). It should be noted that the mechanism of the "locked-in" NPQ in HL spruce is different from the "sustained" NPQ, which is induced in spruce in winter. The "sustained" NPQ was attributed to direct energy transfer from PSII to PSI (so-called spillover) and was associated with a much more pronounced decrease of F_V/F_M (down to 0.2) and dramatic quenching of PSII emission at 77 K (Bag et al. 2020, Grebe et al. 2020).

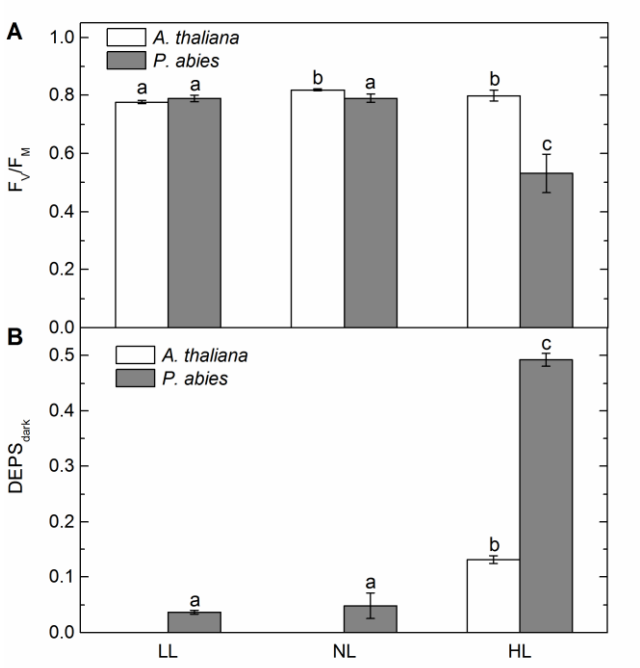

Fig. 14 (A) The maximum quantum yield of PSII photochemistry (F_V/F_M) and **(B)** the de-epoxidation state of xanthophyll cycle pigments ($DEPS_{dark}$) for Arabidopsis (*A. thaliana*) and spruce (*P. abies*) acclimated to low light (LL; 20 µmol m^{-2} s^{-1}), normal light (NL; 100 µmol m^{-2} s^{-1}) and high light (HL; 800 µmol m^{-2} s^{-1}). Measurements were carried out with seedlings adapted to dark for 30 min. DEPS was calculated as (Z+A)/(V+A+Z), where V, A, and Z are violaxanthin, antheraxanthin, and zeaxanthin, respectively. Different letters represent statistically significant differences ($p < 0.05$, two-way ANOVA followed by Tukey's post hoc test). n = 20 and 5 ± S.D. for F_V/F_M and $DEPS_{dark}$, respectively (**Paper II**).

To assess the functional consequences of the different structural adjustments of the photosynthetic complexes after light acclimation in spruce and Arabidopsis, we analyzed the function of PSII and PSI by measurements of Chl fluorescence and P700 redox state, respectively, at various intensities of actinic light. The key photoprotective regulatory mechanism that prevents the overexcitation of PSII reaction centers is light-induced thermal dissipation of absorbed light energy, which can be monitored as non-photochemical quenching of the maximal Chl fluorescence level F_M (i.e. the NPQ parameter; Bilger and Björkman 1990). In spruce, we observed an overall higher NPQ compared to Arabidopsis (Fig. 15A). For example, the actinic light intensity corresponding to NL (100 µmol m^{-2} s^{-1}) induced a 7 times higher level of NPQ in NL spruce than in NL Arabidopsis. The low level of NPQ detected for HL spruce is associated with the pre-existing "locked-in" NPQ mentioned above. As this NPQ is already active in dark-adapted samples, it lowers the value of F_V/F_M (Fig. 14A) and underestimates the real level of NPQ. The measured NPQ parameter thus reflects only the non-photochemical quenching that is induced by actinic light and does not reflect the dark level of NPQ in HL spruce.

As mentioned above, the results of the analysis of 77 K Chl fluorescence emission spectra suggest that there were loosely bound LHCIIs in NL and mainly HL spruce (Fig. 12B). It is known that weakly bound LHCIIs can form aggregates, resulting in quenching of the minimal Chl fluorescence level F_0 (e.g., Belgio et al. 2012, Ware et al. 2015). Therefore, we evaluated non-photochemical quenching of the F_0 level using the parameter SV_0 (Gilmore and Yamamoto 1991), which can be used for the estimation of the light-induced thermal energy dissipation localized in the weakly bound LHCIIs. In Arabidopsis, SV_0 was very low and appeared significantly only in LL plants at higher actinic light intensities (Fig. 15B). We observed much higher SV_0 values in NL and HL spruce, which corresponds to a higher amount of loosely bound LHCII, indicated also by 77 K difference emission spectra (Fig. 12B).

At higher actinic light intensities, PSII photochemistry in spruce, evaluated by the quantum yield Y(II) (Fig. 15C; Genty et al. 1989), was down-regulated due to high NPQ, which should keep PSII reaction centers more open. However, the fraction of open centers (qL; Kramer et al. 2004) was also very low for NL and HL spruce (Fig. 15D). To understand why PSII reaction centers in spruce were closed despite strong NPQ, we analyzed the redox state of PSI by the determination of PSI-related complementary quantum yields, i.e. the quantum yield of PSI photochemistry Y(I), non-photochemical energy dissipation due to PSI donor side limitation Y(ND) and acceptor side limitation Y(NA) (Fig. 16; Klughammer and Schreiber 2008). In HL Arabidopsis, the high activity of both PSII and PSI photochemistry, together with the low limitation of electron transport at both the donor and acceptor sides of PSI, implies that the generation of the trans-thylakoid proton gradient by photosynthetic electron transport and its utilization by ATP synthase were optimized and thus well balanced. In spruce, the Y(I)/Y(II) ratio progressively increased with increasing intensity of actinic light, reaching values 3 - 4 (Fig. 16D). Such high ratios indicate highly imbalanced PSII and PSI photochemistry and the involvement of cyclic electron transport around PSI, which may increase lumen acidification to the level that causes induction of both high NPQ (Miyake et al. 2005) and a pronounced level of regulatory process called photosynthetic control. Photosynthetic control is defined as the slowing down of electron transport at the level of cytochrome b_6f complex activated by the thylakoid lumen acidification (Tikhonov 2013, Yamamoto and Shikanai 2019). This leads to a higher reduction of the plastoquinone pool, which in turn lowers Y(II) (Fig. 15C) and increases Y(ND) (Fig. 16B). P700 is thus kept in the oxidized state, which is crucial for the photoprotection of PSI, as $P700^+$ acts as a non-photochemical quencher of absorbed light energy (Bukhov and Carpentier 2003).

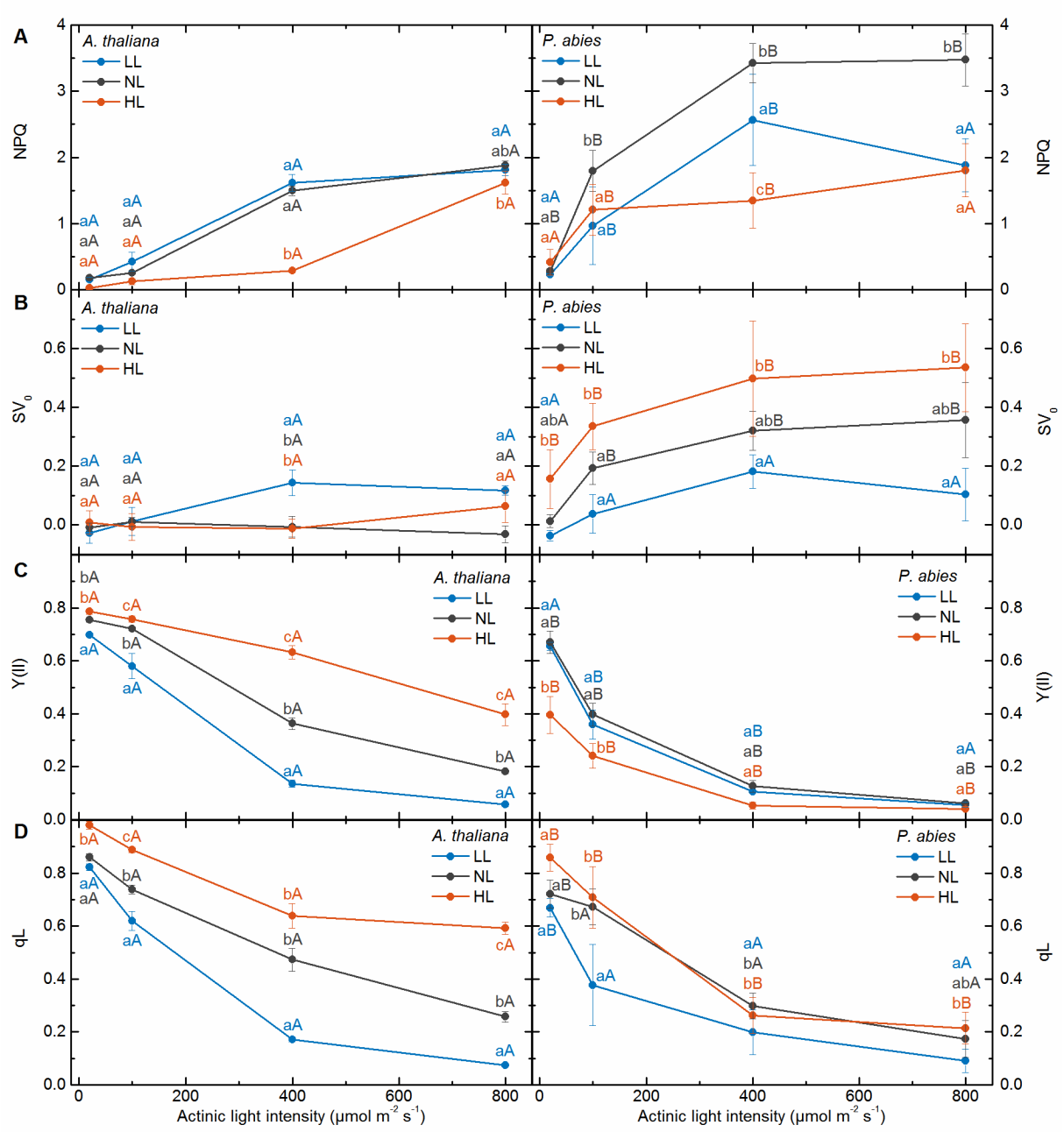

Fig. 15 (A) Non-photochemical quenching of maximal Chl fluorescence (NPQ), **(B)** non-photochemical quenching of minimal Chl fluorescence (SV_0), **(C)** quantum yield of PSII photochemistry [Y(II)] and **(D)** the fraction of open PSII reaction centers (qL) for Arabidopsis (*A. thaliana*) and spruce (*P. abies*) acclimated to low light (LL; 20 µmol m^{-2} s^{-1}), normal light (NL; 100 µmol m^{-2} s^{-1}) and high light (HL; 800 µmol m^{-2} s^{-1}). The parameters were determined after 15 min of exposure to different light intensities (20, 100, 400 and 800 µmol m^{-2} s^{-1}). Different lowercase letters represent statistically significant differences between light acclimation regimes for the same plant species and the same actinic light intensity, while different uppercase letters represent differences between plant species for the same light acclimation intensity and the same actinic light intensity ($p < 0.05$, three-way ANOVA followed by Tukey's post hoc test). n = 4-5 ± S.D. (**Paper II**)

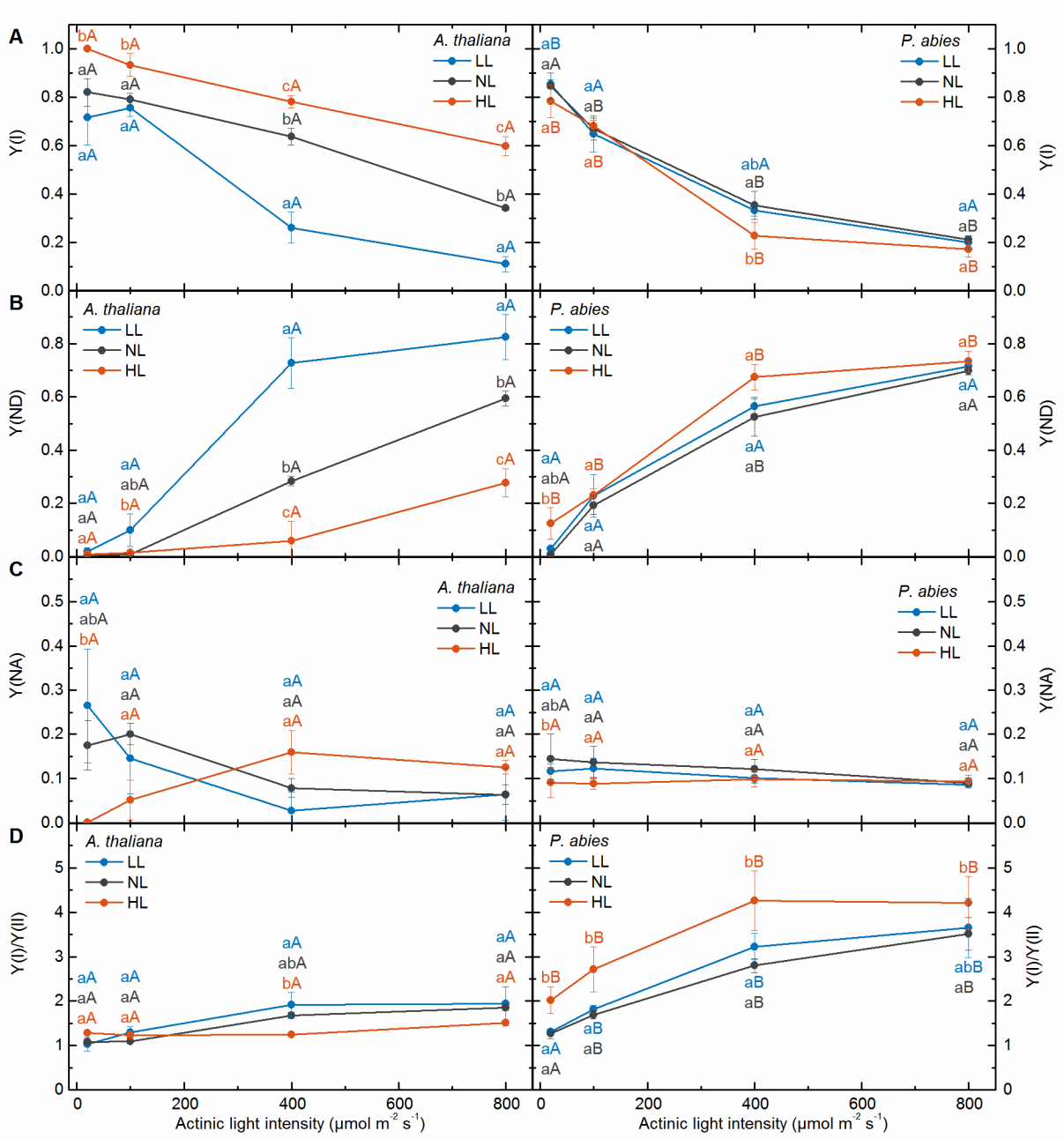

Fig. 16 (A) Quantum yield of PSI photochemistry [Y(I)], **(B)** quantum yield of non-photochemical energy dissipation due to PSI donor side limitation [Y(ND)], **(C)** PSI acceptor side limitation [Y(NA)] and **(D)** the ratio of quantum yields of PSI and PSII photochemistry [Y(I)/Y(II)] for Arabidopsis (*A. thaliana*) and spruce (*P. abies*) acclimated to low light (LL; 20 µmol m^{-2} s^{-1}), normal light (NL; 100 µmol m^{-2} s^{-1}) and high light (HL; 800 µmol m^{-2} s^{-1}). The parameters were determined after 15 min of exposure to different light intensities (20, 100, 400 and 800 µmol m^{-2} s^{-1}). Different lowercase letters represent statistically significant differences between light acclimation regimes for the same plant species and the same actinic light intensity, while different uppercase letters represent differences between plant species for the same light acclimation intensity and the same actinic light intensity ($p < 0.05$, three-way ANOVA followed by Tukey's post hoc test). n = 4-5 ± S.D. (**Paper II**)

The kinetics of PSII and PSI parameters during illumination revealed further differences in the regulation of NPQ (Fig. 17A) and electron transport between spruce and Arabidopsis. We confirmed our previous findings of a very fast induction of NPQ in HL spruce (Chapter 1.3.). This is probably associated with the activity of pseudocyclic electron transport to molecular oxygen, mediated by the flavodiiron enzyme. This alternative pathway is operational on the acceptor side of PSI within one second after the onset of light in all non-flowering plants (including the family Pinaceae), but not in Arabidopsis (Ilík et al. 2017). It contributes to rapid acidification of the thylakoid lumen and thus may be involved in the very fast induction of NPQ in HL spruce. In addition, the flavodiiron-dependent pathway seems to be responsible for the very fast establishment of photosynthetic control, as it required less than 10 s (Fig. 17B). Acceleration of the activation of photosynthetic control by this pathway was confirmed using transgenic Arabidopsis with flavodiiron enzyme from the moss *Physcomitrella patens* (see the supplementary material of **Paper II**).

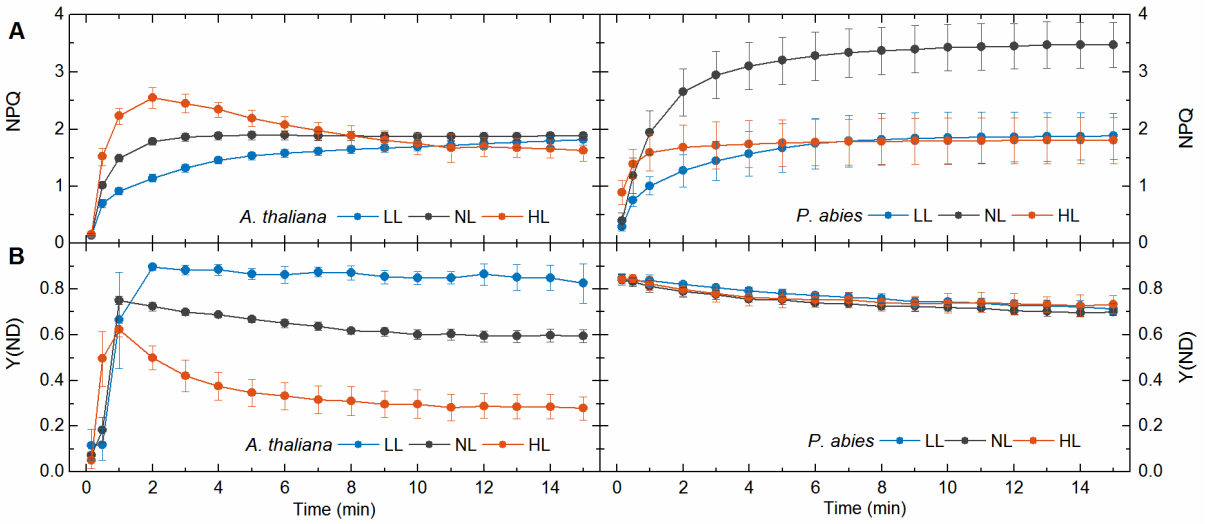

Fig. 17 Kinetics of **(A)** non-photochemical quenching of maximal Chl fluorescence (NPQ) and **(B)** quantum yield of non-photochemical energy dissipation due to PSI donor side limitation [Y(ND)] during light exposure (800 µmol m^{-2} s^{-1}) of Arabidopsis (*A. thaliana*) and spruce (*P. abies*) acclimated to low light (LL; 20 µmol m^{-2} s^{-1}), normal light (NL; 100 µmol m^{-2} s^{-1}) and high light (HL; 800 µmol m^{-2} s^{-1}). *n* = 4-5 ± S.D. (**Paper II**)

In summary, adjustments of the thylakoid protein complexes in Arabidopsis served to increase the capacity of photosynthetic linear electron transport at higher acclimation light intensities. These changes were reflected in the balanced and coordinated increase in the photochemical yields of both PSII and PSI and in the minimization of the involvement of regulatory processes, such as photosynthetic control and NPQ. In contrast, spruce showed a completely different acclimation strategy to changes in light intensity. We observed no adjustment in the stoichiometry of electron transport complexes with increasing acclimation light intensity. In line with these results, the quantum yields of PSII and PSI photochemistry were very similar in spruce acclimated to all light intensities, which was evident mainly at higher intensities of actinic light. The spruce seedlings had a constantly large LHCII antenna. So, how are they able to tolerate excess light despite their light-harvesting apparatus being adjusted to LL? We propose that this is due to the ability of spruce to induce massive NPQ in its antenna system. This type of NPQ is associated with the formation of quenching centers in weakly bound LHCIIs. One of the reasons for this unusually strong NPQ is higher acidification of the thylakoid lumen, which is partly due to a high activity of cyclic electron transport around PSI. Under HL conditions, spruce used additional mechanisms to help it cope with long-term exposure to excessive light. HL spruce downregulated the

amount of PSII and PSI core complexes and induced permanent NPQ that was associated with the formation of LHCII aggregates and reduction of the maximum photochemical yield of PSII (F_V/F_M). At the same time, synthesis of stress proteins (ELIPs) ensured binding of Chls released from degraded photosystems.

2. Effects of UV radiation during barley acclimation

2.1. Effects of UV radiation on the photosynthetic apparatus: damage and protection

In nature, changes in solar irradiance are not limited to photosynthetic active radiation (PAR, 400-700 nm), but also include changes in the level of UV radiation (280-400 nm). UV radiation is more destructive to plants than visible light, as UV-B (280-315 nm) can directly damage DNA, lipids and proteins and also cell membranes through processes of lipid peroxidation (Schmitt et al. 2014). UV-B targets particularly PSII and also the crucial proteins of the photosynthetic apparatus such as Rubisco, ATPase and violaxanthin de-epoxidase (Vass et al. 2005). In PSII, the components susceptible to photodamage due to UV-B are D1 and D2 proteins, water-oxidizing complex, quinone electron acceptors Q_A and Q_B, redox-active tyrosines, and LHCII. Especially, the Mn cluster of the water oxidation complex seems to be the most sensitive to UV-B radiation, and among all the components, it is the initial target of UV-B (Vass et al. 2005, Kataria et al. 2014). In addition to direct effects of UV-B radiation on the photosynthetic apparatus, photosynthetic activity can also be indirectly affected by UV-B-induced stomatal closure (Tossi et al. 2014).

The model experiments have clearly demonstrated the damaging potential of UV-B, but they were performed usually with unrealistically high doses of UV-B, unrealistic ratios between UV-B, UV-A (315-400 nm) and PAR or with isolated thylakoid membrane complexes lacking protective functions, i.e. lacking UV-B-absorbing compounds and antioxidative components. Plants growing under field conditions rarely show signs of UV-induced damage because of the lower doses of UV-B and efficient means of protection evolved by plants, minimizing UV-B penetration into leaf tissues and repairing potential damage (Jansen et al. 1998). Nevertheless, the damaging effects of UV-B observed in laboratory experiments may be relevant to studies under natural conditions if the antioxidant network and/or repair systems are overwhelmed by the presence of additional stress factors.

The important process that protects the photosynthetic apparatus from UV radiation is the accumulation of phenolic compounds, both in the epidermis and mesophyll, which absorb in the UV part of the solar radiation spectrum (Fig. 18). This screening function of UV-absorbing compounds can be assessed by comparison of Chl fluorescence intensity excited by blue (or red) and UV radiation (Bilger et al. 2001). In this method, blue or red light is used as a reference beam, because it is not absorbed by phenolic compounds. Thus, the accumulation of UV-absorbing compounds reduces the level of Chl fluorescence excited by the UV beam without affecting the level of fluorescence excited by the reference beam. Another key function of phenolic compounds is their antioxidant activity, which protects plants by scavenging reactive oxygen species (Agati et al. 2020). Concerning the repair processes of UV-induced damage, plants possess mechanisms that repair both DNA and the D1 and D2 proteins of PSII reaction center (Jansen et al. 1998).

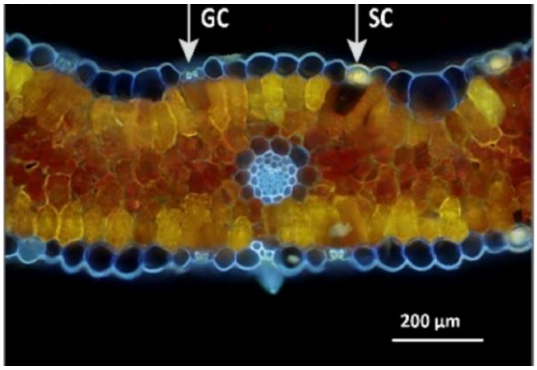

Fig. 18 Cross-sections of barley leaves, treated with Naturstoff reagent A and acquired under UV light, showing the presence of UV-screening phenolics as blue autofluorescence in epidermal cell walls, as well as in stomatal guard cells (GC) and as yellow fluorescence from flavonoids reacting with the reagent in the mesophyll layers adjacent to epidermis and in stomatal subsidiary cells (SC). Red color corresponds to Chl fluorescence. For further details of the methodology, see Hunt et al. (2021).

Solar UV-B should not be regarded only as a stress factor, but also as a regulatory stimulus that modulates gene expression, plant metabolism and development (Hideg et al. 2013). Many regulatory effects of UV-B on plant morphology and development have been reported (Robson et al. 2015). For example, exposure to UV-B generally reduces extension growth and leaf expansion and increases leaf thickness and axillary branching. Under low UV-B conditions, specific signalling pathways activate antioxidant defenses and pre-dispose plants to a state of low alert before potential oxidative stress (Hideg et al. 2013). At high UV-B doses, the impact of generated reactive oxygen species is mitigated by induction of antioxidants, such as ascorbic acid and α-tocopherol, and antioxidant enzymes, such as superoxide dismutase, ascorbic acid peroxidase, glutathione reductase, and guaiacol peroxidase (Kataria et al. 2014).

In a natural environment, plants are exposed to 10-100 times more UV-A photons than UV-B photons. The UV component of sunlight is made up of approximately 95 % UV-A and 5 % UV-B (Rai et al. 2021). UV-A radiation is less reactive per photon than UV-B and can cause both inhibitory and stimulatory effects on biomass accumulation and morphology, while UV-B effects are mainly negative (Verdaguer et al. 2017). UV-A effects depend on other environmental factors, as well as on the species or even the genotype (Cooley et al. 2001). On the basis of *in vitro* studies, UV-A has been considered to be a damaging factor that targets the same components of the photosynthetic apparatus as UV-B (Vass et al. 2005, Verdaguer et al. 2017). However, under field conditions, various protective mechanisms operating in intact leaves (such as UV-shielding or antioxidant defenses) can mitigate or eliminate photoinhibition caused by UV-A. The differences between UV-B and UV-A effects on plant growth and development and on the accumulation of photoprotective phenolics may reflect diverse UV-perception mechanisms with multiple photoreceptors operating in the UV-A range. Blue-light photoreceptors, such as phototropins and cryptochromes, absorb also in the UV-A part of the spectrum (Christie et al. 2015). In contrast, plants perceive UV-B radiation through the photoreceptor UV RESISTANCE LOCUS 8 (UVR8), which has been recently found to also mediate perception of short-wavelength UV-A (315-350 nm) (Rai et al. 2021).

It has been observed that UV-A can enhance photosynthetic rates, particularly under low PAR conditions (e.g., Mantha et al. 2001, Sullivan et al. 2003, Kataria and Guruprasad 2012, **Paper VI**). This can be explained by the following three mechanisms: 1) direct absorption of UV-A by Chls and Cars, which have minor absorption peaks in the UV-A region (Lichtenthaler 1987, Johnson and Day 2002, Turnbull et al. 2013), 2) re-absorption by photosynthetic pigments of UV-A-induced blue-green fluorescence emitted by phenolic compounds (Mantha et al. 2001, Johnson and Day 2002) and 3) increased stomatal opening due to the absorption of UV-induced blue fluorescence by cryptochromes located in stomata (Mantha et al. 2001).

2.2. Contribution of UV-shielding and carotenoid-mediated photoprotection to PSII resistance during acclimation to elevated PAR and UV radiation

In the following three chapters, I will summarize the main findings from field studies dealing with acclimation of barley plants to the change in the level of PAR together with UV radiation. In the experiment presented in **Paper III**, seven-day-old barley seedlings grown from seeds in shaded conditions in a greenhouse were transferred to outdoor conditions with predominantly bright sunny days. At solar noon, the level of PAR and UV radiation in the greenhouse was only approximately 9 %

and 2 % of the outside level, respectively. We monitored the content of photosynthetic pigments, PSII function, and UV-shielding on the primary leaves for 6 days after transfer of plants.

The barley photosynthetic apparatus was successfully acclimated to stressful outdoor conditions, as documented by the recovery of the maximum quantum yield of PSII photochemistry (F_V/F_M) after an initial decline (Fig. 19A) and also by an enhanced electron transport rate through PSII and increased content of Chls and Cars per leaf area (**Paper III**). The absence of PSII photoinhibition is related to immediate carotenoid-mediated photoprotection, reflected by the strongly increased capacity of NPQ (expressed as non-photochemical quenching of minimal fluorescence, SV_0; Fig. 19B) and the Car *x+c*/Chl *a* ratio (Fig. 19C) already after one day under outdoor conditions.

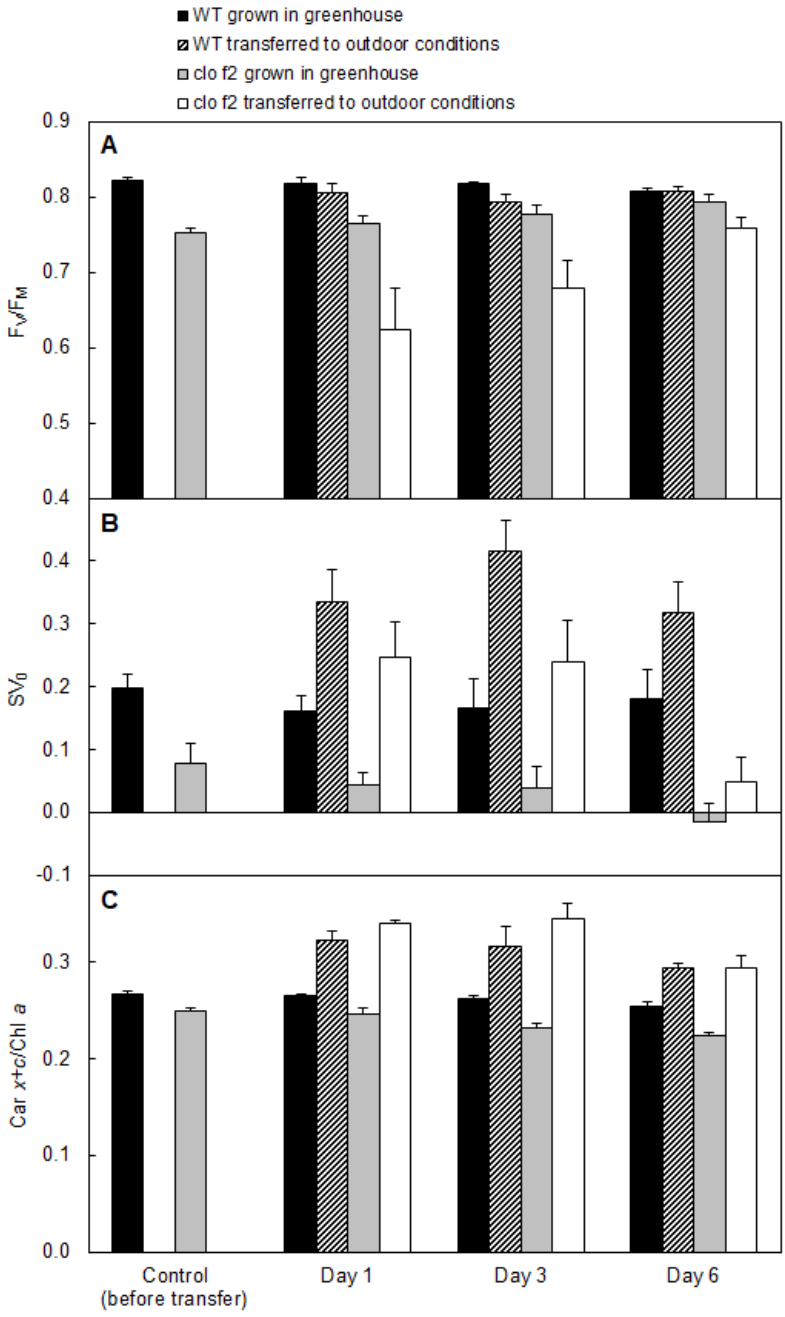

Fig. 19 (A) The maximum quantum yield of PSII photochemistry (F_V/F_M), **(B)** non-photochemical quenching of minimal Chl fluorescence (SV_0) and **(C)** the ratio of total carotenoids to Chl *a* (Car *x+c*/Chl *a*) for barley wild-type (WT) and *chlorina f2* mutant (*clo f2*) grown in the greenhouse and transferred to outdoor conditions. The transfer started with 7-day-old seedlings (control). F_V/F_M was determined after 15 min of dark adaptation, SV_0 after 10 min of illumination with saturating white light of 2000 µmol m^{-2} s^{-1}. *n* = 6 ± S.D. (**Paper III**)

Based on the ratios of blue- to UV-excited Chl fluorescence, we found that UV-shielding increased clearly after transfer to outdoor conditions, already after the first day, and reached a saturation level after three days (Fig. 20). The use of a fluorescence imaging technique allowed us to analyze the spatial distribution of UV-shielding within leaves. UV-shielding was found to increase from the leaf base to the leaf tip. This longitudinal leaf gradient of UV-shielding can be explained by the fact that the leaf tip is more expanded and thus more exposed to light than the enrolled base. Furthermore, since the meristems in barley are on the leaf base, the leaf tip is the oldest leaf tissue that is exposed to light for the longest time. In addition, we observed that the development of UV-shielding under elevated PAR and UV radiation depended on the position within the leaf. After one day under outdoor conditions, the increase of UV-shielding level was pronouncedly greater at the leaf base than at the leaf tip and still continued after 6 days, in contrast to the leaf tip (Fig. 20B). This is apparently related to the different age and developmental stage of the tissue along the leaf blade. Thus, a greater development of UV-shielding was observed in the young leaf regions at the leaf base as compared to the mature regions at the leaf tip.

The acclimation response to elevated PAR and UV radiation was also investigated in Chl *b*-less barley mutant *chlorina f2* (*clo f2*) in order to evaluate the complementarity of two photoprotective mechanisms in acclimation of the assimilatory apparatus, namely carotenoid-mediated photoprotection and UV-shielding. In our earlier study of *clo f2* acclimation to high PAR, we observed that this mutant is resistant to high PAR due to efficient carotenoid-mediated photoprotection. We found that a high amount of de-epoxidized xanthophyll cycle pigments can act as a filter for excitation energy, preventing the transfer of excitation energy to Chl *a* (**Štroch et al. 2004**). Another factor contributing to the resistance of PSII in *clo f2* is the reduced functional antenna size. As a result of Chl *b* absence, *clo f2* has reduced LHCs of PSI and PSII by 30 and 80 %, respectively (Harrison et al. 1993). Compared to wild type, *clo f2* during outdoor treatment exhibited supressed induction of UV-shielding (Fig. 20B) and enhanced development of carotenoid-mediated photoprotection, indicated by a higher increase of SV_0 and the Car *x+c*/Chl *a* ratio (Fig. 19B, C). Thus, it seems that the contributions of these two photoprotective processes to PSII photoprotection might be mutually dependent. We propose that the photoprotective action of de-epoxidized xanthophylls in *clo f2* (i.e., involvement in NPQ, filtering of excitation energy, and their antioxidative function) reduces demand for UV-shielding induction.

Although both UV-shielding and Cars content responded immediately to elevated PAR and UV radiation, in the same time range, the situation is different after eliminating light stress. We observed that while the Car *x+c*/Chl *a* ratio decreased after transfer of wild-type barley and the *clo f2* mutant from high PAR to low PAR conditions, the UV-shielding level remained stable for several days (**Nezval et al. 2017**). Thus, barley plants after elimination of high PAR stress flexibly and rapidly (within a few days) adjusted their composition of photosynthetic pigments, mainly the content of xanthophyll cycle pigments. Furthermore, we have revealed that phenolic compounds with antioxidative function (such as lutonarin and feruloylquinic acid) were also flexibly down-regulated. In contrast, the major phenolic compound in barley, saponarin, remained stable after transfer to low PAR conditions, making it the cause of the constant level of UV-shielding (**Nezval et al. 2017**). The stability of UV-shielding was confirmed for barley plants after their transfer from conditions with elevated PAR (both alone and with UV radiation) to conditions with low PAR and no UV radiation (**Paper V**, see Chapter 2.4.).

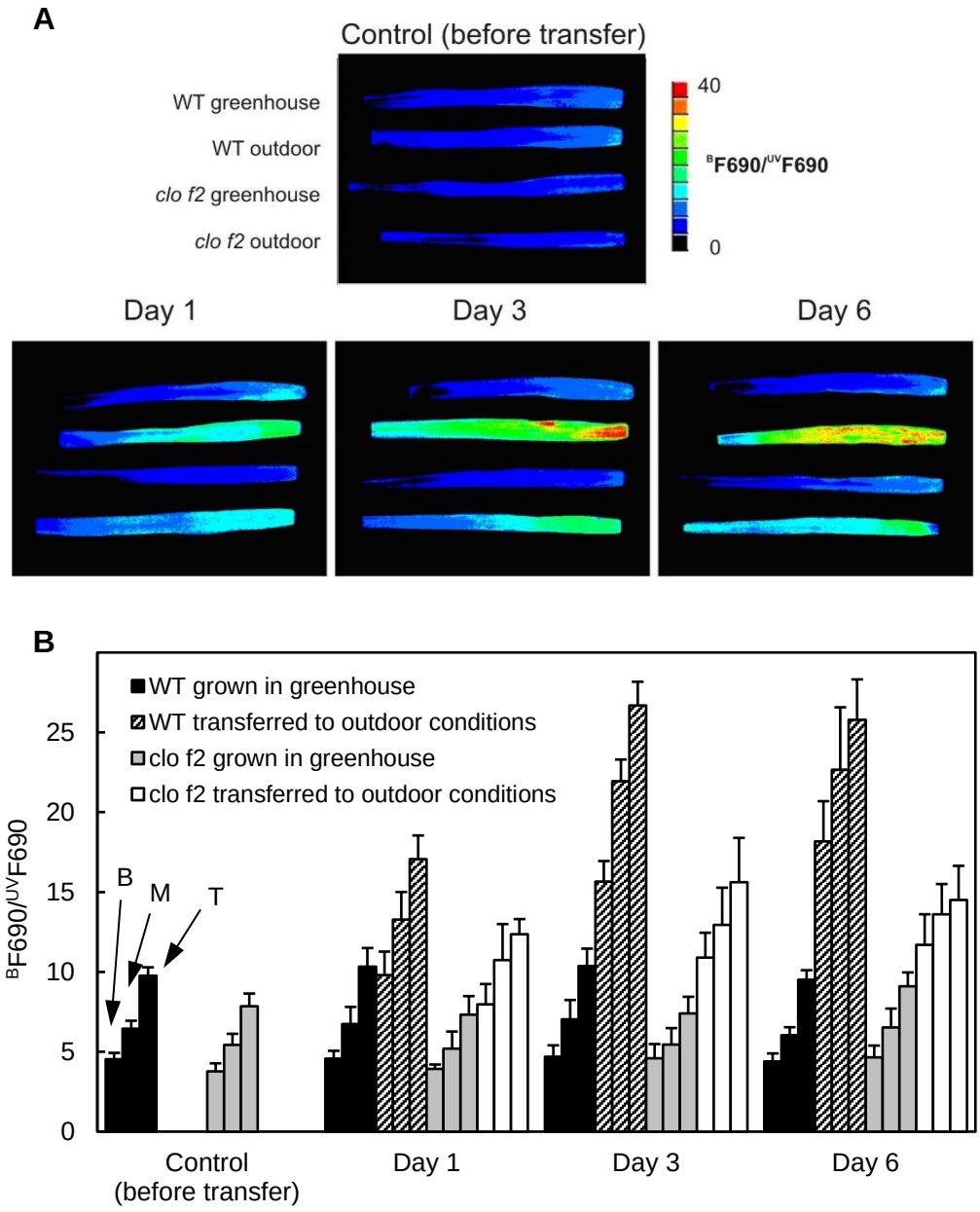

Fig. 20 (A) Representative images of the ratio of blue- to UV-excited Chl *a* fluorescence at 690 nm (^{B}F690/^{UV}F690) reflecting UV-shielding for wild-type barley (WT) and *chlorina f2* mutant (*clo f2*) grown in the greenhouse and transferred to outdoor conditions. The transfer started with 7-day-old seedlings (control). **(B)** The ^{B}F690/^{UV}F690 ratios determined from fluorescence images of the leaves divided into three parts of equal length. In each group, the left bars correspond to the leaf base (B), the middle bars to the middle part (M), and the right bars to the leaf tip (T). *n* = 6 ± S.D. (**Paper III**)

2.3. Effect of acclimation to elevated PAR and UV radiation on tolerance to high radiation stress

In another study, we examined the effect of acclimation to elevated PAR and UV radiation on photoprotection in barley leaves (**Paper IV**). The experiment was carried out in the field with two barley varieties that differ in their sensitivity to photooxidative stress, sensitive Barke and resistant Bonus, to test their photoprotective capacities. First, plants were pre-cultivated for 2 weeks under reduced PAR (to 25 % of natural sunlight) and without UV radiation. The plants were then transferred to three different treatments: [UV-PAR-] corresponding to the pre-cultivation conditions, i.e., UV exclusion and reduction of outdoor PAR to 25 %, [UV-PAR+] representing ambient PAR and UV exclusion, and [UV+PAR+] representing ambient PAR and supplemental UV radiation (doubled solar UV irradiance with the same UV-A/UV-B ratio as under ambient UV conditions). The second leaves, which were used for all measurements, had already been fully formed at the beginning of the individual UV/PAR acclimation treatments. After 7 days of acclimation, plants were exposed to high radiation stress (HRS) for 4 h, defined by high intensities of PAR (1000 µmol m^{-2} s^{-1}), UV-A (10 W m^{-2}) and UV-B (2 W m^{-2}). Our objective was to examine whether acclimation to supplemental UV radiation will enhance the photoprotective capacity of plants, resulting in suppression of photoinhibition caused by HRS.

Our results demonstrate the importance of PAR in the induction of UV-shielding (accumulation of flavonols), as it pronouncedly increased after [UV-PAR+] treatment compared to [UV-PAR-] treatment (Fig. 21A). The sensitive variety Barke showed a lower constitutive level of UV-shielding (determined for [UV-PAR-] treatment) compared to the tolerant variety Bonus. UV exposure under [UV+PAR+] treatment increased UV-shielding only in Barke, but not in Bonus. Thus, inducible UV-shielding can compensate for differences in constitutive protection between barley genotypes. As expected, the relative content of xanthophyll cycle pigments (VAZ/Chls) increased under elevated PAR, but also under supplemental UV radiation, more pronouncedly in the Barke variety (Fig. 21B).

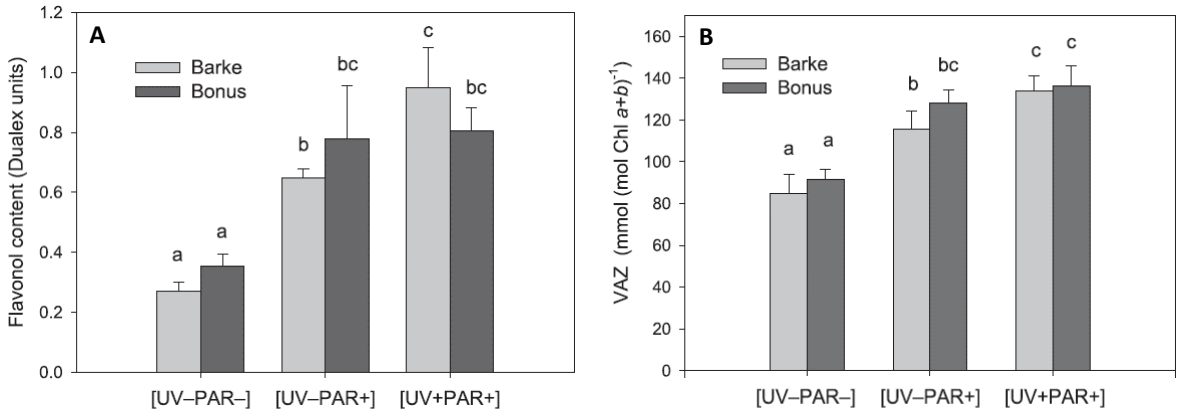

Fig. 21 (A) Flavonol content determined *in vivo* (UV-shielding) and **(B)** total content of xanthophyll cycle pigments (VAZ) expressed per Chl *a+b* in different varieties of barley, sensitive Barke and tolerant Bonus, after 7-day acclimation to individual UV/PAR treatments. [UV-PAR-] corresponds to UV exclusion and reduction of ambient PAR to 25 %, [UV-PAR+] to UV exclusion and ambient PAR, and [UV+PAR+] to supplemental UV radiation (doubled solar UV) and ambient PAR. Different letters denote statistically significant differences ($p \leq 0.05$; Tukey's ANOVA post hoc test). $n \geq 5 \pm$ S.D. (**Paper IV**)

The tolerance to short-term HRS was evaluated by determining the light-saturated CO_2 assimilation rate (A_{max}) and the maximum quantum yield of PSII photochemistry (F_V/F_M) (Fig. 22). We observed that a significant reduction of A_{max} after HRS in barley acclimated to [UV-PAR-] treatment was mitigated in plants acclimated to elevated PAR (fully in the tolerant Bonus and partially in the sensitive Barke) (Fig. 22A, B). UV radiation together with elevated PAR during acclimation resulted in maintained A_{max} after HRS also in the Barke variety. The responses of F_V/F_M after HRS were found to be the same as those of A_{max} (Fig. 22C, D). Thus, acclimation to elevated PAR both alone (without UV radiation) and with supplemental UV radiation ameliorates the negative impact of HRS on photosynthesis. However, the presence of UV radiation is necessary to fully induce photoprotective mechanisms in the sensitive Barke variety.

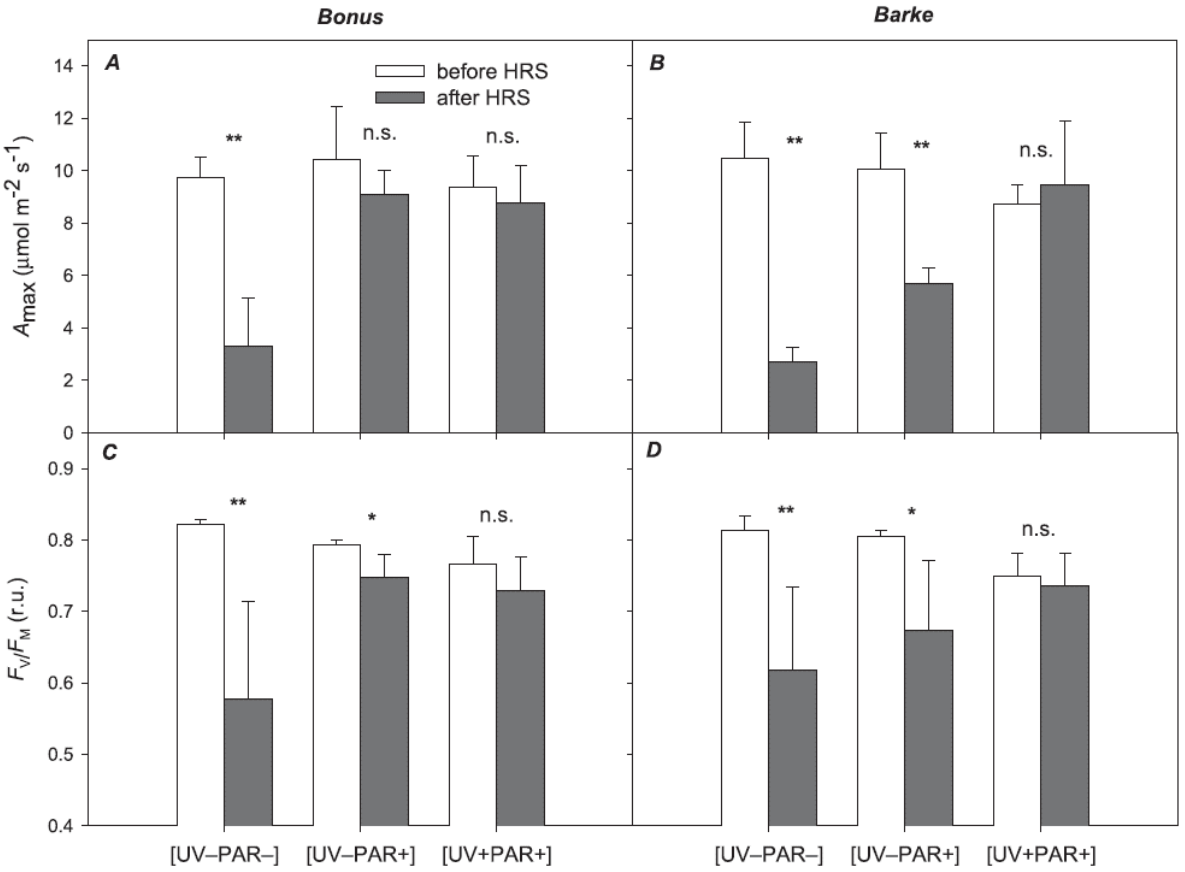

Fig. 22 The light-saturated CO_2 assimilation rate (A_{max}; **A, B**) and the maximum quantum yield of PSII photochemistry (F_V/F_M; **C, D**) before and after short-term (4 h) high radiation stress (HRS). Barley varieties, sensitive Barke and tolerant Bonus, were acclimated for 7 days to individual UV/PAR treatments before HRS application. [UV-PAR-] corresponds to UV exclusion and reduction of ambient PAR to 25 %, [UV-PAR+] to UV exclusion and ambient PAR, and [UV+PAR+] to supplemental UV radiation (doubled solar UV) and ambient PAR. HRS means application of high intensities of PAR (1000 µmol m^{-2} s^{-1}), UV-A (10 W m^{-2}) and UV-B (2 W m^{-2}). A_{max} was measured at PAR of 1200 µmol m^{-2} s^{-1}; F_V/F_M was determined after 25 min in darkness. Significant differences between means before and after HRS were tested using Student's *t*-test (* $p \leq 0.05$; ** $p \leq 0.01$; n.s. non-significant). $n \geq 5 \pm$ S.D. (**Paper IV**)

The accumulation of both flavonols and xanthophyll cycle pigments was recognized as a determining factor in barley for the induction of photoprotection against HRS. The reductions in A_{max} and F_V/F_M caused by HRS were inversely proportional to the contents of both flavonols and VAZ (Fig. 23). In conclusion, growth under elevated PAR can increase the photoprotective capacity of barley plants compared to plants grown under low PAR. Furthermore, we demonstrated that supplemental UV radiation can lead to enhanced photoprotective capacity, thus contributing to the induction of tolerance to HRS in barley.

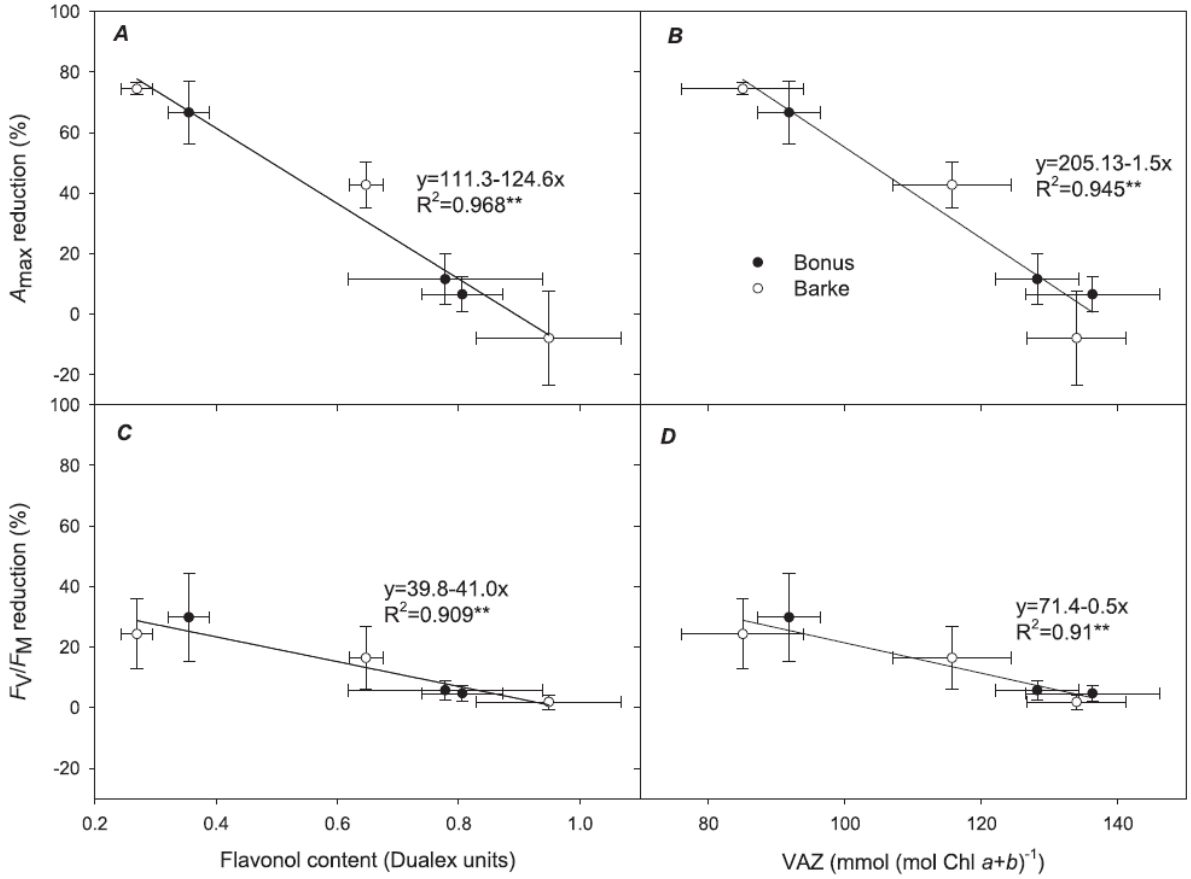

Fig. 23 Relationships between *in vivo* flavonol content **(A, C)**, total content of xanthophyll cycle pigments (VAZ) **(B, D)** and the relative reductions of the light-saturated CO_2 assimilation rate (A_{max}) **(A, B)** and the maximum quantum yield of PSII photochemistry (F_V/F_M) **(C, D)** after high radiation stress. Data were taken from Figs. 21 and 22. Linear functions were fitted to the data of both barley varieties (Barke, Bonus) together. Means (points) and standard deviations (vertical and horizontal error bars) are presented ($n \geq 5$). (**Paper IV**)

2.4. Modulation of PAR- and UV-induced phenolics accumulation and UV-shielding by leaf ontogeny

As mentioned in previous chapter, the development of UV-shielding is dependent on the barley genotype. We were also interested in the effect of PAR and UV radiation on the accumulation of individual phenolic compounds. We addressed the question of how the constitutive and UV- or PAR-induced accumulation of individual phenolic compounds is affected by leaf age and how their accumulation is linked to the accumulation of VAZ pigments (**Paper V**). For this purpose, measurements were made on the second mature barley leaves that were already fully developed at the onset of UV/PAR treatments and on the third young leaves developing during UV/PAR treatments.

UV-shielding was significantly higher in young leaves compared to mature leaves, regardless of barley genotype and radiation treatment (Fig. 24). HPLC analysis revealed in young leaves higher contents of hydroxycinnamic acid derivatives, 3-feruloylquinic acid, lutonarin, and one luteolin derivative (**Paper V**). On the other hand, some phenolics (apigenin derivative in both varieties and other luteolin derivative and saponarin in Bonus) accumulated to higher levels in mature leaves. The high differences in UV-shielding and phenolics contents between young and mature leaves under [UV-PAR-] treatment demonstrate the important role of leaf age in controlling the constitutive accumulation of UV-screening flavonols. Consistent with our previous findings (**Nezval et al. 2017**), Fig. 24 shows the stability of induced UV-shielding (accumulated flavonols) for 10 days after transfer of plants to [UV-PAR-] conditions, regardless of barley genotype, UV/PAR treatment and leaf age.

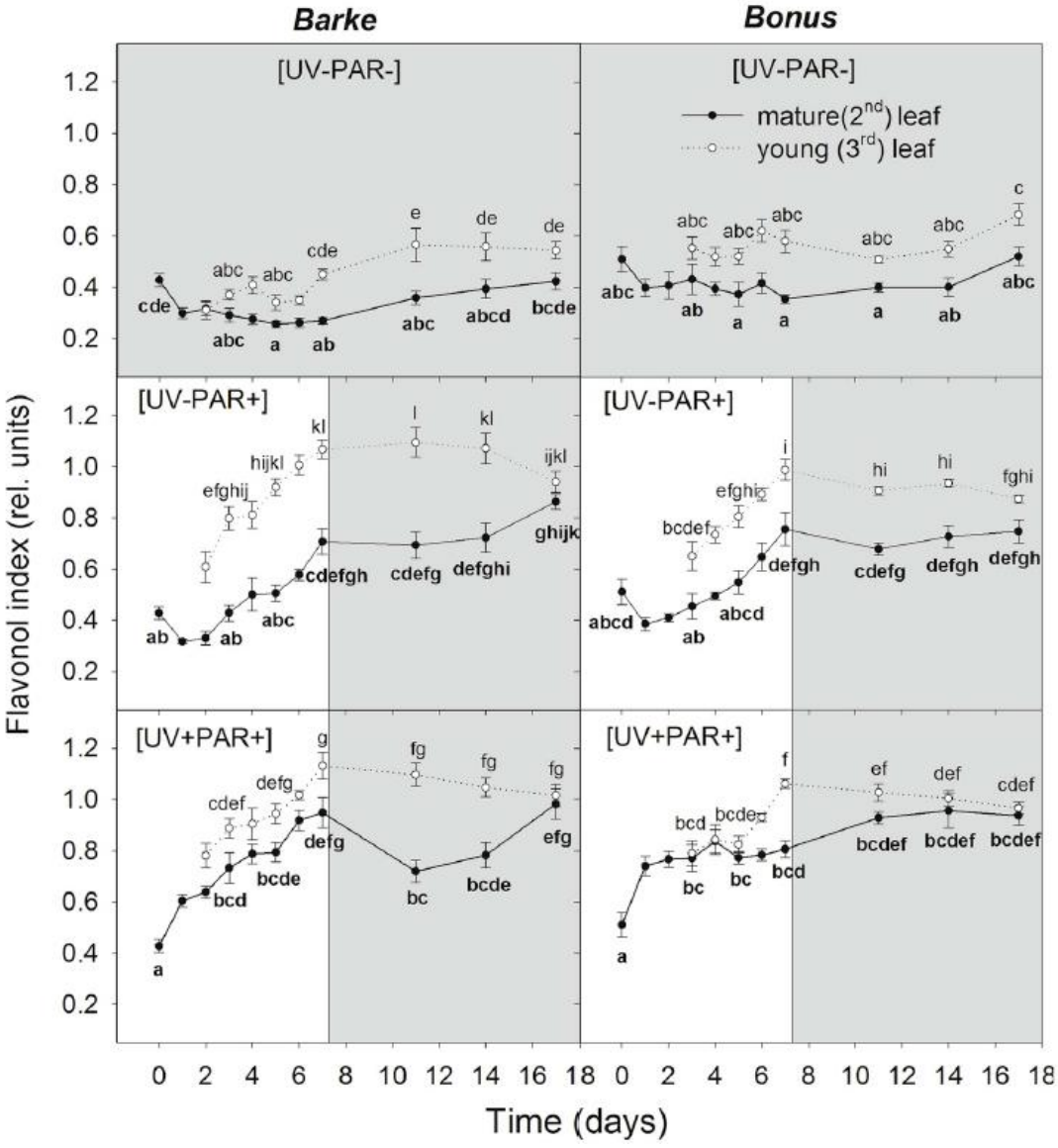

Fig. 24 Flavonol content determined *in vivo* (UV-shielding) in mature (2nd) and young (3rd) leaves of two barley varieties, sensitive Barke and tolerant Bonus, during 7-day acclimation to individual UV/PAR treatments and the following 10-day relaxation, when plants were transferred to [UV-PAR-] conditions. [UV-PAR-] corresponds to UV exclusion and reduction of ambient PAR to 25 %; [UV-PAR+] to UV exclusion and ambient PAR and [UV+PAR+] to supplemental UV radiation (doubled solar UV) and ambient PAR. Different letters denote statistically significant differences ($p \leq 0.05$; Tukey's ANOVA post hoc test) between dates of measurement and the leaves within individual varieties and UV/PAR treatments. $n \geq 5 \pm$ S.E. (**Paper V**)

UV/PAR treatments altered the differences between leaf age classes. Elevated PAR itself induced a much higher difference in UV-shielding between young and mature leaves of the sensitive variety Barke compared to the tolerant variety Bonus. In comparison with [UV-PAR+] treatment, [UV+PAR+] treatment resulted in a decrease in the difference between young and mature leaves in Barke, but an unchanged difference in Bonus. Since no significant differences in UV-shielding were found between [UV-PAR+] and [UV+PAR+] treatments in young leaves, we assume that elevated PAR is sufficient to saturate the accumulation of UV-screening phenolics in young leaves. On the other hand, UV radiation was necessary to achieve maximum UV-shielding level in mature leaves of the Barke variety (Figs. 21A and 24). This may be related to a general assumption that young leaves require more efficient protection against photooxidative stress, since they are more important for plant growth than mature leaves (Reifenrath and Müller 2007). Under higher PAR conditions, elevated photosynthetic carbon fixation is probably coupled with increased demand for biosynthesis of phenolic compounds, since about 20 % of the fixed carbon is estimated to flow through the shikimate pathway, forming phenolic compounds (Rippert et al. 2004). We can conclude that accumulation of both constitutive and UV/PAR-inducible phenolic compounds is modulated by leaf ontogeny, however, this modulation is compound-specific.

The VAZ content (expressed per Chls) was slightly, but often statistically non-significantly, higher in young leaves than in mature leaves of both barley varieties (**Paper V**). We found a strong positive association of VAZ and lutonarin accumulation, irrespective of leaf age (Fig. 25). This relationship reveals a hyperbolic character, particularly for the Barke variety. At first, a slight increase of lutonarin content is accompanied by a considerable increase of VAZ pool size, but later on, VAZ becomes almost saturated, whereas the accumulation of lutonarin continues. Similar results were also found for the relationships between VAZ pool and the contents of hydroxycinnamic acid and luteolin derivatives. Thus, in mature Barke leaves, insufficient accumulation of lutonarin, which contributes to antioxidative protection, can be compensated by a high content of VAZ pigments.

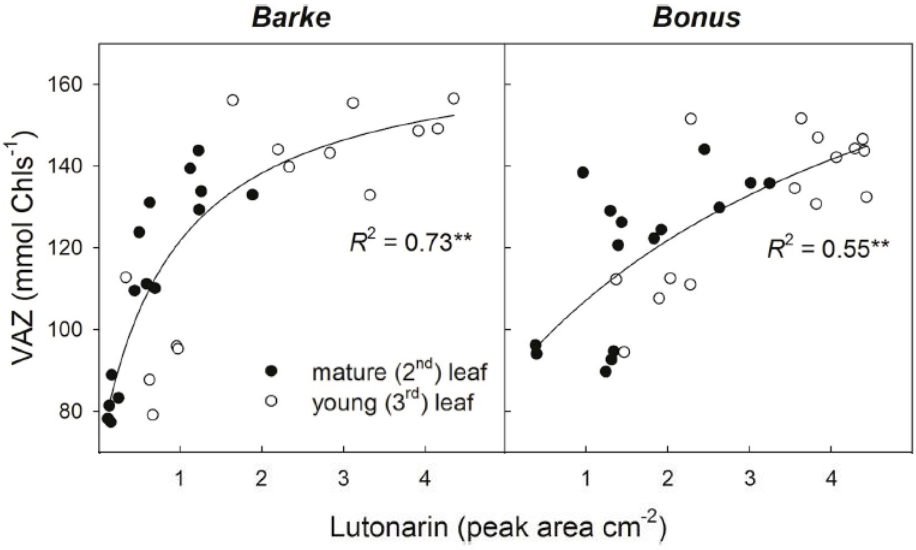

Fig. 25 Relationships between the total content of xanthophyll cycle pigments (VAZ) and the lutonarin content in two barley varieties (Barke, Bonus) at the end of UV/PAR treatments (described in the legend of Fig. 24). A hyperbolic function was fitted to the data of both mature and young leaves together. Points represent individual replicates. The coefficients of determination (R^2) and significance levels (** $p \leq 0.01$) are shown. (**Paper V**)

2.5. Protective action of UV-A radiation during UV-B acclimation

We performed a laboratory experiment to evaluate whether the presence of UV-A radiation during acclimation of barley to a stressful UV-B level prevents UV-B-induced damage to the photosynthetic apparatus (**Paper VI**). Our next objective was to assess the effect of UV-A pre-acclimation on the subsequent acclimation response to a simultaneous exposure to UV-A and UV-B radiation. Barley plants were grown from seeds under low PAR (50 µmol m^{-2} s^{-1}) in the absence or presence of UV-A radiation (UVA- and UVA+ plants, respectively). We used a low PAR level in order to minimize the well-known protective effect of a higher PAR level itself against UV-B exposure (Krizek 2004). UV-A irradiation was 8 W m^{-2} for 16 h per day, together with PAR. After 8 days of development, plants were exposed simultaneously to UV-A and UV-B radiation (0.05 W m^{-2} for 16 h per day) for the next 6 days (UVAB treatment). This duration of acclimation was chosen because we previously found the adjustment of the barley photosynthetic apparatus under increased PAR and UV radiation within this period of time (**Paper III**). In order to monitor the influence of UV-B radiation itself, UVA- plants were also exposed to UVB treatment (without UV-A radiation). The measurements were carried out on the primary leaves of 14-day-old plants, i.e., control UVA- and UVA+ plants and plants at the end of UVAB and UVB treatments (UVA- UVAB, UVA+ UVAB and UVA- UVB plants; see Fig. 26). Taking into account the rapid growth of barley plants, treatments were so short to avoid the effects of ageing of the primary leaves.

As expected, UVB treatment led to negative responses, indicating a disruption of the photosynthetic apparatus function. Exposure of plants grown under low PAR without UV-A (UVA- plants) to UV-B radiation alone resulted in a significant reduction in the CO_2 assimilation rate (A_N; by 44 %), Chl *a+b* content (by 22 %) and the maximum quantum yield of PSII photochemistry (F_V/F_M; from 0.82 to 0.74) (Fig. 26 A-C). Unlike Chls, Cars were not sensitive to UV-B radiation (Fig. 26D). To cope with UV-B radiation, plants retained Cars, maintaining the potential to protect the photosynthetic apparatus under UV-B stress. On the other hand, F_V/F_M remained the same and A_N, total Chls and Cars contents increased in UVA- plants exposed to UVAB treatment. Thus, the presence of UV-A radiation during acclimation to a simultaneous action of UV-A and UV-B radiation not only mitigated, but completely eliminated any negative influence of UV-B radiation on the functioning of the barley photosynthetic apparatus. It can be expected that a higher level of UV-B stress would only lead to a mitigation of UV-B-induced damage by the simultaneous UV-A action (Gartia et al. 2003, Joshi et al. 2007, 2013).

The response of the monitored characteristics to UVAB treatment was not affected by UV-A pre-acclimation, although the increase of both Chls and Cars contents in UVA+ barley under UVAB exposure was statistically insignificant (Fig. 26). Interestingly, while the functional state of PSII was not affected by UV-A pre-acclimation (since both UVA- and UVA+ control plants showed a similar value of F_V/F_M), UVA+ plants had a pronouncedly higher A_N (by 63 %) and a higher content of both total Chls (by 13 %) and total Cars (by 16 %) compared to UVA- plants. This response resembles a typical acclimation response of the photosynthetic apparatus under elevated PAR (Lichtenthaler and Babani 2004). This suggests that the long-wave UV-A spectral region (350-400 nm) used in our experiment can be effectively utilised in photosynthetic reactions, thus compensating for a low level of PAR. Such a pronounced enhancement of A_N per unit leaf area in UVA+ plants was not associated with greater leaf thickness or greater stomatal conductance (**Paper VI**). It seems likely that increased A_N was related to acclimation of the photosynthetic apparatus induced by direct absorption of UV-A radiation by Chls and Cars. As already mentioned in Chapter 2.1., re-absorption of UV-A-induced blue-green

fluorescence emitted by phenolic compounds may contribute to increased A_N (Mantha et al. 2001, Johnson and Day 2002). However, based on a very low level of UV-shielding (and thus a low concentration of phenolic compounds) in UVA+ plants (**Paper VI**), we suppose that this effect is negligible. To conclude, despite the fact that UV-A pre-acclimation led to the adjustment of the photosynthetic apparatus generally observed under elevated PAR, with the potential to better cope with UV-B stress, it was not required for development of the UV-A-induced resistance against UV-B irradiation.

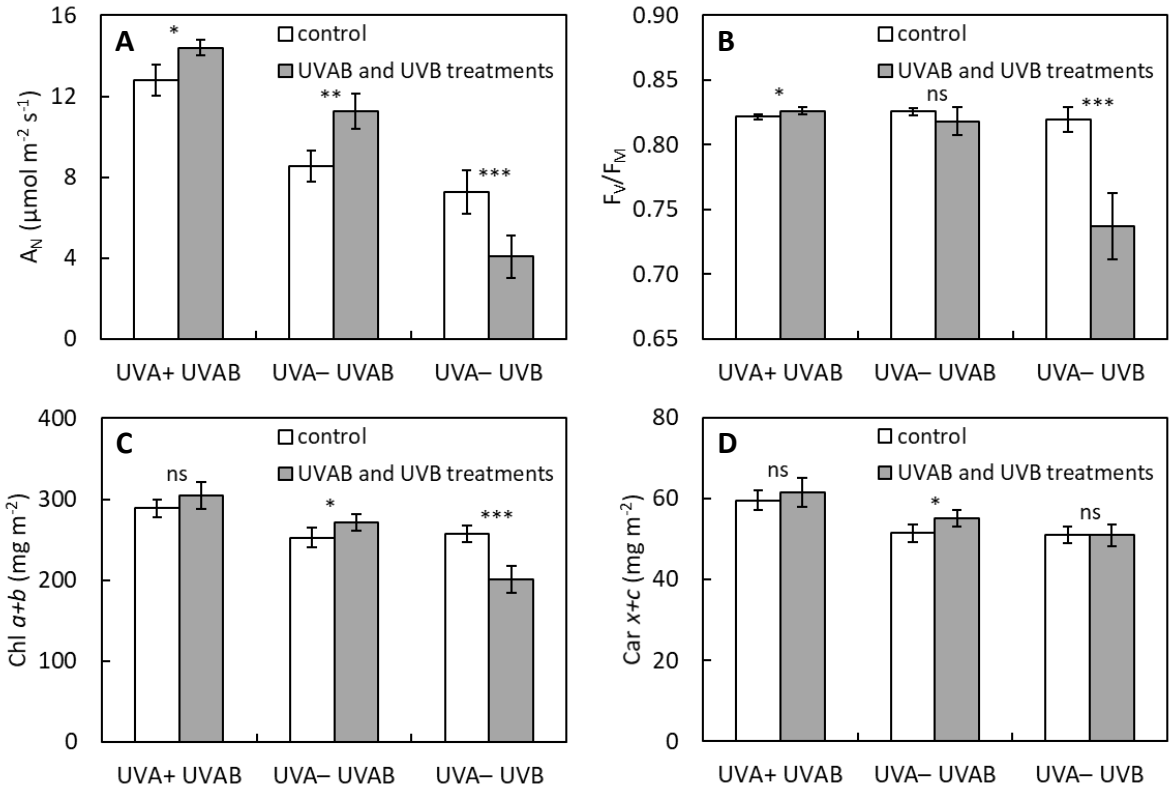

Fig. 26 (A) The CO_2 assimilation rate (A_N), **(B)** the maximum quantum yield of PSII photochemistry (F_V/F_M) and the contents of **(C)** total chlorophylls (Chl *a+b*) and **(D)** total carotenoids (Car *x+c*) per leaf area for barley grown under low PAR (50 µmol m^{-2} s^{-1}) in the presence or absence of UV-A radiation (UVA+ control and UVA- control) after 6 days of acclimation to a simultaneous action of UV-A and UV-B radiation (UVAB) or to UV-B radiation alone (UVB). Measurements were made on 14-day-old plants. A_N was determined in steady state under PAR of 1200 µmol m^{-2} s^{-1}, F_V/F_M was determined after at least 2 h of dark adaptation. Differences between means were tested using Student's *t*-test (*** $p < 0.001$; ** $p < 0.01$; * $p < 0.05$; ns, non-significant). n = 3-6 ± S.D. (**Paper VI**)

3. Acclimation of the photosynthetic apparatus to monochromatic green light

3.1. Effects of green light on plant leaves

While isolated photosynthetic pigments in solution absorb very weakly in the green spectral range (500-600 nm), the absorption of green light (GL) in intact leaves is much higher due to light scattering, which is caused by the water-air interfaces between the water saturated cell walls and the air of the intracellular spaces (Ouzounis et al. 2015; Fig. 27). Although the absorption of GL by leaves is reduced in comparison with other wavelengths of visible light, it represents a substantial fraction of the absorbed light. Typical values of absorptance at 550 nm range from 50 % in *Lactuca sativa* (lettuce) to 90 % in evergreen broad-leaved trees (Inada 1976). The corresponding absorptance values for blue and red lights range from 80 to 95 %. Moreover, on an absorbed quantum basis, the quantum yield of photosynthesis is comparable between GL and red light and greater for GL than for blue light (Hogewoning et al. 2012, Landi et al. 2020). The low quantum yield of blue light is probably due to the fact that some carotenoids (absorbing in the blue spectral region) do not transfer excitation energy to reaction centers, or transfer with an efficiency significantly less than 1.0 (Akimoto and Mimuro 2005).

Based on the absorption spectrum of Chls (Fig. 27A), the penetration of blue, green, and red light into the leaf differs. Blue and red lights are efficiently absorbed close to the surface, whereas GL penetrates deeper into the mesophyll (Brodersen and Vogelmann 2010) and contributes more to photosynthesis in deeper leaf layers, thus decreasing the potentially negative effect of the internal light gradient within the leaf. As a result, GL considerably enhances the efficiency of photosynthetic CO_2 assimilation at the entire leaf level, particularly under moderate and strong white light (Terashima et al. 2009). Similarly, at the canopy level, GL drives photosynthesis in the lower layers of the leaves, where other wavelengths are in limited supply (Smith et al. 2017).

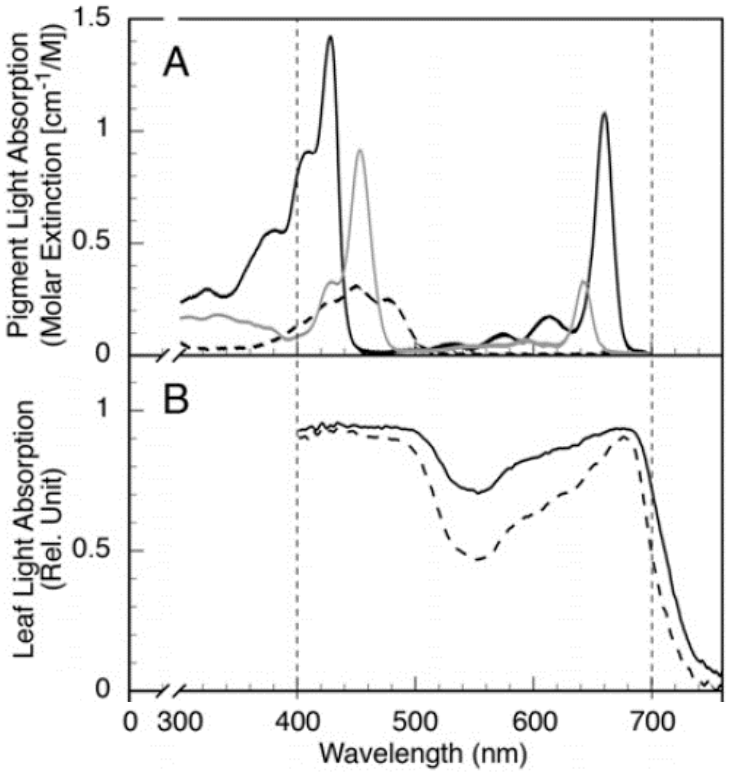

Fig. 27 (A) Absorption spectrum of Chl *a* (black line) and Chl *b* (gray line) in diethyl ether, and β-carotene (dashed line) in hexane. **(B)** Light absorption of the fresh leaf (solid line) of *Chrysanthemum morifolium* and vacuum infiltrated leaf by water (dashed line) to eliminate light scattering (Ouzounis et al. 2015).

Our current understanding of GL photoperception is based on the residual perception by red and blue photoreceptors. No specific green photoreceptor has been identified yet. GL is absorbed by the cryptochromes, photoreceptors that also absorb UV-A and blue light (Bouly et al. 2007). Absorption of GL inactivates cryptochrome and reverses UV-A/blue light-induced physiological responses, such as stomatal opening (Talbott et al. 2002) or anthocyanin accumulation (Bouly et al. 2007, Zhang and Folta 2012). Although phytochromes are characterized as red/far-red sensors, they have a broad absorption spectrum that extends into the green region. This suggests a role for phytochromes as green photoreceptors (Battle et al. 2020). In Arabidopsis plants grown under enriched GL conditions, it was observed that GL induces shade avoidance symptoms (independent of cryptochroms and phytochromes), including petiole elongation and upward orientation of leaves (Zhang et al. 2011). Thus, in addition to an increased proportion of far-red light (a low ratio of red to far-red light), GL is another signal for activating shading responses, enabling plants to adapt development to a low-light environment within a canopy. Green and far-red light together augment shade-induced responses more than green or far-red light alone (Wang et al. 2015).

Supplemental GL has been reported to have a beneficial role in plant growth and photosynthesis (Liu et al. 2017, Bian et al. 2018, Schenkels et al. 2020). On the other hand, acclimation to monochromatic GL adversely affects plant growth, as documented by changes in several morphological and anatomical parameters (for a review, see Landi et al. 2020). For example, GL-grown plants have a reduced number of leaves and leaf area (Su et al. 2014, Gao et al. 2020) as well as a lower stomatal density (Muneer et al. 2014, Liu et al. 2018). The impairment of plant growth can be partly attributed to negative impacts on the photosynthetic apparatus. Compared to plants grown under blue, red or white light, plants grown under GL have lower Chl content, CO_2 assimilation rate, Rubisco content, and PSII efficiency (Muneer et al. 2014, Su et al. 2014, Liu et al. 2018, Gao et al. 2020).

3.2. Identification of an unknown pigment accumulated in barley grown under green light

In barley plants grown under green light (GL; maximum at wavelength of 535 nm, full width at half maximum 35 nm), HPLC analysis of photosynthetic pigment extracts has revealed an extra peak as compared to control plants grown under white light (WL) of the same photosynthetic photon flux density (240 µmol m^{-2} s^{-1}) (Fig. 28; **Paper VII**). The peak of this unknown pigment was eluted between Chl *a* and Chl *b*. Comparing the fractions of unknown pigment and Chl *a* obtained by HPLC, we found no differences in their fluorescence excitation and emission, absorption, and circular dichroism spectra (**Paper VII**), indicating that the unknown pigment could be a Chl *a* derivative.

GL-grown barley contained lower amounts of Chl *a* (Fig. 29A) and approximately 8 and 16 % of Chl *a* derivative relative to the total Chls content after cultivation for 7 and 14 days, respectively (Fig. 29B). When 7 day-old GL plants were exposed to WL for 7 days, the reduction of the Chl *a*/Chls ratio induced by GL was recovered (Fig. 29A) and the accumulation of Chl *a* derivative disappeared almost completely (Fig. 29B). Similarly, pre-cultivation under WL for 7 days caused a pronounced reduction of Chl *a* derivative accumulation by subsequent GL treatment, as compared to barley grown under GL from seeds.

The absence of differences in spectral characteristics between Chl *a* and the Chl *a* derivative in the visible spectrum indicates that the structural difference between these two Chls should be located in the phytyl part of the molecule (Milenković et al. 2012). To confirm this, we performed a mass spectrometry analysis that revealed the presence of different molecular ions for Chl *a* (m/z 891.52)

and the Chl *a* derivative (m/z 889.50). Fragmentation of these two molecular ion adducts led to the same products of m/z 542 and 614, which correspond to tetrapyrrole parts of the Chl *a* molecule (Wei et al. 2013). The mass difference between Chl *a* and its derivative, together with the production of the same tetrapyrrole fragments, suggested the presence of an additional double bond in the phytyl chain of the Chl *a* derivative molecule. Thus, Chl *a* derivative was identified as Chl *a* with a tetrahydrogeranylgeraniol side chain, i.e. containing two double bonds in a phytyl side chain (unlike one double bond in Chl *a* molecule).

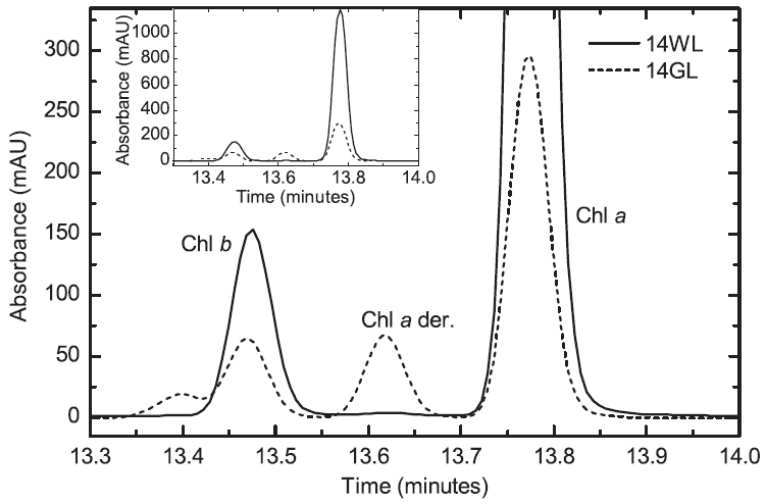

Fig. 28 HPLC chromatograms of photosynthetic pigment extracts from barley plants grown for 14 days under white light (14WL, solid line) and green light (14GL, dashed line), showing the peaks of Chl *b*, Chl *a* derivative (Chl *a* der.) and Chl *a* (**Paper VII**).

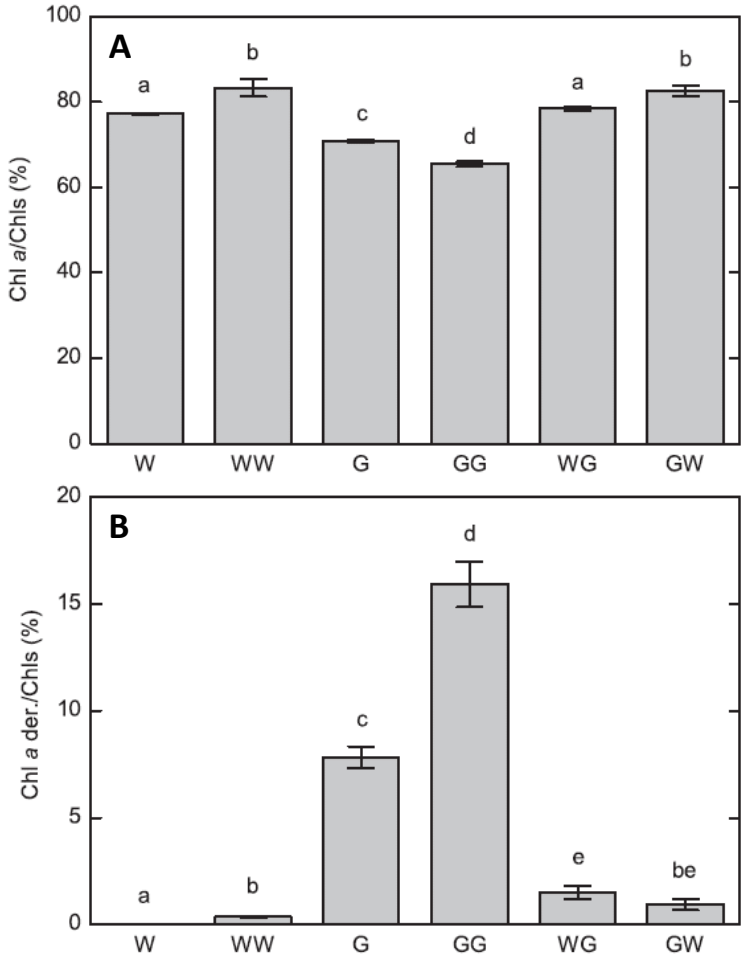

Fig. 29 (A) Chl *a* and **(B)** Chl *a* derivative contents relative to total Chls (Chl *a+b*) in barley plants grown under white light and green light for 7 days (W, G) or 14 days (WW, GG) and plants grown for 7 days under white light followed by 7 days under green light (WG) and vice versa (GW). Chl *a* and Chl *a* derivative in green light-cultivated barley were summed. Different letters denote statistically significant differences (one-way ANOVA followed by Tukey's post hoc test). *n* = 3-4 ± S.D. (**Paper VII**)

This Chl *a* derivative is an intermediate in the final step of the Chl *a* synthesis pathway, driven by the enzyme geranylgeranyl reductase (GGR) (Tanaka et al. 2010). GGR is responsible for the reduction of geranylgeranyl pyrophosphate to phytyl pyrophosphate and the stepwise reduction of Chl *a* with geranylgeraniol (four double bonds) to Chl *a* with dihydrogeranylgeraniol (three double bonds), tetrahydrogeranylgeraniol (two double bonds) and finally to normal phytylated Chl *a* with one double bond. Our result showing the presence of Chl *a* derivative with two double bonds in GL-grown barley suggested a defect in the last step of Chl *a* biosynthesis catalyzed by GGR. Therefore, we assessed the level of GGR by immunodetection and surprisingly found a much higher GGR content in GL-grown plants compared to WL plants (Fig. 30). This demonstrated that the observed accumulation of Chl *a* derivative was not caused by a reduced GGR level, but more likely by an impaired function of this enzyme. However, the exact mechanism of GL-induced accumulation of tetrahydrogeranylgeranyl Chl *a* accompanied by a greatly increased GGR level is not known. We have speculated that the association of Chl *a* derivative with GGR, required to finalize phytol formation, is somehow limited as a result of structural changes in thylakoid membranes and/or a low level of nicotinamide adenine dinucleotide phosphate (NADPH) serving as a cofactor.

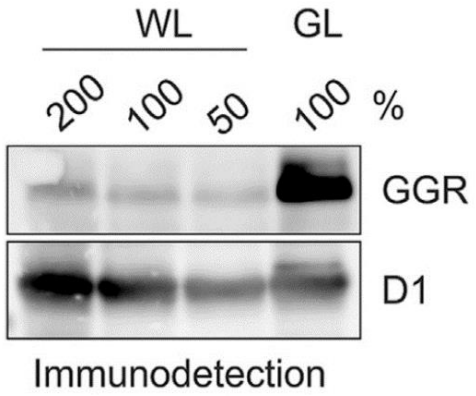

Fig. 30 Levels of geranylgeranyl reductase (GGR) in barley plants grown under white light (WL) and green light (GL). Isolated fractions of membrane proteins were separated by sodium dodecyl sulfate-polyacrylamide gel electrophoresis. Proteins were stained by SYPRO Orange stain, transferred to a polyvinylidene fluoride membrane and probed with antibodies to GGR and the D1 protein of PSII reaction center (**Paper VII**).

3.3. Effects of geranylgeranylated chlorophylls on PSII organization and function in Arabidopsis

When Arabidopsis plants grown under WL (100 µmol m^{-2} s^{-1}) for 8 weeks were transferred to GL of the same photosynthetic photon flux density for 2 weeks, newly developed leaves under GL conditions contained various Chl derivatives with different degree of the phytyl chain saturation (**Paper VIII**). This is in contrast to GL-grown barley, when only one type of Chl *a* derivative was detected (Fig. 28). HPLC chromatograms of photosynthetic pigment extracts have revealed peaks corresponding to different Chl *a* and Chl *b* derivatives, because they had the same absorption spectra as Chl *a* and Chl *b*, suggesting that structural differences are located on the phytyl side chain (Fig. 31). On the basis of mass spectrometry analysis, we could conclude that the detected Chl derivatives contain tetrahydrogeranylgeranyl (THGG), dihydrogeranylgeranyl (DHGG), or geranylgeranyl (GG) side chains instead of the phytyl. Chl, Chl_{THGG}, Chl_{DHGG}, and Chl_{GG} molecules have one, two, three, and four double bonds on their side chains, respectively.

Arabidopsis leaves developed under GL contained large amounts of geranylgeranylated Chls *a* and *b* (more than 50 %; Fig. 32A). The most abundant Chl derivative was Chl_{GG}. In order to determine the localization of Chl derivatives in the individual pigment-protein complexes, we estimated their contents in complexes separated by Clear-native polyacrylamide gel electrophoresis. Analysis of the

gel images showed increased amounts of the smaller protein complexes (LHCII trimers and monomers) at the expense of large supercomplexes in GL-acclimated plants compared to WL plants. Both Chl *a* and Chl *b* derivatives were present in all pigment-protein complexes and PSII supercomplexes (Fig. 32B). The distribution of Chl derivatives among the individual complexes indicated their increasing proportion with the decreasing size of the complexes. The proportion of the total Chl derivatives in the largest investigated complex, PSII supercomplex C2S2M2, was approximately 20 % less than in the thylakoid membranes. On the other hand, the proportion in the smallest LHCII monomers was about 10 % higher as compared to thylakoid membranes. The presence of geranylgeranylated Chls *a* and *b* did not affect the ratio of Chl *a/b* and the amount of total carotenoids and their composition in the individual pigment-protein complexes (see the supplementary material of **Paper VIII**).

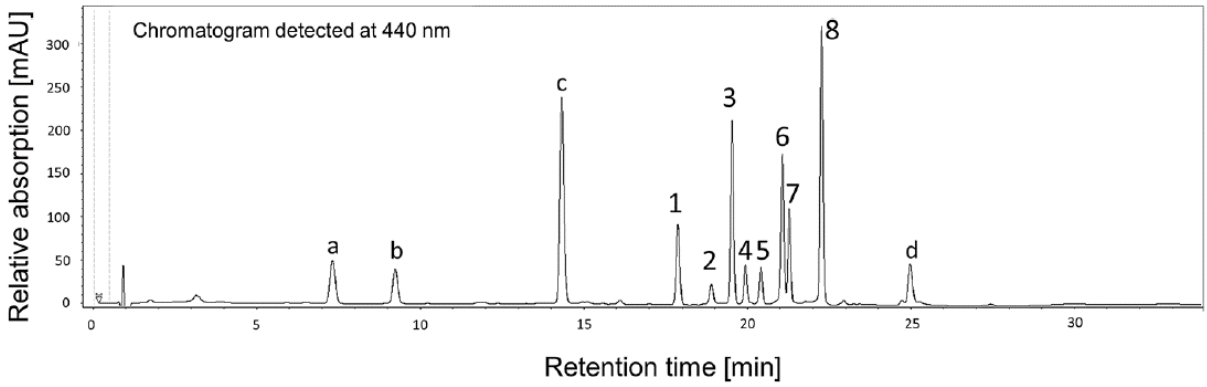

Fig. 31 HPLC chromatogram of photosynthetic pigment extract from Arabidopsis leaves developed during two weeks under green light. Peak 1 – Chl b_{GG}, 2 – Chl b_{DHGG}, 3 – Chl a_{GG}, 4 – Chl b_{THGG}, 5 – Chl a_{DHGG}, 6 – Chl *b*, 7 – Chl a_{THGG}, 8 – Chl *a*, a – neoxanthin, b – violaxanthin, c – lutein + zeaxanthin, d – β-carotene. THGG – tetrahydrogeranylgeranyl, DHGG – dihydrogeranylgeranyl, GG – geranylgeranyl (**Paper VIII**)

We found that accumulation of geranylgeranylated Chls impaired photosynthetic performance. As already mentioned, the formation of PSII and PSI supercomplexes and megacomplexes was reduced in GL plants. We observed a pronouncedly lower PSII activity, as indicated by a reduction of the maximum quantum yield of PSII photochemistry (F_V/F_M) to a value of 0.65. This decrease was mainly due to a twofold increase in minimal fluorescence (F_0) corresponding to Chls functionally uncoupled from the PSII reaction centers (Belgio et al. 2012, Ware et al. 2015). This appears to be associated with the accumulation of LHCII trimers and monomers that are not connected with the super- and megacomplexes. The presence of free LHCIIs in GL-acclimated plants resulted in a strong F_0 quenching (SV_0) that was 10 times higher than in WL plants after 10 min of exposure to WL with an intensity of 1200 µmol m^{-2} s^{-1}.

Circular dichroism and 77 K fluorescence spectroscopy were used to assess the organization of pigment-protein complexes in the thylakoid membranes. The low-temperature spectra of Chl fluorescence emission clearly showed that the organization of both PSII and PSI was affected (Fig. 33A). PSI emission maximum in GL plants was shifted by 4 nm to shorter wavelengths. This can be explained by increased emission from the PSI core (720 nm) at the expense of LHCI emission (735 nm), which can be seen in the differential spectra (GL minus WL). This shift of PSI emission maximum can be a sign of PSI-LHCI destabilization (Nellaepalli et al. 2014) or alternatively, the association of geranylgeranylated Chls with the respective apoproteins affects the structure of the PSI-LHCI supercomplex. Further, GL-acclimated plants revealed a lower emission from LHCII (680 nm) and a pronounced emission at 700 nm originating from LHCII aggregates (Chmeliov et al. 2016).

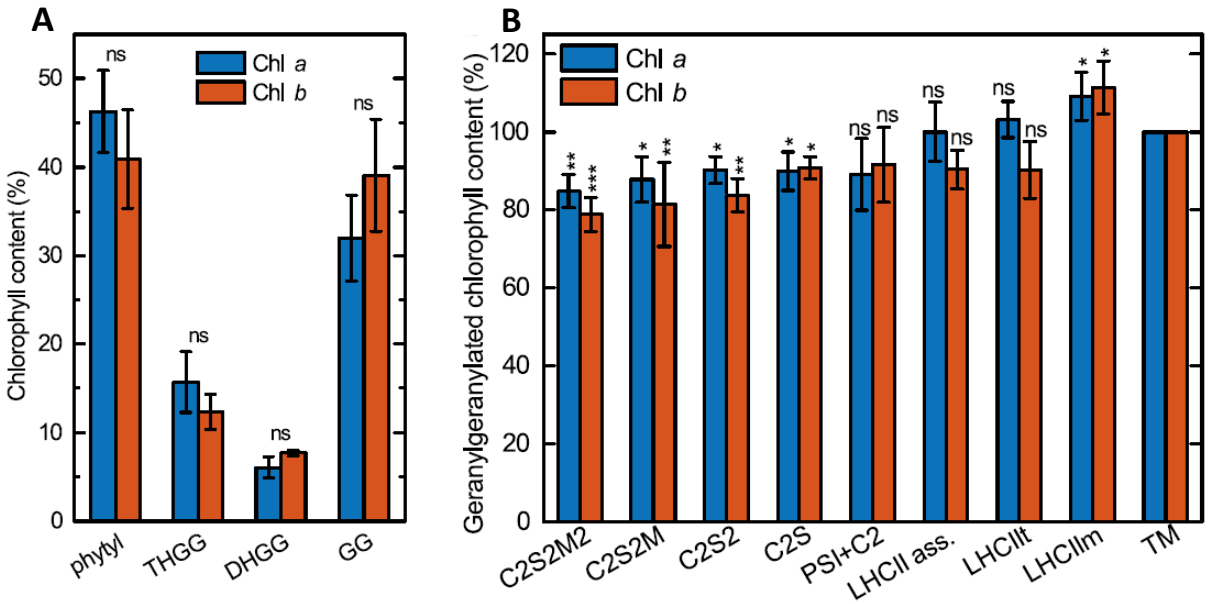

Fig. 32 (A) Amounts of phytylated (phytyl), tetrahydrogeranylgeranylated (THGG), dihydrogeranylgeranylated (DHGG), and geranylgeranylated (GG) Chls *a* and *b* relative to their total contents in the thylakoid membranes isolated from Arabidopsis leaves developed during two weeks under green light. $n = 4 \pm$ S.D. (ns, non-significant difference, Student's *t*-test). **(B)** Amounts of geranylgeranylated Chls *a* and *b* (sum of THGG, DHGG and GG Chls) in the individual pigment-protein complexes and PSII supercomplexes (C2S2M2, C2S2M, C2S2, C2S) relative to their amounts in the thylakoid membranes. The asterisks indicate statistically significant differences (Kruskal–Wallis ANOVA followed by Dunn's post hoc test) between the given protein complexes and the thylakoid membranes (* $p < 0.05$; ** $p < 0.01$; *** $p < 0.001$). $n = 3 \pm$ S.D. (C2 – PSII core dimer, S and M – strongly and moderately bound LHCII trimers, LHCII ass. – LHCII assembly (LHCII-Lhcb4-Lhcb6), LHCIIt – LHCII trimers, LHCIIm – LHCII monomers, TM – thylakoid membranes) (**Paper VIII**)

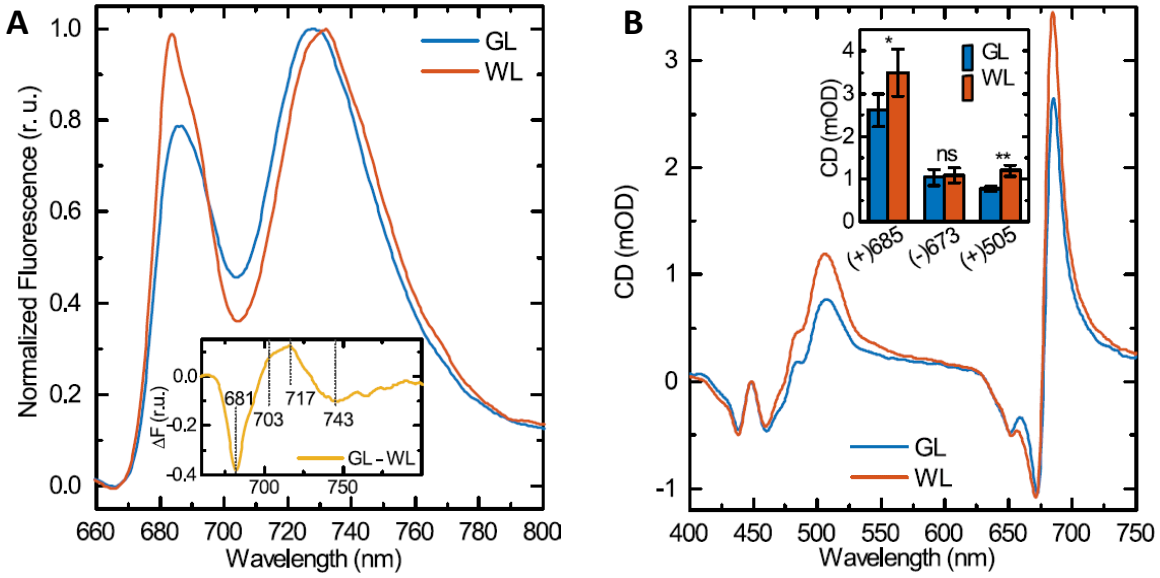

Fig. 33 (A) 77 K Chl fluorescence emission spectra of thylakoid membranes isolated from Arabidopsis acclimated to green light (GL) and white light (WL). The spectra were excited at 476 nm and normalized to PSI emission. Average spectra of four replicates are presented. The inset shows the differential spectrum (GL minus WL). **(B)** Circular dichroism (CD) spectra of thylakoid membranes isolated from GL- and WL-acclimated Arabidopsis. Average spectra normalized to the Q_y absorbance maximum are presented. The inset shows the amplitudes of Ψ-type CD bands. Asterisks indicate statistically significant differences (Student's *t*-test) between GL and WL (* $p < 0.05$; ** $p < 0.01$; ns, non-significant difference). $n = 4 \pm$ S.D. (**Paper VIII**)

The circular dichroism spectra of GL plants showed lower amplitudes of the Ψ-type bands (+)685 nm and (+)505 nm, which depend on the lateral supramolecular organization of PSII and PSII-LHCII supercomplexes (Tóth et al. 2016) (Fig. 33B). The third main Ψ-type band (-)673 nm, which is preferentially associated with grana stacking (Garab et al. 1991), remained unchanged compared to WL control plants. We can therefore conclude that acclimation to GL led to a reduced chiral macro-organization of PSII-LHCII supercomplexes, while not affecting the formation of LHCII trimers and granal stacking. In addition, we also performed an analysis of the thermal stability of pigment-protein complexes and found that the accumulation of geranylgeranylated Chls reduced the thermal stability of the photosystem complexes, especially that of LHCII trimers (**Paper VIII**). The higher thermal susceptibility of LHCII trimers compared to those of the PSI-LHCI and PSII-LHCII supercomplexes corresponds to the observed higher content of Chl derivatives in LHCII.

Conclusions

We have demonstrated that Norway spruce and Arabidopsis (the representative of annual angiosperms) use largely different regulatory mechanisms in the adjustment of their photosynthetic processes and photoprotection in light acclimation (**Paper II**). While Arabidopsis controls the photosynthetic performance and photoprotection through specific modulation of the amounts of individual components of the photosynthetic apparatus, Norway spruce relies only on the activation of strong photoprotective mechanisms, without maximization of its photosynthetic performance. This corresponds to the lifeform of slowly growing long-lived evergreen species that must have a high level of photoprotection and resistance to stress in order to survive prolonged periods of severe environmental conditions. As crucial photoprotective mechanisms in spruce, we have identified cyclic electron transport around PSI, photosynthetic control maintaining P700 in the photoprotective oxidized state, and mainly "locked-in" NPQ, which is associated with the presence of LHCIIs weakly bound to the PSII core.

An interesting question is whether the different acclimation strategy in spruce is due to its unique PSII and PSI organization, or rather reflects the evergreen lifeform. Our data indicate that high light (HL) acclimation of spruce shares common features with HL acclimation of *Monstera deliciosa*, a shade-tolerant tropical evergreen angiosperm species, such as synthesis of stress proteins and a strong "locked-in" NPQ associated with retention of zeaxanthin and a pronounced PSII down-regulation (Demmig-Adams et al. 2006). Unlike spruce, Monstera possess genes for both Lhcb3 and Lhcb6 proteins (Michael et al. 2017). Therefore, it seems that the absence of Lhcb3 and Lhcb6 proteins is not a prerequisite for the acclimation strategy that we described in spruce. In this context, it would be worth studying the acclimation strategy of larch with a life strategy different from spruce, as it is a deciduous conifer, but it lacks Lhcb3 and Lhcb6 proteins like spruce, because it belongs to the same family of Pinaceae (Kouřil et al. 2016). It is possible that the specific light acclimation strategy of Norway spruce might be common to many shade-tolerant evergreen plants, even from evolutionarily distant plant groups in the land plant kingdom. These plants, which include a large group of non-flowering plants and perennial angiosperms, appear to have a low ability to regulate LHCII size after change in light intensity, i.e., they have stable Chl *a/b* ratios as spruce (see Ferroni et al. 2016 for lycophytes, Gerotto et al. 2011 for bryophytes, and Murchie and Horton 1997 for angiosperms).

The specific light acclimation strategy in spruce, described in **Paper II**, occurs under excess light conditions that result in a permanently reduced maximum photochemical efficiency of PSII (F_V/F_M). In another study, spruce was exposed to elevated acclimation light intensity, but at a non-excessive level, as F_V/F_M remained optimal (**Paper I**). In this case, the LHCII size was modulated after transfer of plants from low light conditions to elevated irradiance, although the Chl *a/b* value of our low light-acclimated needles was relatively high, close to sun-exposed needles under field conditions (compare with data in Špunda et al. 1998 or Urban et al. 2012). Thus, it seems that the degree of light stress, the hallmark of which is the level of F_V/F_M lowering, determines the resulting acclimation response under elevated irradiance. In any case, it would be worthwhile to carry out mass spectrometry analysis that would unequivocally confirm whether increase of Chl *a/b* in HL-acclimated spruce without PSII photoinhibition was indeed associated with a reduction of LHCII antenna. We further pointed to the importance of non-assimilatory electron transport pathways (probably photorespiration) in the adjustment of photosynthetic performance of spruce under combined effect of elevated irradiance and air temperature (**Paper I**).

In the field study of acclimation of wild-type barley and its Chl *b*-less mutant *chlorina f2* to naturally occurring high levels of visible and UV light, we have demonstrated the complementarity of UV-shielding and carotenoid-dependent processes in PSII photoprotection (**Paper III**). The age dependence of UV-shielding development has been reported for leaves of different age (e.g., Bilger et al. 2001, Klem et al. 2012). Using the Karlsruhe fluorescence imaging system (Lenk and Buschmann 2006) we have revealed that the differences in UV-shielding induction among the leaves of different age occur also within the leaf blade, which is related to a different development stage of a leaf tissue.

Both PAR and UV radiation represent important environmental factors that control the photoprotective capacity of plants. The findings of the study with the barley variety Barke, which is sensitive to photooxidative stress, have highlighted the importance of the presence of UV radiation under elevated PAR conditions in the accumulation of photoprotective phenolics and xanthophyll cycle pigments, and subsequent resistance to high radiation stress (**Paper IV**). We found that supplemental UV radiation during acclimation of barley can induce enhanced photoprotection and thus contribute to acquired high radiation stress tolerance.

Furthermore, we have shown in barley that both genotype and leaf age can strongly modulate constitutive and UV/PAR-inducible accumulation of phenolic compounds and UV-shielding (**Paper V**). The accumulation of phenolic compounds is orchestrated by the accumulation of xanthophyll cycle pigments (VAZ) to provide balanced protective functions in plants. The observed relationships between contents of VAZ and some phenolic compounds (particularly lutonarin) indicate that the accumulation of VAZ can compensate for the insufficient efficiency of antioxidative protection mediated by phenolic compounds.

Another important finding is the protective role of UV-A radiation (at least the long-wave spectral region above 350 nm) under UV-B stress. Our results revealed that UV-A radiation during acclimation of low PAR-grown barley to simultaneous exposure to UV-A and UV-B prevented UV-B-induced damage to the photosynthetic apparatus regardless of whether the plants were pre-acclimated to UV-A or not (**Paper VI**). We found that barley grown under low PAR with supplemental UV-A radiation adjusted its photosynthetic apparatus as in the case of acclimation to elevated PAR. This could be due to the absorption of UV-A radiation by photosynthetic pigments and specific photoreceptors.

It has long been known that blue light initiates changes of leaf characteristics that occur during HL acclimation (Buschmann et al. 1978, Lichtenthaler and Buschmann 1978, Hogewoning et al. 2010). There are indications that photoreceptors are involved in the regulation of light acclimation (Kleine et al. 2007, Costa et al. 2013). Blue-light photoreceptors, phototropins and cryptochromes, absorb also in the UV-A spectral region (Christie et al. 2015). Based on this we suppose that the observed response in barley under UV-A exposure, resembling the response of HL-acclimated plants, could be induced by the effect of UV-A radiation as described earlier for blue light.

In barley plants grown under monochromatic green light (GL; 500-590 nm), we have revealed an unusual accumulation of tetrahydrogeranylgeranyl Chl *a*, which is a Chl *a* derivative containing two double bonds in the phytyl side chain instead of one in the Chl *a* molecule (**Paper VII**). A large amount of this intermediate of Chl *a* synthesis was accompanied by a massive increase in the level of the enzyme geranylgeranyl reductase (GGR), which is responsible for the reduction of phytyl chain double bonds in the Chl *a* synthesis pathway. This led us to conclude that the GGR function is impaired in barley grown under GL. This surprising sensitivity of the GGR enzymatic step to GL appears to be common to higher plants. The same effect of GL as in barley (monocotyledonous angiosperm) we also observed in basil, sunflower and Arabidopsis (dicotyledonous angiosperms with C3 metabolism),

amaranth (dicotyledonous angiosperm with C4 metabolism) and Norway spruce (gymnosperm), although the level of accumulation of Chl *a* derivative was species-dependent (**Papers VII and VIII**). Recently, GL-induced accumulation of geranylgeranylated chlorophylls was also detected in the representative of green algae, the marine chlorophyte *Picochlorum sp.* (Paper et al. 2022).

In the study with GL-acclimated Arabidopsis plants, we detected geranylgeranylated Chl *a* and *b* with a different degree of the phytyl chain saturation (**Paper VIII**). These Chl derivatives were found to be incorporated in all photosystem complexes, although their accumulation was preferred in LHCII at the expense of PSII supercomplexes. The presence of geranylgeranylated Chls hampered the formation of PSII and PSI supercomplexes and megacomplexes as well as their assembly into chiral macrodomains. Other findings include impaired photosynthetic performance in GL Arabidopsis and reduced thermal stability of thylakoid pigment-protein complexes, especially LHCII trimers. We evaluated the consequences of the accumulated geranylgeranylated Chls on the structure and function of the photosynthetic apparatus, however, the role of GL in determining the deficiency of GGR activity remains to be elucidated.

References

Agati G, Brunetti C, Fini A, Gori A, Guidi L, Landi M, Sebastiani F, Tattini M (2020) Are flavonoids effective antioxidants in plants? Twenty years of our investigation. *Antioxidants* 9: 1098

Akimoto S, Mimuro M (2005) Excitation relaxation dynamics of carotenoids probed by ultrafast fluorescence spectroscopy. In: Wada N, Mimuro M (eds.), *Recent Progress of Bio/Chemiluminescence and Fluorescence Analysis in Photosynthesis*, Research Signpost, Kerala, India, pp 213–214

Albanese P, Manfredi M, Meneghesso A, Marengo E, Saracco G, Barber J, Morosinotto T, Pagliano C (2016) Dynamic reorganization of photosystem II supercomplexes in response to variations in light intensities. *Biochim Biophys Acta-Bioenerg* 1857: 1651–1660

Albanese P, Manfredi M, Re A, Marengo E, Saracco G, Pagliano C (2018) Thylakoid proteome modulation in pea plants grown at different irradiances: quantitative proteomic profiling in a non-model organism aided by transcriptomic data integration. *Plant J* 96: 786–800

Albanese P, Manfredi M, Marengo E, Saracco G, Pagliano C (2019) Structural and functional differentiation of the light-harvesting protein Lhcb4 during land plant diversification. *Physiol Plant* 166: 336–350

Allen JF (2017) Why we need to know the structure of phosphorylated chloroplast light-harvesting complex II. *Physiol Plant* 161: 28–44

Allen JF, Forsberg J (2001) Molecular recognition in thylakoid structure and function. *Trends Plant Sci* 6: 317–326

Anderson JM (1986) Photoregulation of the composition, function, and structure of thylakoid membranes. *Annu Rev Plant Physiol Plant Mol Biol* 37: 93–136

Andersson B, Aro E-M (1997) Proteolytic activities and proteases of plant chloroplasts. *Physiol Plant* 100: 780–793

Arshad R, Saccon F, Bag P, Biswas A, Calvaruso C, Bhatti AF, Grebe S, Mascoli V, Mahbub M, Muzzopappa F, Polyzois A, Schiphorst C, Sorrentino M, Streckaité S, van Amerongen H, Aro E-M, Bassi R, Boekema EJ, Croce R, Dekker J, van Grondelle R, Jansson S, Kirilovsky D, Kouřil R, Michel S, Mullineaux CW, Panzarová K, Robert B, Ruban AV, van Stokkum I, Wientjes E, Büchel C (2022) A kaleidoscope of photosynthetic antenna proteins and their emerging roles. *Plant Physiol* 189: 1204–1219

Bag P, Chukhutsina V, Zhang ZS, Paul S, Ivanov AG, Shutova T, Croce R, Holzwarth AR, Jansson S (2020) Direct energy transfer from photosystem II to photosystem I confers winter sustainability in Scots Pine. *Nat Commun* 11: 6388

Bai TY, Guo L, Xu MY, Tian LR (2021) Structural diversity of Photosystem I and its light-harvesting system in eukaryotic algae and plants. *Front Plant Sci* 12: 781035

Bailey S, Walters RG, Jansson S, Horton P (2001) Acclimation of *Arabidopsis thaliana* to the light environment: the existence of separate low light and high light responses. *Planta* 213: 794–801

Bailey S, Horton P, Walters RG (2004) Acclimation of *Arabidopsis thaliana* to the light environment: the relationship between photosynthetic function and chloroplast composition. *Planta* 218: 793–802

Baker NR (2008) Chlorophyll fluorescence: a probe of photosynthesis *in vivo*. *Annu Rev Plant Biol* 59: 89–113

Ballottari M, Dall'Osto L, Morosinotto T, Bassi R (2007) Contrasting behavior of higher plant photosystem I and II antenna systems during acclimation. *J Biol Chem* 282: 8947–8958

Barber J (1995) Molecular basis of the vulnerability of photosystem II to damage by light. *Austr J Plant Physiol* 22: 201–208

Bassi R, Dall'Osto L (2021) Dissipation of light energy absorbed in excess: The molecular mechanisms. *Annu Rev Plant Biol* 72: 47–76

Battle MW, Vegliani F, Jones MA (2020) Shades of green: untying the knots of green photoperception. *J Exp Bot* 71: 5764–5770

Belgio E, Johnson MP, Juric S, Ruban AV (2012) Higher plant photosystem II light-harvesting antenna, not the reaction center, determines the excited-state lifetime-both the maximum and the nonphotochemically quenched. *Biophys J* 102: 2761–2771

Bian ZH, Yang QC, Li T, Cheng RF, Barnett Y, Lu CG (2018) Study of the beneficial effects of green light on lettuce grown under short-term continuous red and blue light-emitting diodes. *Physiol Plant* 164: 226–240

Bilger W, Björkman O (1990) Role of the xanthophyll cycle in photoprotection elucidated by measurements of light-induced absorbance changes, fluorescence and photosynthesis in leaves of *Hedera canariensis*. *Photosynth Res* 25: 173–185

Bilger W, Johnsen T, Schreiber U (2001) UV-excited chlorophyll fluorescence as a tool for the assessment of UV-protection by the epidermis of plants. *J Exp Bot* 52: 2007–2014

Bouly J-P, Schleicher E, Dionisio-Sese M, Vandenbussche F, Van Der Straeten D, Bakrim N, Meier S, Batschauer A, Galland P, Bittl R, Ahmad M (2007) Cryptochrome blue light photoreceptors are activated through interconversion of flavin redox states. *J Biol Chem* 282: 9383–9391

Brodersen CR, Vogelmann TC (2010) Do changes in light direction affect absorption profiles in leaves? *Funct Plant Biol* 37: 403–412

Brugnoli E, Scartazza A, De Tullio MC, Monteverdi MC, Lauteri M, Augusti A (1998) Zeaxanthin and non-photochemical quenching in sun and shade leaves of C_3 and C_4 plants. *Physiol Plant* 104: 727–734

Bukhov NG, Carpentier R (2003) Measurement of photochemical quenching of absorbed quanta in photosystem I of intact leaves using simultaneous measurements of absorbance changes at 830 nm and thermal dissipation. *Planta* 216: 630–638

Buschmann C, Meier D, Kleudgen HK, Lichtenthaler HK (1978) Regulation of chloroplast development by red and blue light. *Photochem Photobiol* 27: 195–198

Caffarri S, Tibiletti T, Jennings RC, Santabarbara S (2014) A comparison between plant photosystem I and photosystem II architecture and functioning. *Curr Protein Pept Sci* 15: 296–331

Chmeliov J, Gelzinis A, Songaila E, Augulis R, Duffy CDP, Ruban AV, Valkunas L (2016) The nature of self-regulation in photosynthetic light-harvesting antenna. *Nat Plants* 2: 16045

Christie JM, Blackwood L, Petersen J, Sullivan S (2015) Plant flavoprotein photoreceptors. *Plant Cell Physiol* 56: 401–413

Cooley NM, Higgins JT, Holmes MG, Attridge TH (2001) Ecotypic differences in responses of *Arabidopsis thaliana* L. to elevated polychromatic UV-A and UV-B+A radiation in the natural environment: a positive correlation between UV-B+A inhibition and growth rate. *J Photochem Photobiol B: Biol* 60: 143–150

Costa BS, Jungandreas A, Jakob T, Weisheit W, Mittag M, Wilhelm C (2013) Blue light is essential for high light acclimation and photoprotection in the diatom *Phaeodactylum tricornutum*. *J Exp Bot* 64: 483–493

Demmig-Adams B (1998) Survey of thermal energy dissipation and pigment composition in sun and shade leaves. *Plant Cell Physiol* 39: 474–482

Demmig-Adams B, Adams WW (2006) Photoprotection in an ecological context: the remarkable complexity of thermal energy dissipation. *New Phytol* 172: 11–21

Demmig-Adams B, Adams WW III, Barker DH, Logan BA, Bowling DR, Verhoeven AS (1996) Using chlorophyll fluorescence to assess the fraction of absorbed light allocated to thermal dissipation of excess excitation. *Physiol Plant* 98: 253–264

Demmig-Adams B, Ebbert V, Mellman DL, Mueh KE, Schaffer L, Funk C, Zarter CR, Adamska I, Jansson S, Adams WW III (2006) Modulation of PsbS and flexible vs sustained energy dissipation by light environment in different species. *Physiol Plant* 127: 670–680

Demmig-Adams B, Cohu CM, Muller O, Adams WW III (2012) Modulation of photosynthetic energy conversion efficiency in nature: from seconds to seasons. *Photosynth Res* 113: 75–88

Demmig-Adams B, Koh SC, Cohu CM, Muller O, Stewart JJ, Adams WW III (2014) Non-photochemical fluorescence quenching in contrasting plant species and environments. In: Demmig-Adams B, Garab G, Adams WW III and Govindjee (eds.), *Non-Photochemical Quenching and Energy Dissipation in*

Plants, Algae and Cyanobacteria. Advances in Photosynthesis and Respiration 40, Springer, Dordrecht, pp 531–552

Eberhard S, Finazzi G, Wollman FA (2008) The dynamics of photosynthesis. *Annu Rev Genet* 42: 463–515

Ferroni L, Suorsa M, Aro EM, Baldisserotto C, Pancaldi S (2016) Light acclimation in the lycophyte *Selaginella martensii* depends on changes in the amount of photosystems and on the flexibility of the light-harvesting complex II antenna association with both photosystems. *New Phytol* 211: 554–568

Floris M, Bassi R, Robaglia C, Alboresi A, Lanet E (2013) Post-transcriptional control of light-harvesting genes expression under light stress. *Plant Mol Biol* 82: 147–154

Franco AC, Matsubara S, Orthen B (2007) Photoinhibition, carotenoid composition and the co-regulation of photochemical and non-photochemical quenching in neotropical savanna trees. *Tree Physiol* 27: 717–725

Gao S, Liu XN, Liu Y, Cao BL, Chen ZJ, Xu K (2020) Photosynthetic characteristics and chloroplast ultrastructure of welsh onion (*Allium fistulosum* L.) grown under different LED wavelengths. *BMC Plant Biol* 20: 78

Garab G, Kieleczawa J, Sutherland JC, Bustamante C, Hind G (1991) Organization of pigment-protein complexes into macrodomains in the thylakoid membranes of wild-type and chlorophyll *b*-less mutant of barley as revealed by circular dichroism. *Photochem Photobiol* 54: 273–281

Gartia S, Pradhan MK, Joshi PN, Biswal UC, Biswal B (2003) UV-A irradiation guards the photosynthetic apparatus against UV-B-induced damage. *Photosynthetica* 41: 545–549

Genty B, Briantais JM, Baker NR (1989) The relationship between the quantum yield of photosynthetic electron transport and quenching of chlorophyll fluorescence. *Biochim Biophys Acta* 990: 87–92

Gerotto C, Alboresi A, Giacometti GM, Bassi R, Morosinotto T (2011) Role of PSBS and LHCSR in *Physcomitrella patens* acclimation to high light and low temperature. *Plant Cell Environ* 34: 922–932

Gilmore AM, Yamamoto HY (1991) Zeaxanthin formation and energy-dependent fluorescence quenching in pea chloroplasts under artificially mediated linear and cyclic electron transport. *Plant Physiol* 96: 635–643

Grebe S, Trotta A, Bajwa AA, Suorsa M, Gollan PJ, Jansson S, Tikkanen M, Aro EM (2019) The unique photosynthetic apparatus of Pinaceae: analysis of photosynthetic complexes in *Picea abies*. *J Exp Bot* 70: 3211–3225

Grebe S, Trotta A, Bajwa AA, Mancini I, Bag P, Jansson S, Tikkanen M, Aro EM (2020) Specific thylakoid protein phosphorylations are prerequisites for overwintering of Norway spruce (*Picea abies*) photosynthesis. *Proc Natl Acad Sci USA* 117: 17499–17509

Harrison MA, Nemson JA, Melis A (1993) Assembly and composition of the chlorophyll *a-b* light-harvesting complex of barley (*Hordeum vulgare* L.): immunochemical analysis of chlorophyll *b*-less and chlorophyll *b*-deficient mutants. *Photosynth Res* 38: 141–151

Hendrickson L, Furbank RT, Chow WS (2004) A simple alternative approach to assessing the fate of absorbed light energy using chlorophyll fluorescence. *Photosynth Res* 82: 73–81

Hideg É, Jansen MAK, Strid Å (2013) UV-B exposure, ROS, and stress: inseparable companions or loosely linked associates? *Trends Plant Sci* 18: 107–115

Hogewoning SW, Trouwborst G, Maljaars H, Poorter H, van Ieperen W, Harbinson J (2010) Blue light dose-responses of leaf photosynthesis, morphology, and chemical composition of *Cucumis sativus* grown under different combinations of red and blue light. *J Exp Bot* 61: 3107–3117

Hogewoning SW, Wientjes E, Douwstra P, Trouwborst G, van Ieperen W, Croce R, Harbinson J (2012) Photosynthetic quantum yield dynamics: from photosystems to leaves. *Plant Cell* 24: 1921–1935

Huang W, Zhang J-L, Zhang S-B, Hu H (2014) Evidence for the regulation of leaf movement by photosystem II activity. *Environ Exp Bot* 107: 167–172

Hunt L, Klem K, Lhotáková Z, Vosolsobě S, Oravec M, Urban O, Špunda V, Albrechtová J (2021) Light and CO_2 modulate the accumulation and localization of phenolic compounds in barley leaves. *Antioxidants* 10: 385

Hutin C, Nussaume L, Moise N, Moya I, Kloppstech K, Havaux M (2003) Early light-induced proteins protect Arabidopsis from photooxidative stress. *Proc Natl Acad Sci USA* 100: 4921–4926

Ilík P, Pavlovič A, Kouřil R, Alboresi A, Morosinotto T, Allahverdiyeva Y, Aro EM, Yamamoto H, Shikanai T (2017) Alternative electron transport mediated by flavodiiron proteins is operational in organisms from cyanobacteria up to gymnosperms. *New Phytol* 214: 967–972

Inada K (1976) Action spectra for photosynthesis in higher plants. *Plant Cell Physiol* 17: 355–365

Jahns P, Holzwarth AR (2012) The role of the xanthophyll cycle and of lutein in photoprotection of photosystem II. *Biochim Biophys Acta-Bioenerg* 1817: 182–193

Jansen MAK, Gaba V, Greenberg BM (1998) Higher plants and UV-B radiation: balancing damage, repair and acclimation. *Trends Plant Sci* 3: 131–135

Johnson GA, Day TA (2002) Enhancement of photosynthesis in *Sorghum bicolor* by ultraviolet radiation. *Physiol Plant* 116: 554–562

Joshi PN, Ramaswamy NK, Iyer RK, Nair JS, Pradhan MK, Gartia S, Biswal B, Biswal UC (2007) Partial protection of photosynthetic apparatus from UV-B-induced damage by UV-A radiation. *Environ Exp Bot* 59: 166–172

Joshi PN, Gartia S, Pradhan MK, Panigrahi S, Nayak L, Biswal B (2013) Acclimation of clusterbean cotyledon to UV-B radiation in the presence of UV-A: partial restoration of photosynthetic energy balance and redox homeostasis. *Acta Physiol Plant* 35: 2323–2328

Kalina J, Urban O, Čajánek M, Kurasová I, Špunda V, Marek MV (2001) Different responses of Norway spruce needles from shaded and exposed crown layers to the prolonged exposure to elevated CO_2 studied by various chlorophyll *a* fluorescence techniques. *Photosynthetica* 39: 369–376

Karlický V, Kurasová I, Ptáčková B, Večeřová K, Urban O, Špunda V (2016) Enhanced thermal stability of the thylakoid membranes from spruce. A comparison with selected angiosperms. *Photosynth Res* 130: 357–371

Kataria S, Guruprasad KN (2012) Intraspecific variations in growth, yield and photosynthesis of sorghum varieties to ambient UV (280-400 nm) radiation. *Plant Sci* 196: 85–92

Kataria S, Jajoo A, Guruprasad KN (2014) Impact of increasing Ultraviolet-B (UV-B) radiation on photosynthetic processes. *J Photochem Photobiol B: Biol* 137: 55–66

Kirchhoff H (2013) Architectural switches in plant thylakoid membranes. *Photosynth Res* 116: 481–487

Kleine T, Kindgren P, Benedict C, Hendrickson L, Strand Å (2007) Genome-wide gene expression analysis reveals a critical role for CRYPTOCHROME1 in the response of Arabidopsis to high irradiance. *Plant Physiol* 144: 1391–1406

Klem K, Ač A, Holub P, Kováč D, Špunda V, Robson TM, Urban O (2012) Interactive effects of PAR and UV radiation on the physiology, morphology and leaf optical properties of two barley varieties. *Env Exp Bot* 75: 52–64

Klughammer C, Schreiber U (2008) Saturation pulse method for assessment of energy conversion in PSI. *PAM Application Notes* 1: 11–14

Kouřil R, Dekker JP, Boekema EJ (2012) Supramolecular organization of photosystem II in green plants. *Biochim Biophys Acta-Bioenerg* 1817: 2–12

Kouřil R, Wientjes E, Bultema JB, Croce R, Boekema EJ (2013) High-light vs. low-light: Effect of light acclimation on photosystem II composition and organization in *Arabidopsis thaliana*. *Biochim Biophys Acta-Bioenerg* 1827: 411–419

Kouřil R, Strouhal O, Nosek L, Lenobel R, Chamrád I, Boekema EJ, Šebela M, Ilík P (2014) Structural characterization of a plant photosystem I and NAD(P)H dehydrogenase supercomplex. *Plant J* 77: 568–576

Kouřil R, Nosek L, Bartoš J, Boekema EJ, Ilík P (2016) Evolutionary loss of light-harvesting proteins Lhcb6 and Lhcb3 in major land plant groups - break-up of current dogma. *New Phytol* 210: 808–814

Kouřil R, Nosek L, Opatíková M, Arshad R, Semchonok DA, Chamrád I, Lenobel R, Boekema EJ, Ilík P (2020) Unique organization of photosystem II supercomplexes and megacomplexes in Norway spruce. *Plant J* 104: 215–225

Kovács L, Damkjær J, Kereïche S, Ilioaia C, Ruban AV, Boekema EJ, Jansson S, Horton P (2006) Lack of the light-harvesting complex CP24 affects the structure and function of the grana membranes of higher plant chloroplasts. *Plant Cell* 18: 3106–3120

Kramer DM, Johnson G, Kiirats O, Edwards GE (2004) New fluorescence parameters for the determination of Q_A redox state and excitation energy fluxes. *Photosynth Res* 79: 209–218

Krizek DT (2004) Influence of PAR and UV-A in determining plant sensitivity and photomorphogenic responses to UV-B radiation. *Photochem Photobiol* 79: 307–315

Kurasová I, Čajánek M, Kalina J, Urban O, Špunda V (2002) Characterization of acclimation of *Hordeum vulgare* to high irradiation based on different responses of photosynthetic activity and pigment composition. *Photosynth Res* 72: 71–83

Kurasová I, Kalina J, Štroch M, Urban O, Špunda V (2003a) Response of photosynthetic apparatus of spring barley (*Hordeum vulgare* L.) to combined effect of elevated CO_2 concentration and different growth irradiance. *Photosynthetica* 41: 209–219

Kurasová I, Kalina J, Urban O, Štroch M, Špunda V (2003b) Acclimation of two distinct plant species, spring barley and Norway spruce, to combined effect of various irradiance and CO_2 concentration during cultivation in controlled environment. *Photosynthetica* 41: 513–523

Landi M, Živčák M, Sytar O, Brestič M, Allakhverdiev SI (2020) Plasticity of photosynthetic processes and the accumulation of secondary metabolites in plants in response to monochromatic light environments: a review. *Biochim Biophys Acta-Bioenerg* 1861: 148131

Lenk S, Buschmann C (2006) Distribution of UV-shielding of the epidermis of sun and shade leaves of the beech (*Fagus sylvatica* L.) as monitored by multi-colour fluorescence imaging. *J Plant Physiol* 163: 1273–1283

Lichtenthaler HK (1987) Chlorophylls and carotenoids: pigments of photosynthetic biomembranes. In: Colowick SP, Kaplan NO (eds.), *Methods in Enzymology* 148, Academic Press, San Diego/New York, pp 350–382

Lichtenthaler HK (2015) Fifty-Five Years of Research on Photosynthesis, Chloroplasts, and Stress Physiology of Plants: 1958–2013. In: Lüttge U, Beyschlag W (eds.), *Progress in Botany*, Progress in Botany 76, Springer, pp 3–42

Lichtenthaler HK, Babani F (2004) Light adaptation and senescence of the photosynthetic apparatus. Changes in pigment composition, chlorophyll fluorescence parameters and photosynthetic activity. In: Papageorgiou GC, Govindjee (eds.), *Chlorophyll a Fluorescence: a Signature of Photosynthesis*, Springer, Dordrecht, pp 713–736

Lichtenthaler HK, Buschmann C (1978) Control of chloroplast development by red light, blue light and phytohormones. In: Akoyunoglou G et al. (eds.), *Chloroplast Development*, Elsevier/North Holland Biomedical Press, Amsterdam, pp 801–816

Lichtenthaler HK, Ač A, Marek MV, Kalina J, Urban O (2007) Differences in pigment composition, photosynthetic rates and chlorophyll fluorescence images of sun and shade leaves of four tree species. *Plant Physiol Biochem* 45: 577–588

Liu H, Fu Y, Wang M, Liu H (2017) Green light enhances growth, photosynthetic pigments and CO_2 assimilation efficiency of lettuce as revealed by 'knock out' of the 480–560 nm spectral waveband. *Photosynthetica* 55: 144–152

Liu Y, Wang TL, Fang SZ, Zhou MM, Qin J (2018) Responses of morphology, gas exchange, photochemical activity of photosystem II, and antioxidant balance in *Cyclocarya paliurus* to light spectra. *Front Plant Sci* 9: 1704

Mantha SV, Johnson GA, Day TA (2001) Evidence from action and fluorescence spectra that UV-induced violet-blue-green fluorescence enhances leaf photosynthesis. *Photochem Photobiol* 73: 249–256

Michael TP, Bryant D, Gutierrez R, Borisjuk N, Chu P, Zhang HZ, Xia J, Zhou JF, Peng H, El Baidouri M, ten Hallers B, Hastie AR, Liang T, Acosta K, Gilbert S, McEntee C, Jackson SA, Mockler TC, Zhang WX, Lam E (2017) Comprehensive definition of genome features in *Spirodela polyrhiza* by high-depth physical mapping and short-read DNA sequencing strategies. *Plant J* 89: 617–635

Milenković SM, Zvezdanović JB, Andelković TD, Marković DZ (2012) The identification of chlorophyll and its derivatives in the pigment mixtures: HPLC-chromatography, visible and mass spectroscopy studies. *Adv Technol* 1: 16–24

Miyake C, Miyata M, Shinzaki Y, Tomizawa K (2005) CO_2 response of cyclic electron flow around PSI (CEF-PSI) in tobacco leaves - Relative electron fluxes through PSI and PSII determine the magnitude of non-photochemical quenching (NPQ) of Chl fluorescence. *Plant Cell Physiol* 46: 629–637

Muneer S, Kim EJ, Park JS, Lee JH (2014) Influence of green, red and blue light emitting diodes on multiprotein complex proteins and photosynthetic activity under different light intensities in lettuce leaves (*Lactuca sativa* L.). *Int J Mol Sci* 15: 4657–4670

Murchie EH, Horton P (1997) Acclimation of photosynthesis to irradiance and spectral quality in British plant species: Chlorophyll content, photosynthetic capacity and habitat preference. *Plant Cell Environ* 20: 438–448

Murchie EH, Lawson T (2013) Chlorophyll fluorescence analysis: a guide to good practice and understanding some new applications. *J Exp Bot* 64: 3983–3998

Nellaepalli S, Zsiros O, Tóth T, Yadavalli V, Garab G, Subramanyam R, Kovács L (2014) Heat- and light-induced detachment of the light harvesting complex from isolated photosystem I supercomplexes. *J Photochem Photobiol B: Biol* 137: 13–20

Nezval J, Štroch M, Materová Z, Špunda V, Kalina J (2017) Phenolic compounds and carotenoids during acclimation of spring barley and its mutant *Chlorina f2* from high to low irradiance. *Biol Plant* 61: 73–84

Nystedt B, Street NR, Wetterbom A, Zuccolo A, Lin YC, Scofield DG, Vezzi F, Delhomme N, Giacomello S, Alexeyenko A, Vicedomini R, Sahlin K, Sherwood E, Elfstrand M, Gramzow L, Holmberg K, Hallman J, Keech O, Klasson L, Koriabine M, Kucukoglu M, Kaller M, Luthman J, Lysholm F, Niittyla T, Olson A, Rilakovic N, Ritland C, Rossello JA, Sena J, Svensson T, Talavera-Lopez C, Theissen G, Tuominen H, Vanneste K, Wu ZQ, Zhang B, Zerbe P, Arvestad L, Bhalerao R, Bohlmann J, Bousquet J, Gil RG, Hvidsten TR, de Jong P, MacKay J, Morgante M, Ritland K, Sundberg B, Thompson SL, Van de Peer Y, Andersson B, Nilsson O, Ingvarsson PK, Lundeberg J, Jansson S (2013) The Norway spruce genome sequence and conifer genome evolution. *Nature* 497: 579–584

Ouzounis T, Rosenqvist E, Ottosen C-O (2015) Spectral effects of artificial light on plant physiology and secondary metabolism: a review. *HortScience* 50: 1128–1135

Paper M, Glemser M, Haack M, Lorenzen J, Mehlmer N, Fuchs T, Schenk G, Garbe D, Weuster-Botz D, Eisenreich W, Lakatos M, Brück TB (2022) Efficient green light acclimation of the green algae *Picochlorum sp.* triggering geranylgeranylated chlorophylls. *Front Bioeng Biotechnol* 10: 885977

Peng LW, Fukao Y, Fujiwara M, Takami T, Shikanai T (2009) Efficient operation of NAD(P)H dehydrogenase requires supercomplex formation with photosystem I via minor LHCI in *Arabidopsis*. *Plant Cell* 21: 3623–3640

Pfündel EE, Latouche G, Meister A, Cerovic ZG (2018) Linking chloroplast relocation to different responses of photosynthesis to blue and red radiation in low and high light-acclimated leaves of *Arabidopsis thaliana* (L.). *Photosynth Res* 137: 105–128

Powles SB (1984) Photoinhibition of photosynthesis induced by visible light. *Annu Rev Plant Physiol Plant Mol Biol* 35: 15–44

Rai N, Morales LO, Aphalo PJ (2021) Perception of solar UV radiation by plants: photoreceptors and mechanisms. *Plant Physiol* 186: 1382–1396

Reifenrath K, Müller C (2007) Species-specific and leaf-age dependent effects of ultraviolet radiation on two Brassicaceae. *Phytochemistry* 68: 875–885

Rippert P, Scimemi C, Dubald M, Matringe M (2004) Engineering plant shikimate pathway for production of tocotrienol and improving herbicide resistance. *Plant Physiol* 134: 92–100

Robson TM, Klem K, Urban O, Jansen MAK (2015) Re-interpreting plant morphological responses to UV-B radiation. *Plant Cell Environ* 38: 856–866

Ruban AV, Wilson S (2021) The mechanism of non-photochemical quenching in plants: localization and driving forces. *Plant Cell Physiol* 62: 1063–1072

Schenkels L, Saeys W, Lauwers A, De Proft MP (2020) Green light induces shade avoidance to alter plant morphology and increases biomass production in *Ocimum basilicum* L. *Sci Hortic* 261: 109002

Schmitt F-J, Renger G, Friedrich T, Kreslavski VD, Zharmukhamedov SK, Los DA, Kuznetsov VV, Allakhverdiev SI (2014) Reactive oxygen species: re-evaluation of generation, monitoring and role in stress-signaling in phototrophic organisms. *Biochim Biophys Acta-Bioenerg* 1837: 835–848

Schöttler MA, Tóth SZ (2014) Photosynthetic complex stoichiometry dynamics in higher plants: environmental acclimation and photosynthetic flux control. *Front Plant Sci* 5: 188

Schulze E-D, Beck E, Buchmann N, Clemens S, Müller-Hohenstein K, Scherer-Lorenzen M (2019) Plant Ecology, Second Edition, Springer

Semer J, Štroch M, Špunda V, Navrátil M (2018) Partitioning of absorbed light energy within photosystem II in barley can be affected by chloroplast movement. *J Photochem Photobiol B: Biol* 186: 98–106

Semer J, Navrátil M, Špunda V, Štroch M (2019) Chlorophyll fluorescence parameters to assess utilization of excitation energy in photosystem II independently of changes in leaf absorption. *J Photochem Photobiol B: Biol* 197: 111535

Shen LL, Huang ZH, Chang SH, Wang WD, Wang JF, Kuang TY, Han GY, Shen JR, Zhang X (2019) Structure of a $C_2S_2M_2N_2$ type PSII-LHCII supercomplex from the green alga *Chlamydomonas reinhardtii*. *Proc Natl Acad Sci USA* 116: 21246–21255

Sheng X, Watanabe A, Li AJ, Kim E, Song CH, Murata K, Song DF, Minagawa J, Liu ZF (2019) Structural insight into light harvesting for photosystem II in green algae. *Nat Plants* 5: 1320–1330

Smith HL, McAusland L, Murchie EH (2017) Don't ignore the green light: exploring diverse roles in plant processes. *J Exp Bot* 68: 2099–2110

Špunda V, Čajánek M, Kalina J, Lachetová I, Šprtová M, Marek MV (1998) Mechanistic differences in utilization of absorbed excitation energy within photosynthetic apparatus of Norway spruce induced by the vertical distribution of photosynthetically active radiation through the tree crown. *Plant Sci* 133: 155–165

Štroch M (2006) Photochemical and non-photochemical de-excitation processes in relation to acclimation of the photosynthetic apparatus of higher plants to different irradiances. PhD. Thesis, Palacký University, Olomouc, Czech Republic

Štroch M, Čajánek M, Kalina J, Špunda V (2004) Regulation of the excitation energy utilization in the photosynthetic apparatus of *chlorina f2* barley mutant grown under different irradiances. *J Photochem Photobiol B: Biol* 75: 41–50

Štroch M, Kuldová K, Kalina J, Špunda V (2008) Dynamics of the xanthophyll cycle and non-radiative dissipation of absorbed light energy during exposure of Norway spruce to high irradiance. *J Plant Physiol* 165: 612–622

Su NN, Wu Q, Shen ZG, Xia K, Cui J (2014) Effects of light quality on the chloroplastic ultrastructure and photosynthetic characteristics of cucumber seedlings. *Plant Growth Regul* 73: 227–235

Su XD, Ma J, Wei XP, Cao P, Zhu DJ, Chang WR, Liu ZF, Zhang XZ, Li M (2017) Structure and assembly mechanism of plant $C_2S_2M_2$-type PSII-LHCII supercomplex. *Science* 357: 815–520

Sullivan JH, Gitz DC, Peek MS, McElrone AJ (2003) Response of three eastern tree species to supplemental UV-B radiation: leaf chemistry and gas exchange. *Agric For Meteorol* 120: 219–228

Talbott LD, Nikolova G, Ortiz A, Shmayevich I, Zeiger E (2002) Green light reversal of blue-light-stimulated stomatal opening is found in a diversity of plant species. *Am J Bot* 89: 366–368

Tanaka R, Rothbart M, Oka S, Takabayashi A, Takahashi K, Shibata M, Myouga F, Motohashi R, Shinozaki K, Grimm B, Tanaka A (2010) LIL3, a light-harvesting-like protein, plays an essential role in chlorophyll and tocopherol biosynthesis. *Proc Natl Acad Sci USA* 107: 16721–16725

Terashima I, Fujita T, Inoue T, Chow WS, Oguchi R (2009) Green light drives leaf photosynthesis more efficiently than red light in strong white light: revisiting the enigmatic question of why leaves are green. *Plant Cell Physiol* 50: 684–697

Tikhonov AN (2013) pH-dependent regulation of electron transport and ATP synthesis in chloroplasts. *Photosynth Res* 116: 511–534

Tossi V, Lamattina L, Jenkins GI, Cassia RO (2014) Ultraviolet-B-induced stomatal closure in Arabidopsis is regulated by the UV RESISTANCE LOCUS8 photoreceptor in a nitric oxide-dependent mechanism. *Plant Physiol* 164: 2220–2230

Tóth TN, Rai N, Solymosi K, Zsiros O, Schröder WP, Garab G, van Amerongen H, Horton P, Kovács L (2016) Fingerprinting the macro-organisation of pigment-protein complexes in plant thylakoid membranes in vivo by circular-dichroism spectroscopy. *Biochim Biophys Acta-Bioenerg* 1857: 1479–1489

Turnbull TL, Barlow AM, Adams MA (2013) Photosynthetic benefits of ultraviolet-A to *Pimelea ligustrina*, a woody shrub of sub-alpine Australia. *Oecologia* 173: 375–385

Urban O, Klem K, Ač A, Havránková K, Holišová P, Navrátil M, Zitová M, Kozlová K, Pokorný R, Šprtová M, Tomášková I, Špunda V, Grace J (2012) Impact of clear and cloudy sky conditions on the vertical distribution of photosynthetic CO_2 uptake within a spruce canopy. *Funct Ecol* 26: 46–55

Vass I, Szilárd A, Sicora C (2005) Adverse effects of UV-B light on the structure and function of the photosynthetic apparatus. In: Pessarakli M (ed.), *Handbook of Photosynthesis, second edition*. CRC Press, Taylor and Francis Group, Boca Raton, pp 827–843

Verdaguer D, Jansen MAK, Llorens L, Morales LO, Neugart S (2017) UV-A radiation effects on higher plants: Exploring the known unknown. *Plant Sci* 255: 72–81

Wada M (2013) Chloroplast movement. *Plant Sci* 210: 177–182

Wada M (2016) Chloroplast and nuclear photorelocation movements. *Proc Jpn Acad Ser B-Phys Biol Sci* 92: 387–411

Walters RG (2005) Towards an understanding of photosynthetic acclimation. *J Exp Bot* 56: 435–447

Wang YH, Zhang TT, Folta KM (2015) Green light augments far-red-light-induced shade response. *Plant Growth Regul* 77: 147–155

Ware MA, Belgio E, Ruban AV (2015) Photoprotective capacity of non-photochemical quenching in plants acclimated to different light intensities. *Photosynth Res* 126: 261–274

Way DA, Sage RF (2008) Elevated growth temperatures reduce the carbon gain of black spruce [*Picea mariana* (Mill.) B.S.P.]. *Glob Change Biol* 14: 624–636

Wei J, Li HL, Barrow MP, O'Connor PB (2013) Structural characterization of chlorophyll-*a* by high resolution tandem mass spectrometry. *J Am Soc Mass Spectr* 24: 753–760

Wientjes E, van Amerongen H, Croce R (2013) LHCII is an antenna of both photosystems after long-term acclimation. *Biochim Biophys Acta-Bioenerg* 1827: 420–426

Yamamoto H, Shikanai T (2019) PGR5-dependent cyclic electron flow protects photosystem I under fluctuating light at donor and acceptor sides. *Plant Physiol* 179: 588–600

Yang D-H, Webster J, Adam Z, Lindahl M, Andersson B (1998) Induction of acclimative proteolysis of the light-harvesting chlorophyll *a/b* protein of photosystem II in response to elevated light intensities. *Plant Physiol* 118: 827–834

Zhang TT, Folta KM (2012) Green light signaling and adaptive response. *Plant Signal Behav* 7: 75–78

Zhang TT, Maruhnich SA, Folta KM (2011) Green light induces shade avoidance symptoms. *Plant Physiol* 157: 1528–1536

Appendix - Author's publications

Eight original publications presented in the habilitation thesis are attached, including supplementary material to some publications that is published online. Publications are listed on page 5.